Biomechanics and Energetics of Bipedal Locomotion on Uneven Terrain

by

Alexandra S. Voloshina

A dissertation submitted in partial fulfillment
of the requirements for the degree of
Doctor of Philosophy
(Kinesiology and Mechanical Engineering)
in The University of Michigan
2015

Doctoral Committee:

        Professor Daniel P. Ferris, Co-chair
        Assistant Professor C. David Remy, Co-chair
        Senior Lecturer Monica A. Daley, Royal Veterinary College
        Associate Professor Brent Gillespie
        Associate Professor Scott G. McLean

To my family,
for all their love, support and encouragement throughout the years.

ACKNOWLEDGEMENTS

TABLE OF CONTENTS

LIST OF FIGURES

LIST OF TABLES

LIST OF APPENDICES

Appendix

ABSTRACT

Biomechanics and Energetics of Bipedal Locomotion on Uneven Terrain

by

Alexandra S. Voloshina

Chair: Daniel P. Ferris

Humans navigate uneven terrain in their everyday lives. From trails, grass, and uneven sidewalks, we constantly adapt to various surfaces in our environment. Past research has shown that walking on natural terrain, compared to walking on smooth flat surfaces, results in increased energy expenditure during locomotion. However, the biomechanical adaptations responsible for this energetic increase are unclear, since locomotion research is often conducted either on short walkways or in an outdoor setting, thus limiting data collections. To further our understanding of human locomotion on uneven terrain, I focused on quantifying the biomechanical and energetic changes due to increased terrain variability during walking and running. First, this thesis presents modifications to a regular exercise treadmill to allow for attachment of a separate uneven surface. Using this treadmill, I collected kinetic, kinematic, electromyographic, and energy expenditure data during continuous human walking and running. I showed that humans walking at $1.0\,\mathrm{m/s}$ on an uneven surface, with a $2.5\,\mathrm{cm}$ height variability, increased energy expenditure by $0.73\,\mathrm{W/kg}$ (approx. 28%) compared to walking on smooth terrain. Greater energy expenditure was primarily caused by increased positive work at the hip and knee, with minor contributions from increased muscle activity and step parameter adaptations. I then showed that running at $2.3\,\mathrm{m/s}$ on the same surface resulted in an energetic increase of $0.48\,\mathrm{W/kg}$ (approx. 5%) compared to running on even terrain. In contrast to walking, humans compensated for uneven terrain during running by reducing positive work produced by the ankle and adapting a more crouched leg posture. The similar absolute increases in energetic cost between walking and running implied that much of this increase is likely due to surface height variability and changes in mechanical work. Finally, this work presents analytical and simulated analyses for the rimless wheel and simplest walker models. These analyses explored the relationship

between gait dynamics, energy input strategies, surface unevenness and the energetic cost of walking. Together, these studies advance our understanding of the relationship between mechanics and energetics of human walking on uneven surfaces and could potentially lead to more robust and energetically efficient legged robots, prostheses and more effective clinical rehabilitation interventions.

CHAPTER I

Introduction

In their everyday lives, humans walk and run on a variety of complex surfaces. Navigating these natural terrains, such as grass, sand or snow, leads to increased energetic cost of locomotion compared to moving over even ground (Davies and Mackinnon, 2006; Pandolf et al., 1976; Pinnington and Dawson, 2001; Soule and Goldman, 1972). However, the biomechanical mechanisms responsible for these energetic increases have scarcely been identified, as locomotion research has been typically conducted on smooth surfaces. This allows for only a partial understanding of the mechanics and energetics of human locomotion on uneven terrain, thus potentially limiting the development of legged robots, exoskeletons, prostheses and clinical interventions during gait rehabilitation. For example, hardware designs for robotic systems have greatly advanced in recent years but reliable controllers that can produce stable, energetically efficient locomotion on uneven surfaces still pose a challenge. In addition, rehabilitation interventions after injury often focus on rebuilding gait on even, level ground, thus potentially limiting patient mobility on natural surfaces. The work presented here attempts to characterize the relationship between the biomechanical and energetic changes that occur during locomotion on uneven ground compared to smooth terrain. Understanding human compensatory techniques to continuous perturbations and the causes behind increased energy expenditure on uneven terrain could have potential applications in clinical, bipedal robotics and rehabilitation robotics fields.

This work focuses on three themes of studying human locomotion on uneven terrain. First, I address how studying locomotion on uneven surfaces is limited by equipment both outdoors and in the laboratory environment. I propose modifications to a regular exercise treadmill to address these issues. Second, I present two separate studies on human walking and running on the modified uneven terrain treadmill. Finally, using a model-based approach, I attempt to provide further insight into the mechanical adaptations seen in human walking on uneven terrain.

The first study (Chapter 2) describes the design and construction of an uneven terrain treadmill. Human locomotion on uneven terrain has traditionally been studied either in a natural environment or using short walkways in the laboratory. Both of these setups are

limiting, since studies conducted outdoors have limited access to measurement equipment and studies in the laboratory setting allow for only short walking or running distances. To bypass such issues, several previous studies, both for animal and human locomotion, have taken advantage of modified treadmills by attaching discrete obstacles (e.g. Daley and Biewener (2011); Domingo and Ferris (2009)). Using a similar concept, I modified a regular exercise treadmill to allow for attachment of a separate uneven surface (based on Sponberg and Full (2008)). Using the terrain treadmill without the uneven surface attached produces ground reaction force and inverse dynamics data comparable to the data obtained using a commercially available, instrumented treadmill. I also show that errors due to the terrain are relatively small, suggesting that such modified equipment can be used to evaluate human biomechanics. As a result, the modified treadmill provides a new method of collecting kinematic and energetic data during continuous human walking or running in the laboratory environment.

The second study (Chapter 3) characterizes changes in human biomechanics and energetics during walking on uneven terrain, compared to a flat smooth surface. Subjects walked on the uneven terrain treadmill with even and uneven surfaces, while I collected metabolic energy expenditure and electromyographic data. As the surfaces were detachable from the treadmill, I used them as a walkway placed over in-ground force platforms to obtain ground reaction force and kinematic data for individual steps. I found that the energetic cost of walking on uneven terrain increased by 28% relative to the cost of walking on the flat surface. Although there were slight changes in muscle activity and step parameter means and variability, the majority of this increase in energy cost could be attributed to increased mechanical work at the knee and hip. This redistribution in joint work could potentially be caused by mistiming push-off and collision during walking. Gait is most energetically efficient when push-off with the trailing leg occurs immediately before ground contact of the leading leg (Kuo, 2002; Kuo et al., 2005), and this balance is likely offset by unexpected perturbations encountered on uneven terrain. Using a model-based analysis, I discuss the question of just how much push-off timing affects energetics in a separate chapter (Chapter 5). First, however, I wanted to determine if the biomechanics and energetics of running are affected by uneven terrain similarly.

The biomechanics of walking and running are inherently different, with walking dynamics often compared to an inverted pendulum (Alexander, 1995; Garcia et al., 1998; Mochon and McMahon, 1980) and running dynamics to a mass-spring model (Blickhan, 1989; McMahon and Cheng, 1990). As a result, the adaptation mechanisms apparent on uneven terrain are likely significantly different between walking and running. To determine this difference in adaptation mechanisms, and to identify changes in biomechanics and energetics between

running on uneven and even terrains, my third study (Chapter 4) examined human running on uneven terrain. Using a similar uneven surface attached to the terrain treadmill, subjects ran continuously while I collected kinetic, kinematic, electromyographic and energy expenditure data. I found that, during running, subjects modified work production at the ankle joint (in contrast to changes in knee and hip joint work seen during walking). This likely led to less efficient energy storage and return in elastic tendons and ligaments. This inefficiency, as well as changes in mechanical work due to center of mass up and down motion, led to a an energy expenditure increase of 5% during running on uneven terrain compared to smooth terrain. However, the absolute increases in energetic cost for walking and running on the uneven surface were similar. This implies that the dominant factor responsible for increased energy expenditure on uneven terrain during both walking and running is likely related to surface height variability and the up and down motion of the center of mass.

The final study presented in this work (Chapter 5) attempts to quantify the effects of push-off timing and surface height variability on the energetic cost of walking on uneven terrain, relative to walking on smooth terrain. This is done using a model-based approach, where I analyzed two simple models of walking: the rimless wheel (McGeer, 1990a) and the simplest walker (Alexander, 1995; Garcia et al., 1998; Kuo, 2002). The models moved over a simulated uneven surface consisting of equal up and down steps of varying step height. I examined several gait and energy input strategies, where gait strategies dictated gait parameters (e.g. equal step durations, equal initial step velocities, etc.) and energy input strategies determined how energy was added into the system (such as through push-off impulses, hip impulses or a combination of both). I then compared model predictions to the empirical results described in Chapter 2 and found that the model-based analysis was in agreement with observed human adaptations. In particular, biological data were most closely associated with model-based gaits that relied on energetically expensive hip-work but still managed to show adaptation to the terrain by adjusting work done through push-off. These results support the hypothesis that increases in energy expenditure during walking on uneven terrain are likely caused by changes in gait mechanics.

This work makes several contributions to the study of human locomotion on uneven terrain. The uneven terrain treadmill presented here can be constructed in the laboratory and equipped with a variety of terrains aimed at mimicking the natural environment. Such equipment could allow experiments not possible with existing methods, as well as be potentially used in clinical settings for rehabilitative purposes. In addition, this work has demonstrated that humans adapt to uneven surfaces differently during walking and running, while the increases in absolute energetic cost for both types of locomotion are very similar. This suggests that the implementation of rehabilitation exercises, as well as the development of controllers

3

for biped robots or exoskeletons, needs to consider the type of environment the patient or robot might encounter. Lastly, this work has quantified the energetic cost of mechanical adaptations for two walking models to uneven terrain. Changes in model cost of transport closely matched empirical data of human walking on uneven terrain. Together, these studies helped further the understanding of the control and adaptations of human locomotion on uneven terrain, with potential applications in the clinical, biped and rehabilitation robotics fields.

CHAPTER II

Design and Construction of an Uneven Terrain Treadmill

Abstract

Understanding human locomotion on uneven terrain could be beneficial to both clinical and robotic applications. However, current approaches of studying human locomotion are limited, since continuous walking or running cannot be studied in the laboratory environment. To this end, we modified a regular exercise treadmill by attaching a separate, uneven surface. We compared data obtained during running on our terrain treadmill without the uneven surface attached to data obtained using a commercially available instrumented treadmill and found only minor differences. In addition, we speculate that any errors introduced to the data by the addition of the uneven surfaces are likely small. As a result, we believe such a terrain treadmill is a viable option for studying human locomotion on uneven surfaces in the laboratory setting.

2.1 Introduction

Understanding human and animal adaptations to natural, uneven surfaces could potentially improve clinical rehabilitations methods or even the design and control of robotic exoskeletons and prosthesis. Terrain can affect human biomechanics and energetics in a multitude of ways, but studying these effects in detail is difficult in both outdoor and laboratory environments. Outdoor studies are typically limited in the biomechanical data it is possible to collect, while laboratory settings do not allow for continuous, natural locomotion. As a result, we propose a way to modify a regular exercise treadmill by adding an uneven surface. This would allow subjects to walk uninterrupted for extended periods of time on simulated terrains and would allow for more detailed analysis of human locomotion biomechanics, energetics and adaptation to uneven surfaces.

Currently, studies focusing on locomotion on uneven terrain are conducted either on short uneven walkways or outside in natural environments, such as on grass, sand, snow and other terrains (e.g. Davies and Mackinnon (2006); Grimmer et al. (2008); Pandolf et al. (1976);

5

Pinnington and Dawson (2001); Soule and Goldman (1972)). However, outdoor studies limit the collection of any data that require externally powered, heavy or sensitive equipment. As a result, it is often not possible to obtain ground reaction forces, muscle electromyography or even kinematic data. Conventional experimental setups within the laboratory are limited in a different manner. Often, walking and running studies in the laboratory environment are conducted on designated walkways, which limit the range over which data can be collected. This makes it difficult to obtain kinetic and kinematic information over more than a few steps or to quantify biomechanical and energetic adaptations over time. For these reasons we sought to construct an uneven terrain treadmill that would allow for experimental control of terrain variation and trial duration. We modified a regular exercise treadmill such that a separate uneven surface could be attached and removed as needed. Such a treadmill allows for biomechanical, metabolic and other gait data to be collected during continuous walking or running, in a laboratory setting.

A variety of surfaces, aimed at mimicking the natural environment, have been constructed in a laboratory setting for past research. For example, foam, sand, ballast and other walkways are commonly used in locomotion research (e.g. Andres et al. (2005); Ferris et al. (1998, 1999); Lejeune et al. (1998)). Often, these walkways include force platforms underneath the terrain, which allows for several steps of ground reaction force and joint kinematic data analysis. Several types of uneven surfaces have also been adopted in the laboratory, such as uneven pathways leading to force platforms, unexpected drops in substrate height, or randomly placed obstacles to be navigated (Grimmer et al., 2008; Daley and Biewener, 2006; Marigold and Patla, 2007; Patla, 1997). Similarly, rough terrain constructed of randomly distributed wooden blocks was developed to study cockroach locomotion (Sponberg and Full, 2008). In addition, some experimental setups modified existing treadmills by attaching either discreet obstacles or even creating a continuous balance beam using a set of narrow blocks (Daley and Biewener, 2011; Domingo and Ferris, 2009). However, these setups are limited in multiple ways: walkways of a limited length do not allow for uninterrupted walking or running on these surfaces and treadmill setups have only included discrete obstacles or tasks, rather than a continuously perturbing uneven terrain. Existing experimental setups are not suitable for measuring biomechanical adaptations or energetic consequences of continuous locomotion on uneven terrain. Instead, we have developed an uneven terrain treadmill with variable surface height, which can be used to collect ground reaction forces and other biomechanical and energetic data during continuous locomotion.

2.2   Methods

2.2.1   Treadmill modifications

We modified a commercially available exercise treadmill (JAS Fitness Systems, Track-master TMX22, Dallas, TX) to facilitate attachment of a separate, uneven surface. First, we separated the motor and electronics box located at the front base of the treadmill from the rest of the treadmill frame. We then shifted and reattached the motor box further forward on the treadmill frame. This created approximately a 10 cm gap between the front treadmill roller and the motor box. Since the motor was now further from the treadmill roller, we replaced the original belt drive with one of appropriate length. These modifications created ample room for any obstacles located on the treadmill belt to curve around the treadmill rollers without being obstructed by the motor box.

So that obstacles could clear the ground under the treadmill and to be able to collect ground reaction force data, we placed the treadmill on two custom-made steel support beams. Only the frame of the treadmill rested on the support beams, with the treadmill belt being unobstructed. This allowed any obstacles on the belt to pass under the treadmill unhindered. Each support beam rested directly on an in-ground force platform. As a result, all ground reaction forces were registered by the two force plates. For subject safety, a custom-made platform surrounded the raised treadmill, onto which subjects could step off directly.

2.2.2   Uneven surface

We designed the uneven surface as a separate belt that could be attached to or removed from the original treadmill belt as needed (Figure 2.1). We sewed the secondary belt out of thick, non-stretch canvas material, to match the width and length of the original treadmill belt. At each short end of the belt we attached 16 loops made out of 1.27 cm-wide durable belting trim. This way, once the secondary belt looped around the treadmill rollers and on top of the original belt, the two ends of the secondary belt could be connected to each other with cable-ties. The cable-ties not only allowed us to remove and attach the surface with ease, but also offered flexibility in tightening the secondary belt around the treadmill rollers. So that blocks could be attached to the secondary belt, we sewed 5 cm-wide strands of industrial grade loop-fabric (Velcro, Manchester, NH, USA) along the length of, and covering the entire width of, the secondary belt. The strands of loop-fabric extended past the short end of the secondary belt by approximately 10 cm. These extended pieces of loop-fabric covered the cable-ties when the secondary belt was in place and created a continuous loop-fabric surface.

We used wooden obstacles of different heights to create the uneven surface (after Sponberg and Full (2008)). Blocks were custom-made from sugar pine and were 2.55 cm wide, 15.2 cm
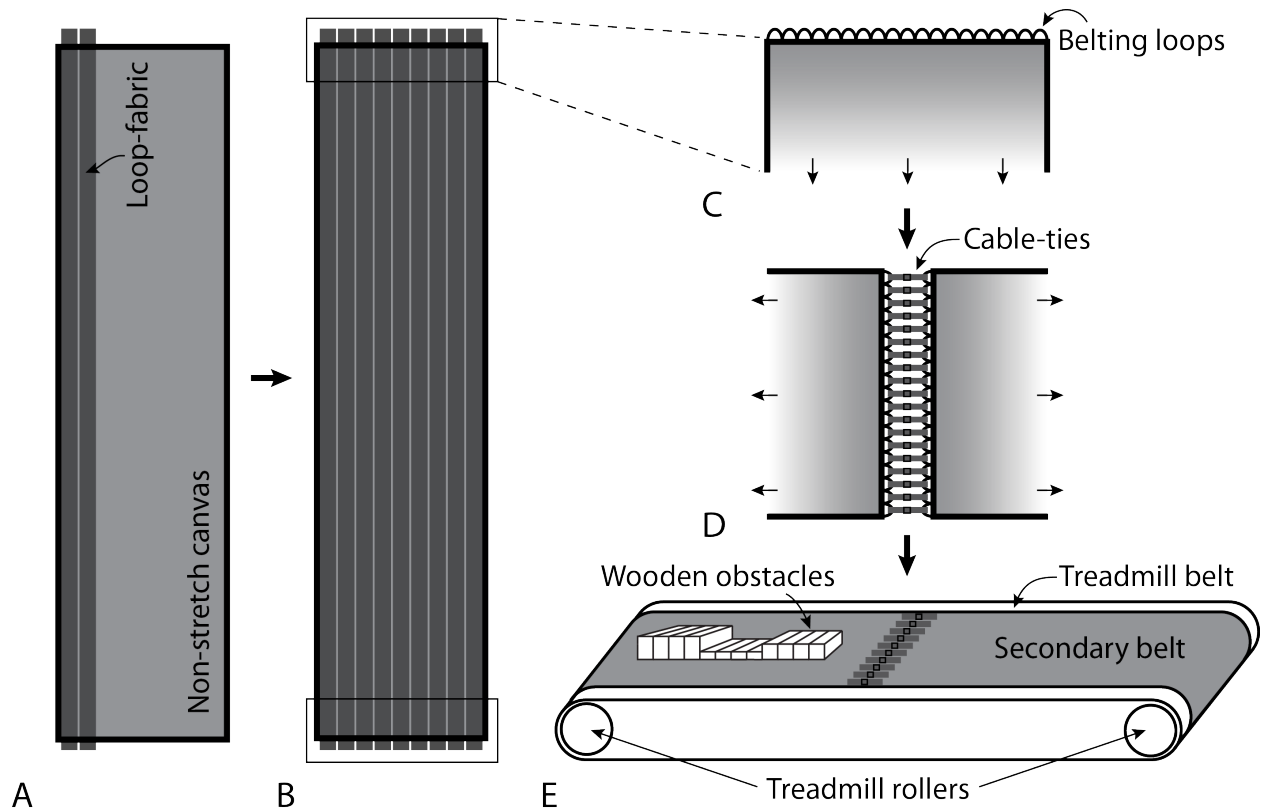
Figure 2.1: Design of the secondary uneven terrain belt. A) Thick, non-stretch fabric is used as the base material. B) Loop fabric is sewed directly onto the canvas, to cover it completely. C) Belting loops are added at each end of the belt. D) Once the secondary belt is placed around the treadmill rollers, the two ends are secured together with cable-ties that go through the belting loops at the end. E) The secondary belt rests on top of the treadmill belt and wooden obstacles are added as desired using hook-and-loop fabric.

long and were three different heights (1.27, 2.54, and 3.81 cm). We glued industrial grade hoop-fabric (Velcro, Manchester, NH, USA) to the bottom of each block. This allowed us to attached and remove obstacles from the loop-fabric on the secondary belt described earlier. Each block was arranged lengthwise across the belt, which allowed the short side of the obstacle to curve around the treadmill rollers. We arranged the blocks in three columns along the length of the belt. The blocks were arranged in 15.2 x 15.2 cm squares, or stepping areas, consisting of six blocks of the same height. These squares alternated by height in each column, with each column height order offset by one. This created a patterned uneven surface, which, due to the arrangement offset in the columns and the relatively short stepping areas, appeared random to individuals walking on the surface (Figure 2.2).
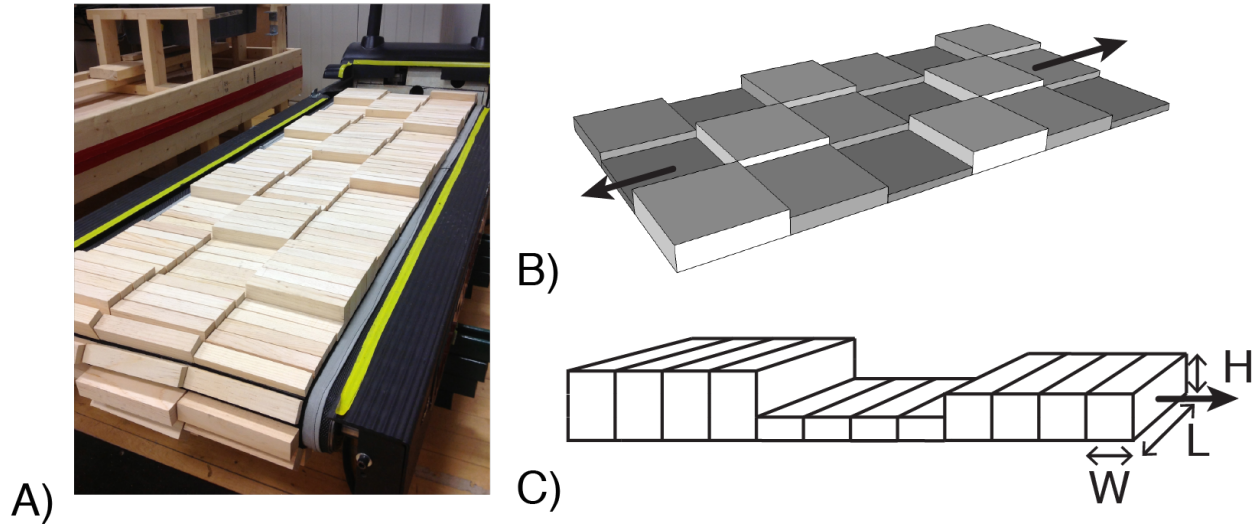
Figure 2.2: Uneven terrain pattern and close-up. A) Photograph of the uneven surface attached to the treadmill. B) Schematic of the uneven surface, with stepping areas of three different heights (arrows indicate the treadmill's long axis). C) Close-up of the blocks comprising the stepping areas. Dimensions: H, 1.27; L, 15.2; W, 2.54.

2.2.3   Force data and moment analysis

Since the uneven terrain treadmill was raised on supports, ground reaction forces and moments were measured substantially below the surface of the treadmill by two force platforms. Such a setup made inverse dynamics calculations non-trivial, as the total force vectors and effective moments were represented by data from two force platforms located underneath the treadmill. To correct for this before any inverse dynamics calculations, we modified the force vector location and moment magnitudes. First, we added force data measured from the force plates to yield the total ground reaction force vector. We then defined a new origin located on the treadmill surface and calculated an effective moment about that point. The effective moment about the new origin was defined as the sum of all moments recorded by the two force plates and the moments created by the ground reaction forces about the new origin. These modified data were then used for inverse dynamics calculations.

2.2.4   Validation of terrain treadmill setup

To test the validity of our setup and data manipulation methods, we tested one representative subject running on an in-ground instrumented treadmill (Bertec, Worthington, OH, USA) and on the terrain treadmill with the uneven surface removed. The terrain treadmill was placed on top of two in-ground force platforms, placed 0.5 m apart (sample rate: 1000 Hz; AMTI, Watertown, MA, USA). We collected ground reaction forces from both setups,
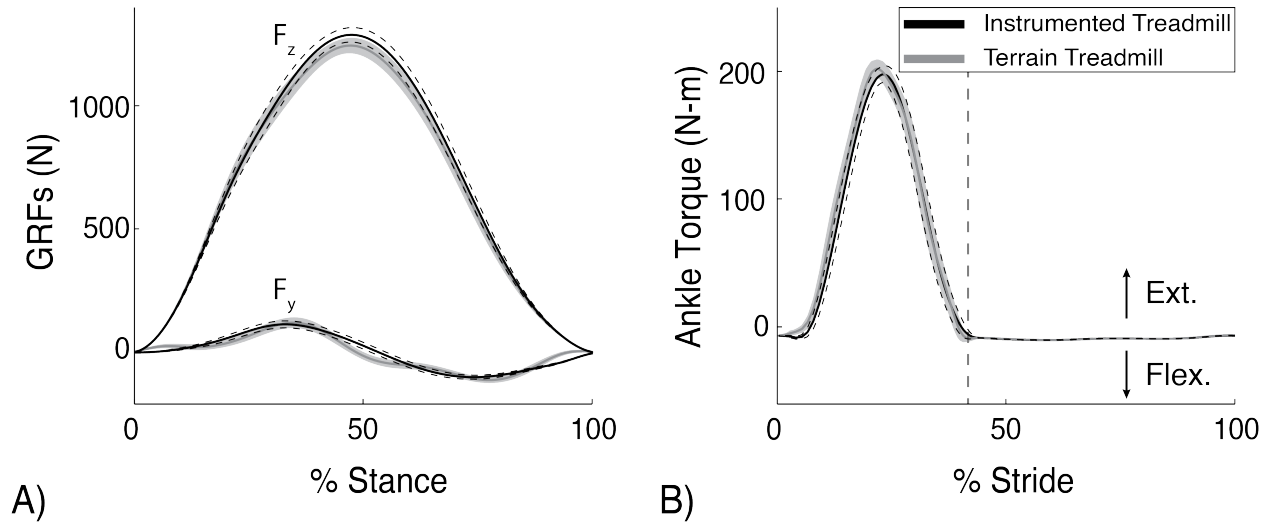
Figure 2.3: Comparison of ground reaction forces and ankle moments during level ground running on instrumented and terrain treadmills. A) Vertical (F_z) and fore-aft (F_y) ground reaction forces for the two running conditions. B) Ankle torques for the two running conditions. Shaded areas denote the standard deviation envelopes of the subject mean for the terrain treadmill condition; dashed for the instrumented treadmill condition. Dashed vertical gray line indicates mean time of toe-off.

as well as the positions of 31 reflective markers, positioned on the lower limbs and pelvis, using a 10-camera motion capture system (frame rate: 100 Hz; Vicon, Oxford, UK). On each treadmill, the subject ran for 2 minutes (approx. 275 steps) at a speed of 2.3 m/s. Force data used to determine the time of heel-strike and for analysis of average ground reaction forces were low-pass filtered at 25 Hz (fourth-order Butterworth filter, zero-lag). For inverse dynamics calculations we low-pass filtered all marker and force data at 6 Hz (fourth-order Butterworth filter, zero-lag) to reduce motion artifact and high noise sensitivity of the ground reaction forces. We used Visual-3D (C-Motion, Germantown, MD, USA) to conduct inverse dynamics calculations and determine center of pressure locations and ankle joint moments. We then averaged force and moment data to create mean profiles and standard deviation envelopes. Differences between conditions for peak vertical ground reaction forces and angle moments for all steps were quantified using a repeated-measure ANOVA, with a post hoc Holm-Sidak multiple comparisons correction. The significance level α was set to 0.05.

Average peak vertical and fore-aft ground reaction forces and average ankle moment profiles were similar for the two treadmill conditions (Figure 2.3A). We found the peak vertical ground reaction forces (F_z) for each step during running on the terrain treadmill and the instrumented treadmill. Maximum F_z were statistically different between the two experimental setups ($p < 0.001$). However, the average peak vertical ground reaction forces were only 3.5% smaller on the terrain treadmill, compared to the instrumented treadmill.

Qualitative examination of the average fore-aft ground reaction forces for the two running conditions did not reveal substantial differences. For the terrain treadmill compared to the instrumented treadmill, force variability, defined as the standard deviation of the mean, was larger by 5% and 30% for the vertical and fore-aft ground reaction forces respectively. The root-mean-square of the fore-aft center of pressure distribution for the two experimental setups was also within 6% of each other. The peak ankle moments on the terrain treadmill were also statistically different than the peak ankle moment on the instrumented treadmill ($p < 0.001$; Figure 2.3B). The average peak ankle moment on the terrain treadmill was less than 2% smaller than on the instrumented treadmill. Ankle moment variabilities were comparable on the two treadmills. In addition, both the ground reaction forces and ankle moment profiles were highly correlated for the two conditions (R > 0.997).

2.3 Discussion

We modified a regular exercise treadmill to allow for the attachment of an uneven terrain surface, such that we could collect continuous biomechanical and energetic data during human locomotion. The artificial uneven surface presented here comprised of stepping areas of three different heights. We arranged the stepping areas in a particular order and our uneven surface clearly exhibited a pattern. Although humans may adapt gait to patterned terrain (such as walking on stepping stones) it is very unlikely that subjects would do so with this particular surface. The stepping areas created by the obstacles were smaller than the length of an average foot, which means that subjects would be perturbed with every step. However, the variability of the terrain height is likely to affect human locomotion. Obstacle heights chosen here were selected based on the maximum several representative subjects could run on. It may be beneficial for future studies to create other, more or less variable, uneven terrain surfaces to examine how changes in terrain variability affect the biomechanics and energetics of human locomotion.

Ground reaction forces and ankle joint moment data were very similar for even running on both the terrain and instrumented treadmills. Although individual step analysis revealed significant differences between the two running setups, the peak average vertical ground reaction force and peak average ankle moment only decreased by 3.5 and 2%, respectively. Considering that ankle moment calculations are based on force data, it is not surprising that the decreases are similar. It is important to note that the decrease in peak force could be caused by a difference in surface stiffness between the two treadmills and not necessarily by the treadmill setup. Past research has shown that humans adjust their leg stiffness and ultimately ground reaction forces in response to changes in surfaces stiffness (Ferris et al.,

1998, 1999). Still, the differences in average ground reaction forces and ankle moments seen due to different setups are likely much smaller than the differences that would be caused by an uneven surface. Result comparisons could also be affected by the relatively low cut-off frequency (of 6 Hz) used to filter force data prior to inverse dynamics calculations. We chose this cut-off frequency over the more traditional cut-off frequency of 25Hz in order to minimize the effects of natural treadmill vibrations on the inverse dynamics analysis. This could, in turn, affect the ground reaction force data by reducing the maximum peak ground reaction forces recorded. In addition, any significance of impact peaks could be reduced. However, since force data from both setups are processed in the same manner, comparisons between the two methods are still valid. In other words, although absolute ground reaction force magnitudes may be underrepresented, any changes in means would still be informative. Thus, we feel confident that data collected from the terrain treadmill with the uneven surface attached is accurate enough to draw conclusions about the effects of terrain on human biomechanics.

Although data obtained using the terrain treadmill and the instrumented treadmill are highly comparable during even running, it is likely that the addition of the uneven surface would introduce error into the inverse dynamics calculations. Since we shift the vertical location of the effective force vector to the lowest point of the terrain surface, actual points of foot contact may be up to 2.54 cm higher due to terrain unevenness. This would, in turn, affect center of pressure and inverse dynamics calculations. If we project the force vector from the highest point on the terrain (where the foot may actually be in contact with the ground) to the surface of the treadmill (where we calculate the force vector to be), we can calculate the center of pressure location error. Given the variability of our terrain, this error is relatively small and is less than 1.5 cm. In addition, during both walking and running, this error would be multidirectional. This means that the overall mean results of the inverse dynamics calculations would likely not be affected. Instead, we are likely to see increased variability in all measurements that rely on center of pressure locations.

In conclusion, the treadmill modifications and uneven surface designs presented here can potentially be useful in many types of biomechanical studies on human locomotion on uneven surfaces. We have also demonstrated that it is possible to obtain reliable results from the terrain treadmill for human running on even ground, compared to those obtained using a commercially available instrumented treadmill. Although results using the terrain treadmill during running on an uneven surface are likely to be more variable, the mean biomechanical changes are likely to be unaffected by calculations errors. As a result, this device can help improve our understanding of human locomotion on surfaces that mimic the natural environment.

CHAPTER III

Biomechanics and Energetics of Walking on Uneven Terrain

Abstract

Walking on uneven terrain is more energetically costly than walking on smooth ground, but the biomechanical factors that contribute to this increase are unknown. To identify possible factors, we constructed an uneven terrain treadmill that allowed us to record biomechanical, electromyographic, and metabolic energetics data from human subjects. We hypothesized that walking on uneven terrain would increase step width and length variability, joint mechanical work, and muscle co-activation compared to walking on smooth terrain. We tested healthy subjects ($N = 11$) walking at 1.0 m/s, and found that, when walking on uneven terrain with up to 2.5 cm variation, subjects decreased their step length by 4% and did not significantly change their step width, while both step length and width variability increased significantly (22% and 36%, respectively; $p < 0.05$). Uneven terrain walking caused a 28% and 62% increase in positive knee and hip work, and a 26% greater magnitude of negative knee work (0.0106, 0.1078, and 0.0425 J/kg, respectively; $p < 0.05$). Mean muscle activity increased in seven muscles in the lower leg and thigh ($p < 0.05$). These changes caused overall net metabolic energy expenditure to increase by 0.73 W/kg (28%; $p < 0.0001$). Much of that increase could be explained by the increased mechanical work observed at the knee and hip. Greater muscle co-activation could also contribute to increased energetic cost but to unknown degree. The findings provide insight into how lower limb muscles are used differently for natural terrain compared to laboratory conditions.

3.1   Introduction

Animals and humans navigate complex terrain in their everyday lives. From uneven sidewalks to natural trails, humans often encounter surfaces that are not smooth. Energetic cost for locomotion increases on natural complex surfaces [e.g. grass, sand, snow; e.g. (Davies and Mackinnon, 2006; Pandolf et al., 1976; Pinnington and Dawson, 2001; Soule and Goldman, 1972)] compared to smooth surfaces, but the biomechanical mechanisms responsible for the increased cost are still unclear. Terrain has many features that might affect locomotion, such as height variations, damping, and coefficient of friction. These could cause a variety of changes to locomotion, yet gait research has typically focused on smooth, level ground. To provide some insight into how complex natural terrain can affect locomotion, we therefore studied metabolic energy expenditure and biomechanics of human walking on a synthesized uneven terrain surface.

There are a number of potential factors that could contribute to greater energy expenditure when walking on uneven terrain compared to smooth terrain. Adjusting step parameters during locomotion is one such factor. Adults typically take shorter and wider steps with increasing age (Murray et al., 1969), while younger individuals respond similarly to continuous perturbations, both physical and visual (Hak et al., 2012; McAndrew et al., 2010). If these are strategies to enhance stability, it is possible that younger adults might do the same on uneven terrain. Such terrain may also perturb gait from step to step and cause greater variability. Step width, in particular, would show increased variability, because lateral balance may be more dependent on active stabilization than fore-aft motion, due to passive dynamic stability (Donelan et al., 2001). Energy expenditure would be expected to increase with changes in mean step parameters (Gordon et al., 2009; Wade et al., 2010) and with changes in step variability as well (O'Connor et al., 2012).

Uneven terrain might also require more mechanical work from the legs, independent of the effect on step parameters. Kuo (2002) previously hypothesized that walking economy is improved by pushing off with the trailing leg just prior to the collision of the leading leg. Push-off redirects the body center of mass and, if properly timed, can reduce the amount of negative work performed in the collision. Uneven terrain may upset the relative timing of these events, so that a collision occurring either earlier or later relative to push-off would be expected to lead to greater negative mechanical work. This would then require muscles to compensate and actively do more positive work elsewhere, as steady walking requires zero work on average. It is difficult to predict how work will be distributed between the lower limb joints, but perturbed timing would be expected to require more work overall, and thus more expenditure of metabolic energy.

Another possible factor contributing to increased energy expenditure is co-activation of muscles. When walking on less secure surfaces such as railroad ballast or ice (Cappellini et al., 2010; Marigold and Patla, 2002; Wade et al., 2010), or when there is an unexpected drop in the surface (Nakazawa et al., 2004), humans increase muscle co-activation about the ankle joint. This compensation may help to stabilize the joints for uncertain conditions. If humans co-activate the corresponding muscles on uneven terrain, energy expenditure may increase even if work does not.

The purpose of this study was to determine the changes in walking biomechanics on uneven terrain, and how they might relate to increased metabolic cost. We developed an uneven terrain surface that allowed us to collect continuous kinematic and energetics data during treadmill and over-ground walking. We expected that walking on uneven terrain would increase the variability of step width and step length. Humans may also adopt wider and shorter steps as a stabilizing strategy, similar to the changes that older adults make to compensate for poorer balance. Regardless of strategy, the perturbations of uneven terrain would be expected to cause subjects to increase joint mechanical work and muscle co-activation on uneven terrain compared to walking on smooth terrain. Walking over natural surfaces involves much greater variation than a smooth treadmill belt or uniform pavement; thus, biomechanics and energetics in uneven terrain are likely to better represent the functional demands that have influenced the evolution of human bipedalism (Pontzer et al., 2009; Sockol et al., 2007).

3.2   Methods

We created an uneven terrain surface by attaching wooden blocks to a treadmill belt. This allowed us to collect biomechanical data and metabolic energetics data simultaneously during continuous walking. The same terrain surface could also be placed over ground-embedded force plates, facilitating collection of joint kinetics data. Each wooden block was covered with a layer of ethylene-vinyl acetate (EVA) cushioning foam, to make the surface comfortable to walk on. To test for effects of the cushioning foam alone, subjects also walked on a smooth treadmill belt surface covered only by the cushioning foam, resulting in conditions termed "Uneven + Foam" and "Even + Foam." We also tested walking on just the normal treadmill belt, termed the "Even" condition. We collected kinematic, kinetic, metabolic, and electromyographic data for each condition, all at a walking speed of 1.0 m/s.
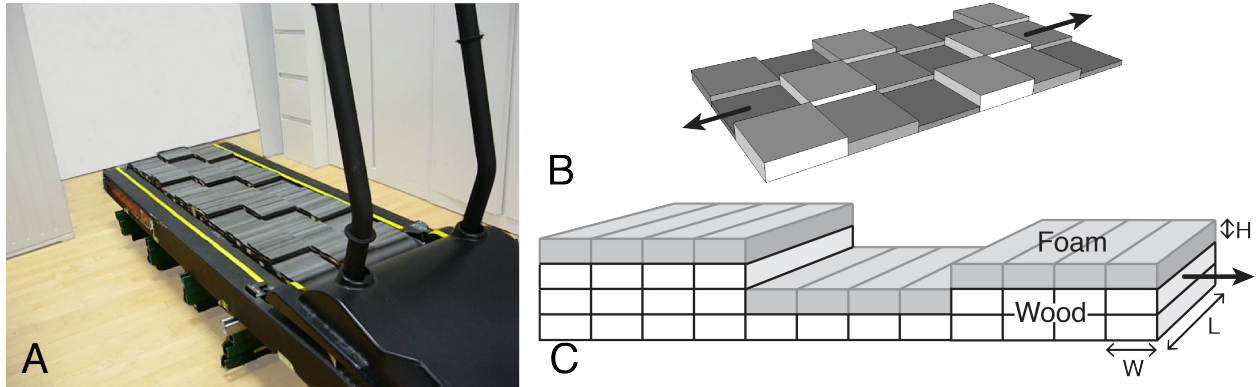
Figure 3.1: Uneven terrain treadmill for walking. A) Treadmill with the uneven terrain surface attached. B) Schematic of the uneven surface layout, consisting of three alternating heights (arrows indicate the treadmill's long axis). C) Close-up representation of the individual blocks comprising each stepping area. Dimensions: H, 1.27 cm; L, 15.2 cm; W, 2.54 cm.

3.2.1 Subjects

Eleven young, healthy subjects (four female, seven male, mean±standard deviation (SD): age 22.9±2.8 years, mass 66.1±13.2 kg and height 172.6±6.4 cm) participated in the study. Data were collected in two sessions on separate days. One session was for treadmill walking to collect oxygen consumption ($N = 7$) , step parameter data ($N = 9$), and electromyographic data ($N = 8$). The other session was for over-ground walking over force plates to collect joint kinematics and kinetics ($N = 10$). Some data were not collected successfully due to technical and logistical issues, resulting in values of N less than eleven in each data subset, noted in parentheses above. Due to these issues, different subject data were excluded from step parameter, kinematic and kinetic, and electromyographic data. Subjects provided written informed consent before the experiment. All procedures were approved by the University of Michigan Health Sciences Institutional Review Board.

3.2.2 Walking Surfaces and Trial Procedures

We modified a regular exercise treadmill (JAS Fitness Systems, Trackmaster TMX22, Dallas, TX) to allow for attachment and replacement of uneven and even terrain surfaces (Figure 3.1). The uneven surface was created from wooden blocks arranged in squares (15.2 x 15.2 cm) and glued together to form three different heights (1.27, 2.54, and 3.81 cm) and create an uneven surface (after Sponberg and Full (2008)). Each square consisted of smaller blocks, 2.55 x 15.2 cm, oriented lengthwise across the belt and affixed to it with hook-and-

loop fabric. The short dimension of the blocks allowed the belt to curve around the treadmill rollers. Each block's surface was covered with a layer of cushioning foam that was 1.27 cm thick, yielding a surface condition referred to as Uneven + Foam. Even though the uneven squares were arranged in a repeating pattern, their length was not an integer fraction of step length, making it difficult for subjects to learn or adopt a periodic compensation for this condition.

The two other surfaces served as control conditions. The Even + Foam condition was formed using only cushioning foam of the same height as the Uneven + Foam condition. The Even condition consisted of the treadmill belt alone, and allowed us to determine the biomechanical effects of only the cushioning foam.

Walking trials were performed for all three conditions in randomized order, both on treadmill and over-ground. All trials were completed with subjects walking at 1.0 m/s while wearing rubber-soled socks for comfort. Subjects were instructed to walk naturally and encouraged not to look down at their feet unless they felt unstable. Subjects participated in only one 10-minute long treadmill trial per condition with at least 5 minutes of resting time between trials. During over-ground trials, speed was verified by optical timers set 4 m apart mid-way in a 7 m path, and trials were only used if they were within 10% of the target time. Subjects completed at least 10 successful over-ground trials for each surface condition.

3.2.3   Kinetics and Kinematics

For all walking trials (both on the treadmill and over-ground), we recorded the position of 31 reflective markers located on the pelvis and lower limbs using a 10-camera motion capture setup (frame rate: 100 Hz; Vicon, Oxford, UK). Markers were taped to the skin or spandex shorts worn by the subjects. Three markers were placed on each thigh and shank, one at the sacrum and one at each of the greater trochanters, anterior superior iliac spine, the medial and lateral epicondyles of the femur, the medial and lateral malleoli, the fifth metatarsals, the calcanei, and the first metatarsals. Medial markers were removed after static marker calibration. Only the last 2.5 min of kinematic data collected from each treadmill trial were used for calculations. Over-ground trials occurred over two force plates, yielding one to two steps per trial for inverse dynamics calculations. The marker data for both legs were low-pass filtered at 6 Hz to reduce motion artifact (fourth-order Butterworth filter, zero-lag), and used to calculate step widths, lengths and heights, as well as to identify successful steps in over-ground trials. Step parameters were calculated using the calcaneous markers on the two feet. Step width and length were defined as the lateral and fore-aft distances between the two markers at their respective heel-strike instants. Step height was defined as the vertical distance between the two markers at heel-strike, and was only used to indicate greater step

height variability expected from uneven terrain. Heel-strike was defined by the onset of ground force for over-ground trials, and by the lowest height of the calcaneous marker for treadmill trials (where forces were not measured). Over-ground data were used to confirm that these timings agreed well with each other. All step measurements were normalized to subject leg length, defined as the average vertical distance between the greater trochanter and calcaneous markers of both legs.

The Uneven + Foam and Even + Foam surfaces could be detached from the treadmill and used as a walkway. During over-ground trials, subjects walked across these two walking surfaces placed on top of two in-ground force platforms, 0.5 m apart (sample rate: 1000 Hz; AMTI, Watertown, MA) for the Uneven + Foam and Even + Foam conditions. The surfaces were not secured to the floor, but did not appear to slip during walking trials. For the Even condition, subjects walked on the bare floor and force plates. The in-ground force plates were re-zeroed between conditions. All force data were low-pass filtered at 6 Hz (fourth-order Butterworth filter, zero lag) and ground reaction force data were synchronized with the kinematic data. Joint angles, moments and powers for the stance limb were determined using inverse dynamics analysis in Visual-3D (C-Motion Inc., Germantown, MD). Positive and negative joint work measures were calculated by integrating the intervals of either positive or negative joint power over time.

3.2.4 Electromyography

We measured electromyography (EMG) in the tibialis anterior (TA), soleus (SO), medial gastrocnemius (MG), lateral gastrocnemius (LG), rectus femoris (RF), vastus medialis (VM), vastus lateralis (VL) and the semitendinosus of the medial hamstring (MH) muscles, during all treadmill trials. All EMG data were collected only for the right leg. Bipolar surface electrodes (sample rate: 1000 Hz; Biometrics Ltd., Ladysmith, VA) were placed over the belly center of the muscle and in parallel to the muscle according to the procedure of Winter and Yack (1987). The inter-electrode distance was 2.0 cm for all trials and electrode diameters were 1.0 cm. The EMG amplifier had a bandwidth of 20 Hz - 460 Hz. As with other measurements, only the last 2.5 min of EMG data were used for data analysis. All electromyography signals were high-pass filtered with a 20 Hz cutoff-frequency (4th order Butterworth filter, zero-lag) and then full-wave rectified. We then normalized each muscle's data to the maximum activation observed for that same muscle over all three conditions for that subject (Winter and Yack, 1987; Yang and Winter, 1984) and averaged over subjects to create representative EMG profiles. Standard deviations of the EMG traces were found at each time point for every subject and condition and also averaged, to determine mean standard deviation envelopes. Although the relationship between EMG variability

18

and metabolic cost is undetermined, this measure can indicate the level of perturbation to gait mechanics from uneven terrain. To determine increases in muscle activation, we found the average of the normalized EMG profile for each subject and condition. These average values were then averaged over subjects. In addition, we assessed muscle co-activation as the amount of mutual contraction (MC) as defined by Thoroughman and Shadmehr (1999) to indicate 'wasted' contraction, for each stride for three pairs of antagonistic muscles (SO/TA, MH/VM, MH/VL). To do so, we used the equation:

$$\text{MC} = \int \min(f_1, f_2)\mathrm{d}t$$

where f_1 and f_2 are the full-wave rectified EMG profiles, averaged over one hundred steps, of the two antagonistic muscles and $\min(f_1, f_2)$ is the minimum of the two profiles at each time point. Integrals were computed over the duration of the whole stride and in 1% increments to identify where in the stride cycle mutual contraction occurred.

3.2.5 Metabolic Rate

For all treadmill walking conditions, we measured the rate of $\dot{V}_{O2}$ using an open-circuit respirometry system (CareFusion Oxycon Mobile, Hoechberg, Germany). We recorded 7 minutes of respirometry data during a quiet standing trial, and 10 minutes for all walking trials. Although 3-minute trials are sufficient to reach steady-state energy expenditure on uniform terrain (Poole and Richardson, 1997), we expected walking on uneven terrain to be an increase in exercise intensity and allowed subjects 7.5 minutes of walking to reach steady-state before collection 2.5 minutes of data. We later confirmed that subjects had reached steady-state in both biomechanics and energetics on the novel terrain conditions by checking that no adaptation trends were still present in the last 2.5 minutes of data. We calculated the metabolic energy expenditure rate of each subject using standard empirical equations yielding metabolic rate $\dot{E}_{met}$ (in W) (Brockway, 1987; Weir, 1949). Net metabolic rate was found by subtracting the standing metabolic power from the metabolic power of all other conditions. We normalized the net metabolic power for all conditions by dividing by subject body mass (kg).

3.2.6 Data and Statistical Analyses

To compare changes in variability for step parameter, joint parameter and EMG data, we averaged the variability for each of the three conditions over all subjects. For step data, we defined variability as the standard deviation of contiguous step distances or periods over

	Even		Even + Foam		Uneven + Foam		p − value	
	Mean(s.d.)	*Step.var.(s.d.)*	*Mean(s.d.)*	*Step.var.(s.d.)*	*Mean(s.d.)*	*Step.var.(s.d.)*	*Mean*	*Step.var.*
Width	0.077 (0.040)	0.027 (0.005)	0.080 (0.036)	0.028 (0.004)	0.102 (0.053)	0.038* (0.006)	0.0336	0.0003
Length	0.672 (0.020)	0.037 (0.009)	0.662 (0.025)	0.037 (0.008)	0.638* (0.024)	0.045* (0.007)	0.0039	0.0006
Height	∼	0.004 (0.001)	∼	0.004 (0.001)	∼	0.008* (0.001)	∼	< 0.0001
StepPeriod(s)	0.568 (0.022)	0.013 (0.003)	0.560 (0.027)	0.014 (0.003)	0.540* (0.038)	0.018* (0.003)	0.0028	0.0017

Table 3.1: Step parameters for walking on even and uneven terrains. Parameters include mean step length, width, and height and their respective variations (all normalized to subject leg length, mean 0.870 m), as well as step period. Shown are averages (and standard deviations, s.d.) across subjects. Step variability is defined as the standard deviation of step distances over a trial, reported as an average (and s.d.) across subjects. Asterisks signify a statistically significant difference of the Uneven + Foam condition from the other two conditions (post-hoc pair-wise comparisons, $\alpha = 0.05$).

time, for each subject. For joint parameter and EMG data, means are found across trials for each point in relative stride cycle timing. Similarly, joint parameter and EMG variability was defined for each subject and condition as the standard deviation across trials for each point. We then report the mean variations (and standard deviations) across subjects for each condition. Differences between the conditions were quantified by performing repeated-measures ANOVAs on the data sets of interest. The significance level α was set at 0.05 and post hoc Holm-Sidak multiple comparison tests were performed where appropriate.

3.3   Results

Walking on uneven terrain resulted in a variety of changes to gait compared to walking on smooth terrain. Subjects walked with slightly shorter step lengths and substantially increased step variability. Gait kinematics remained similar overall but knee and hip mechanical work increased on uneven terrain. We also observed increased mean activity among multiple proximal leg muscles (VM, VL, RF, MH), and greater muscle mutual contraction about all three joints on uneven terrain. In all variables, the two smooth terrain conditions (with and without a foam layer) exhibited negligible differences between each other. We therefore report comparisons mainly between the Uneven + Foam and Even + Foam conditions.

3.3.1   Kinetics and Kinematics

Although mean step parameters changed little, there were large changes in step variability during walking on the uneven surface when compared to the even foam surface (Table 2.1). Of the mean step distances, only step length changed significantly, decreasing by 3.7%. Because walking speed was kept fixed, this was accompanied by a 3.7% decrease in mean step duration. Variability of step width, length and height all increased significantly by
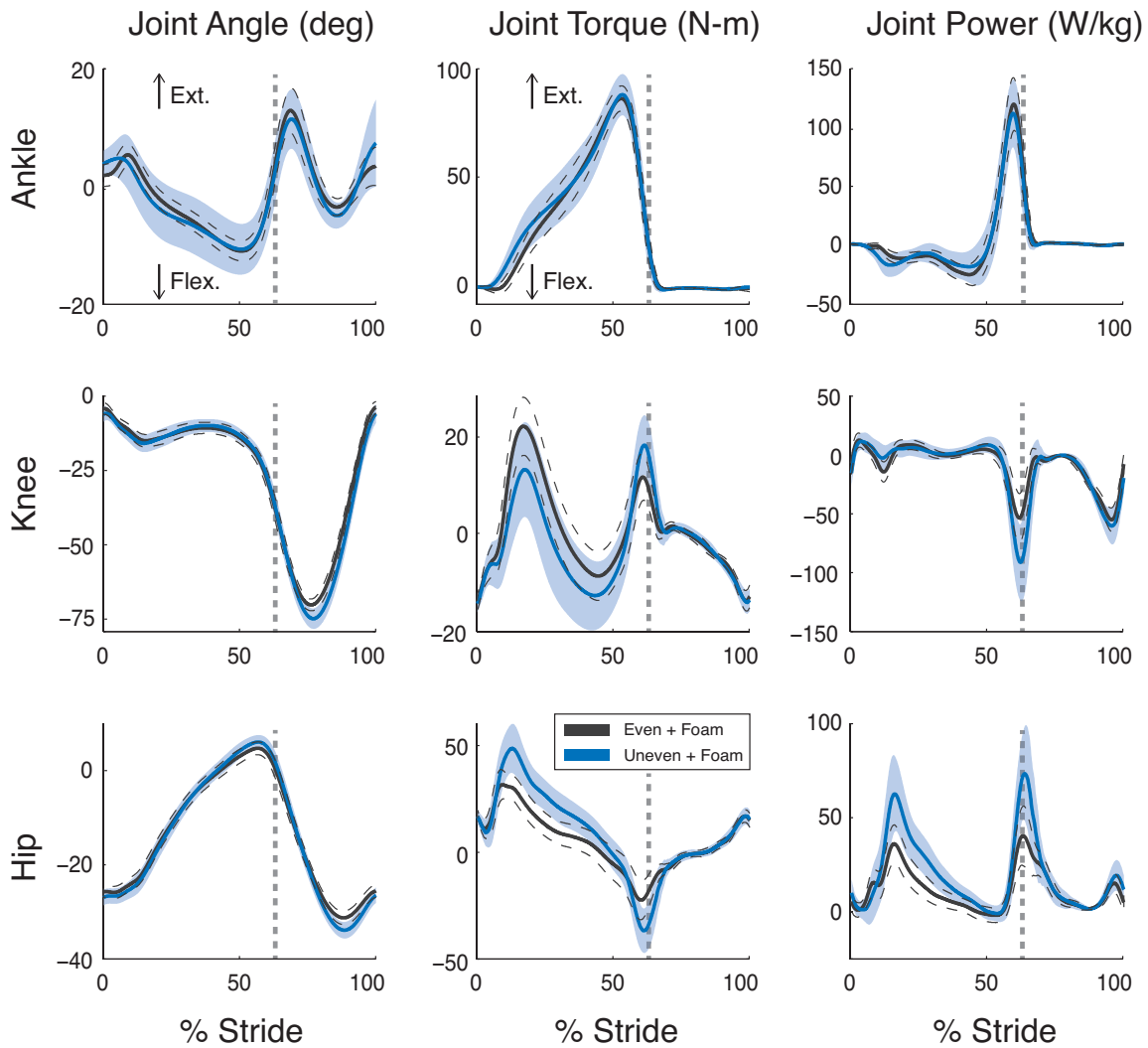
Figure 3.2: JJoint angle, torque and power versus stride time for walking on even and uneven terrains. Mean trajectories for ankle, knee and hip are plotted against percent stride time for uneven and even terrain (both with foam) conditions. Shaded area denotes standard deviation across subjects for Uneven + Foam; dashed lines for Even + Foam. Strides start and end at same-side heel-strike; dashed vertical gray lines indicate toe-off.
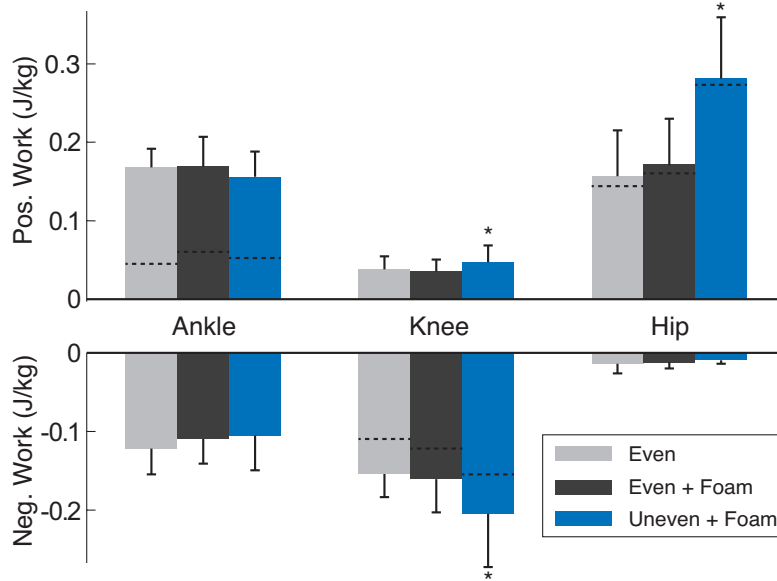
Figure 3.3: Joint work per stride for walking on even and uneven terrains. Values shown are positive and negative work for ankle, knee, and hip, with error bars denoting standard deviations. Dashed lines indicate net work for that specific joint and condition. Asterisks signify a statistically significant difference of the Uneven + Foam condition from the other two conditions ($\alpha = 0.05$)

about 35%, 23%, and 105%, respectively. Step period variability also increased significantly by 26.7%.

A number of effects were observed on joint kinematics and kinetics when subjects walked on uneven terrain when compared to the even surface (Figure 3.2). Qualitative examination of sagittal plane joint angles on uneven terrain suggest slightly greater knee and hip flexion at mid-swing, perhaps associated with greater ground clearance of the swing foot. Mean ankle angle trajectory changed little (Figure 3.2). However, on uneven terrain, we observed larger effects on the joint moments during stance, with increased knee flexion and increased hip extension moments at mid-stance. At the end of stance during push-off, these patterns reversed, with greater knee extension and hip flexion moments. The main changes in joint power were also confined to the knee and hip, with increased peak powers, especially at push-off (by about 65% and 85%, respectively) when walking on the uneven surface. Hip power also increased by 75% during mid-stance, at about 20% of stride time. Toe-off timing in the stride cycle did not appear to differ between conditions. Joint trajectories were more variable on uneven terrain (Figure 3.2). The ankle angle variability more than doubled on uneven terrain, while the knee and hip variability increased by about 30% (all $p < 0.05$). The mean ankle and knee torque variability both increased by approximately 50% (all $p < 0.05$). All joint power variability also increased by 50% or more on the uneven terrain condition (all $p < 0.05$).
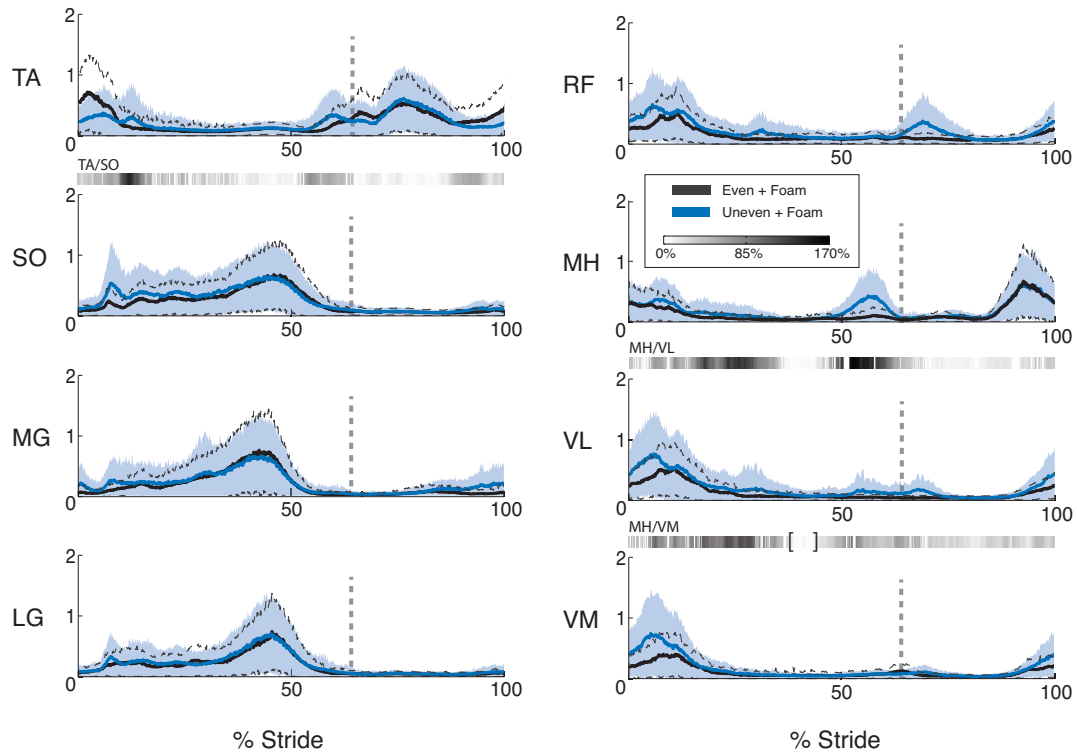
Figure 3.4: Averaged electromyographic (EMG) activity versus stride time for walking on even and uneven terrains. EMG data were normalized to the maximum activation of each muscle for each subject and plotted against % stride time for Uneven and Even terrain (both with Foam). Strides start and end at same-side heel-strikes; dashed vertical gray lines indicate toe-off. Envelopes indicate standard deviations for Uneven (shaded area) and Even terrain (dashed lines) conditions (both with Foam). Gray bars indicate statistically significant increases in mutual muscle contraction, with darker colors indicating larger percent increases, from even terrain mutual muscle contraction to uneven terrain mutual muscle contraction. Brackets indicate time of decreased muscle contraction. TA, tibialis anterior; SO, soleus; MG, medial gastrocnemius; LG, lateral gastrocnemius; VM, vastus medialis; VL, vastus lateralis; RF, rectus femoris; MH, medial hamstring.
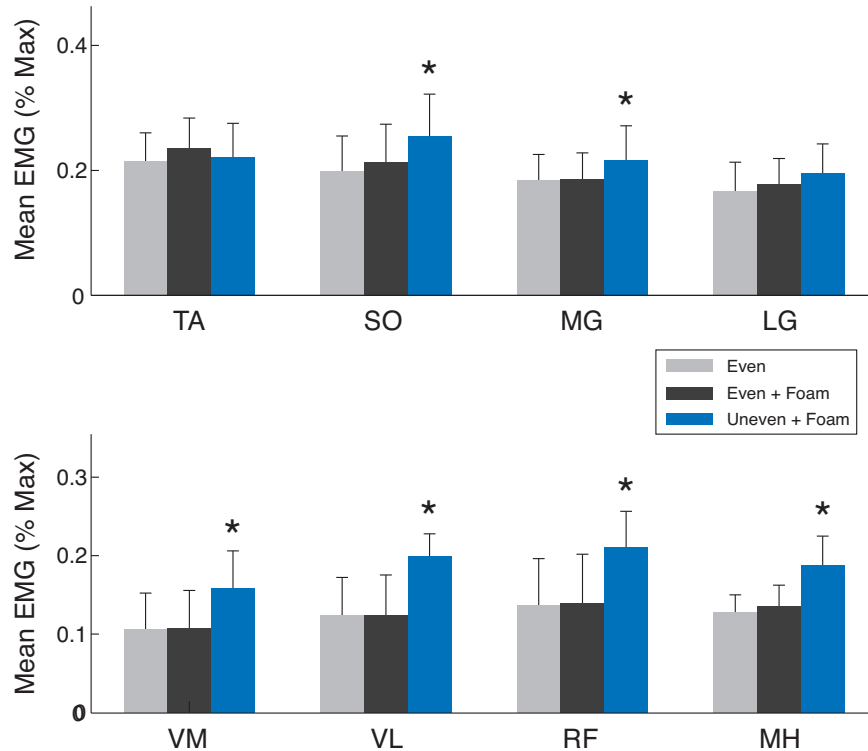
Figure 3.5: Mean rectified EMG activation values for walking on even and uneven terrains. Bars indicate standard deviation across subjects. Single asterisks denote statistically significant differences between the Uneven + Foam condition and the other two conditions. No statistically significant differences were found between the Even and Even + Foam conditions ($\alpha = 0.05$)

The biomechanical effects included greater joint work performed over a stride (Figure 3.3). There was a 0.0106 J/kg (28%) increase in positive knee work and a 0.0425 J/kg (26%) increase in negative knee work ($p = 0.011$ and $p = 0.0019$, respectively). Positive hip work also significantly increased by 0.1078 J/kg (62%; $p < 0.0001$). No statistically significant changes were found in positive or negative ankle work, or negative hip work.

3.3.2 Muscle Activation

Subjects showed increased muscle activity, variability of activity (Figure 3.4), and mutual contraction when walking on the uneven surface. There were significant increases in activation for six of the eight muscles measured (Figure 3.5). Averaged, normalized EMG values increased for all of the thigh muscles: VM, VL, RF and MH increased by 49%, 60%, 54% and 47%, respectively ($p < 0.05$). In the lower leg, SO muscle activity increased by 28%, while the MG muscle activity increased by 17% ($p < 0.05$). The remaining muscles, TA and LG, did not exhibit significant changes in mean activity across the stride, although TA appeared to have slightly decreased activity in the first 10% of stride.

	Even		Even + Foam		Uneven + Foam		p − value
	Mean	s.d.	Mean	s.d.	Mean	s.d.	
TA/SO	115.5	25.59	121.6	28.48	161.3*	38.70	0.0003
MH/VM	97.82	40.31	103.3	44.82	145.5*	52.82	0.0061
MH/VL	102.8	26.08	107.4	33.69	165.6*	40.41	0.0002

Table 3.2: Muscle mutual contraction over the entire stride for walking on even and uneven terrains. Values signify unit-less area under the minimum of the normalized EMG activation curves for the two muscles of interest. Three muscle antagonist pairs are compared: TA/SO for tibialis anterior/soleus, MH/VM for medial hamstring/vastus medialis, MH/VL for medial hamstring/vastus lateralis. Asterisks signify a statistically significant difference of the Uneven + Foam condition ($\alpha = 0.05$). Standard deviations indicate variation between subjects.

Variability of EMG increased significantly for nearly all muscles on the uneven terrain (Figure 3.4). On average, walking on uneven terrain resulted in a larger increase in variability (standard deviation of muscle activity) in the thigh muscles (mean 60% increase) than in the leg muscles (mean 30% increase). For the thigh muscles, RF and VL variability increasing over 80% ($p < 0.05$), and VM and MH muscles showed over 45% increases ($p < 0.05$). The SO, MG and LG muscles in the leg showed a minimum increase in standard deviation of 27%, and as much as 40% for MG ($p < 0.05$).

We also observed changes in co-contraction over the entire stride for all three pairs of antagonistic muscles (Table 2.2). However, upon breaking the stride down into 1% increments, mutual activation for the MH/VM and MH/VL muscle pairs appears to increase substantially only around mid-stance. The MH/VL muscle pair also shows a significant increase pre toe-off. The largest increase of mutual contraction of the TA/SO muscles was seen shortly after heel-strike (Figure 3.4).

3.3.3 Metabolic Energy Expenditure

Walking on the uneven terrain resulted in a significant increase in energy expenditure compared to the other surfaces (Figure 3.6). Net metabolic rate increased from 2.65±0.373 W/kg (mean±s.d.) to 3.38±0.289 W/kg ($p < 0.0001$), about 28%, from the even foam to uneven terrain. There was no difference between the energetic cost of walking on the even surface (mean metabolic rate of 2.53±0.282 W/kg) and the even foam surface ($p = 0.330$). Average standing metabolic rate was found to be 1.48±0.181 W/kg).
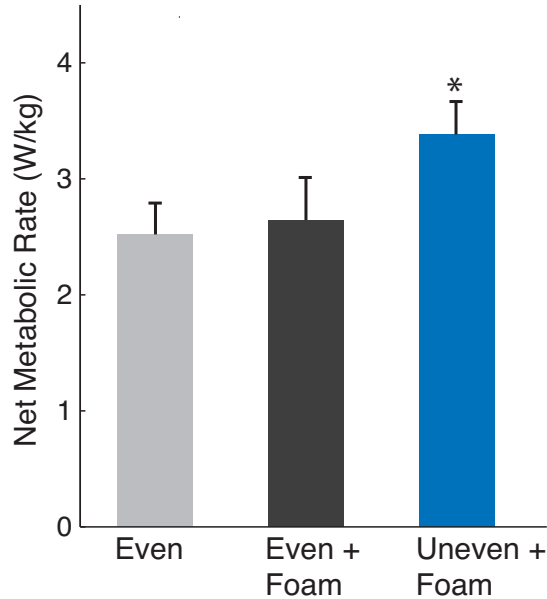
Figure 3.6: Net metabolic rate for walking on even and uneven terrains. Metabolic rates are normalized by subject mass. Values shown are averages over subjects, with error bars indicating standard deviations. Asterisk indicates a statistically significant difference between the Uneven + Foam walking condition and the other two conditions ($\alpha = 0.05$)

3.4 Discussion

On natural terrain, there are many surface properties that can dictate the metabolic cost of locomotion. Surface compliance and damping can affect locomotion energetics and dynamics (Ferris et al., 1998, 1999; Kerdok et al., 2002) as do surface inclines or declines (Margaria, 1976; Minetti et al., 1993). However, few studies have characterized the biomechanics and energetics of walking on uneven surfaces. We examined the effects of uneven terrain compared to smooth surfaces, and found a number of biomechanical factors related to energetic cost. Locomotion on terrain with a surface variability of only 2.5 cm resulted in a 28% increase in net metabolic cost. For comparison, this is approximately energetically equivalent to walking up a 2% steady incline (Margaria, 1968) and is likely comparable to natural terrain variation experienced when moving over trails, grass or uneven pavement.

We observed only modest changes in stepping strategy with uneven terrain. For example, average step length decreased by only 4%, and the increase in step width was not significant. Examination of previous studies on the effects of varying step parameters (Donelan et al., 2001; Gordon et al., 2009; O'Connor and Kuo, 2009) suggests that differences seen here are too small to have a substantial influence on energetic cost. However, we did observe a 22% increase in step length variability and a 36% increase in step width variability. As shown by others (Donelan et al., 2004; O'Connor et al., 2012), it is costlier to walk with
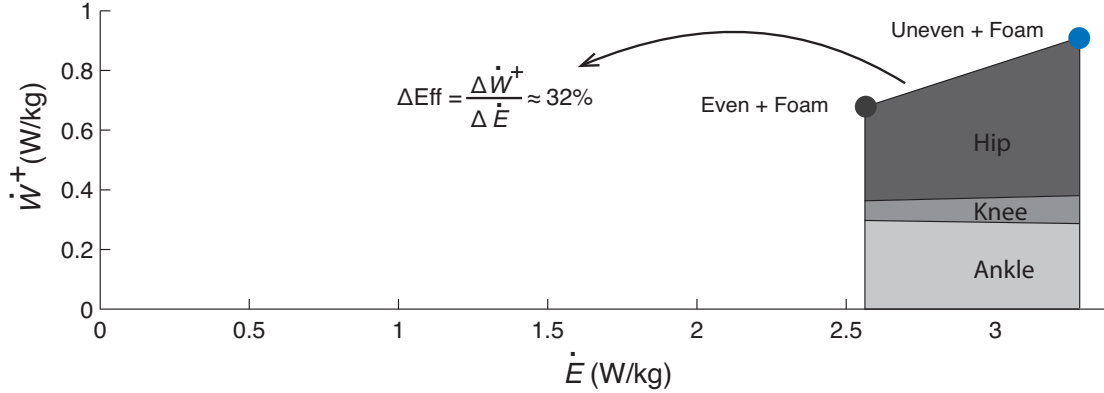
Figure 3.7: Delta efficiency (ΔEff) for walking on even and uneven terrains. Delta efficiency is defined as the ratio between differences in positive mechanical power and metabolic power ($\dot{W}^+$ and $\Delta\dot{E}$, respectively; plotted as filled circles, with units W/kg). Average joint power is shown for ankle, knee, and hip joints.

more variability (e.g. 65% greater step width variability results in 5.9% higher energetic cost), in part because increased step variability reduces the use of passive energy exchange and increases step-to-step transition costs. However, the differences we found in our study would not likely translate to large changes in energetic cost. Available evidence suggests that changes in step distances and variability could account for only a small percent of increased energy expenditure.

One of the biomechanical effects that might explain the energetic cost differences were the amount and distribution of work by lower limb joints. Work performed by the ankle over a stride did not change appreciably on the uneven surface, but the hip performed 62% more positive work and the knee 26% more negative work (Figure 3.3). The greater positive work at the hip occurred during mid-stance and also at push-off, as corroborated by increased medial hamstring and rectus femoris activity (Figs. 4 and 5). The hip accounted for nearly all of the increase in positive joint work. Changes in positive joint work relative to changes in metabolic energy cost yields a delta efficiency (ΔEff = $\Delta\dot{W}^+/\Delta\dot{E}$, where $\dot{W}^+$ is positive mechanical power and $\dot{E}$ is metabolic power) of about 32% (Figure 3.7). If all of the increased metabolic energy cost of walking on uneven terrain came exclusively from positive muscle work, then the delta efficiency would equal approximately 25% (Margaria, 1968). A very low efficiency would imply that energy is expended for costs other than work, such as increased co-activation and force of contraction. But the relatively high ΔEff observed here suggests that the cost of walking on uneven terrain may largely be explained by greater mechanical work, mostly performed at the hip.

By exceeding 25% delta efficiency, the data also suggest that not all of the changes in

joint positive work were due to active muscle work. Joint power trajectories (Figure 3.2) reveal that some of the positive hip work was performed simultaneously with negative knee work at toe-off (at about 60% of stride time). The rectus femoris muscle is biarticular and can flex the hip and extend the knee at the same time. It can thus produce both higher positive work at one joint and a greater negative work at the other, yet experience a smaller change in actual muscle work. In addition, some joint work may be performed passively through elastic energy storage and return by tendon, as has been implicated most strongly for the ankle (Sawicki et al., 2009) but also in the knee and hip (Doke and Kuo, 2007; Geyer et al., 2006). It is therefore likely that positive joint work is an overestimate of actual muscle work, which could explain the relatively high delta efficiency. It is nevertheless evident that there was substantially more positive work at the hip, even discounting hip power at toe-off. The work increase in the first half of stride is not easily explained by simultaneous negative work at another joint, nor by passive elastic work. It therefore appears that much of the increase in metabolic cost could still be explained by active joint work, at a more physiological efficiency.

A possible explanation for the joint work increase on uneven terrain is the timing of push-off and collision during walking. Push-off by the trailing leg can reduce negative work done by the leading leg if it commences just before heel-strike, redirecting the body center of mass prior to collision (Kuo, 2002; Kuo et al., 2005). Stride period was quite consistent on level ground, with variability of about 0.014 s, but increased by about 27% on uneven terrain. This may suggest greater variability in timing between push-off and collision, which may contribute to greater variability of joint power and muscle activity to compensate for collision costs (Figures 3.2 and 3.4, respectively). A more direct test would be to compare variations in consecutive push-off and collision phases. The present force data did not include consecutive steps, and so the proposed effect on redirecting the body center of mass remains to be tested.

Subjects also appeared to have modified their landing strategy following heel-strike. As an indicator of such adaptations, we examined the effective leg length during stance, defined as the straight-line distance from sacrum to calcaneous marker of the stance foot, normalized to subject leg length. The maximum effective leg length occurred immediately after heel-strike, and was reduced by about 2.4% on uneven terrain (mean±sd $=$ 1.140±0.028 for Even + Foam; 1.113±0.026 for Uneven + Foam; $p < 0.0001$). This may suggest that subjects adopted a slightly more crouched posture on uneven terrain, perhaps associated with increased EMG activity in the thigh muscles. Past research has suggested that vertical stiffness decreases with a more crouched posture, for both human running (McMahon et al., 1987) and walking (Bertram et al., 2002). A more crouched limbed posture on uneven terrain

might also increase compliance and provide a smoother gait, albeit at higher energetic cost. We also observed decreased tibialis anterior activation at heel strike, which may be associated with adaptations for variable conditions at heel-strike. These overall changes to landing strategy, along with increased variability in stride period duration, may have contributed to increased joint work and energetic cost during walking on uneven terrain.

There are other factors that may have contributed to the increased energetic cost of walking on uneven terrain compared to even terrain. Co-activation of muscles about a joint can lead to increased metabolic cost in human movement (Cavanagh and Kram, 1985). Although our data suggest an increase in mutual muscle contraction about the ankle and knee joints (Table 2.2), it is difficult to convert relative amounts of co-activation to a prediction of energetic cost. The increased vastus lateralis and vastus medialis activity during stance (Figs. 4 and 5) could also lead to greater energy expenditure. Although much of that cost could be quantified by knee power, production of muscle force may also have an energetic cost beyond that for muscle work (Dean and Kuo, 2009; Doke and Kuo, 2007). Although we cannot estimate a cost for co-activation or force production, it is quite possible that they contributed to the increased metabolic cost on uneven terrain.

There were several limitations to this study. A limitation of the data setup was the arrangement of the force plates during over-ground trials. Force plates placed consecutively would have allowed us to collect force data during consecutive steps and to analyze simultaneous work by the leading and trailing legs. Another limitation was that subjects walked at a controlled walking speed. This might have constrained their freedom to negotiate terrain by varying their speed. We also did not test a range of walking speeds to determine if uneven terrain causes an altered relationship between energy cost and speed. We also tested only one pattern and range of surface heights, with the expectation that greater height variation would largely have a magnified effect on energetics. Subjects were also given little time to become accustomed to the uneven terrain. We had assumed that everyday experience would allow them to adapt to uneven surface relatively quickly. There was also reduced ability for subjects to view the terrain surface ahead of them, due to the limited length of the treadmill. This did not seem to pose an undue challenge for the small perturbations here, but we would expect vision to be increasingly important with greater terrain variations (Patla, 1997).

This study characterizes some of the adaptations that might occur on uneven terrain. These include relatively minor adaptations in stepping strategy, increases in muscle activity, and additional work performed at the hip. A controlled experiment can hardly replicate the limitless variations of the actual environment, nor can it capture the entire range of compensations humans might perform in daily living. But this study does suggest that much of the energetic cost of walking on uneven terrain may be explained by changes in

mechanical work from lower limb muscles. As a result, these findings can potentially influence future designs of robotic exoskeletons used to assist with locomotion on natural surfaces, as well as the development of various legged robots. In addition, numerous studies have been done on the biomechanics and energetics of locomotion in humans and other primates with the intent of highlighting factors driving the evolution of bipedal locomotion (Pontzer et al., 2009; Sockol et al., 2007). Our findings highlight that rather small changes in terrain properties (about 2.5 cm terrain height variation) can have substantial impact on muscular work distribution across the lower limb. Thus, future studies should take into account how properties of natural terrain, such as terrain height variability and terrain damping (Lejeune et al., 1998), can influence potential conclusions relating locomotion biomechanics and energetics of bipedal evolution.

Acknowledgements

Funding

CHAPTER IV

Biomechanics and Energetics of Running on Uneven Terrain

Abstract

In the natural world, legged animals regularly run across uneven terrain with remarkable ease. To gain understanding of how running on uneven terrain affects the biomechanics and energetics of locomotion, we studied human subjects ($N = 12$) running at $2.3\,\mathrm{m/s}$ on an uneven terrain treadmill, with up to a $2.5\,\mathrm{cm}$ height variation. We hypothesized that running on uneven terrain would show increased energy expenditure, step parameter variability and leg stiffness compared to running on smooth terrain. Subject energy expenditure increased by 5% ($0.68\,\mathrm{W/kg}$; $p < 0.05$) when running on uneven terrain compared to smooth terrain. Step width and length variability also increased by 27% and 26%, respectively ($p < 0.05$). Positive and negative ankle work decreased on uneven terrain by 22% ($0.413\,\mathrm{J/kg}$) and 18% ($0.147\,\mathrm{J/kg}$), respectively ($p = 0.0001$ and $p = 0.0008$). Mean muscle activity increased on uneven terrain for three muscles in the thigh ($p < 0.05$). Leg stiffness also increased by 20% ($p < 0.05$) during running on uneven terrain compared to smooth terrain. Calculations of gravitational potential energy fluctuations suggest that about half of the energetic increases can be explained by additional positive and negative mechanical work for up and down steps on the uneven surface. This is consistent between walking and running, as the absolute increases in energetic cost for walking and running on uneven terrain were similar: $0.68\,\mathrm{W/kg}$ and $0.48\,\mathrm{W/kg}$, respectively. These results provide insight into how surface smoothness can affect locomotion biomechanics and energetics in the real world.

4.1 Introduction

Empirical measurements have documented that running on natural surfaces such as sand, grass or irregular trails requires greater metabolic energy expenditure than running on smooth hard surfaces (Jensen et al., 1999; Lejeune et al., 1998; Pinnington and Dawson, 2001; Zamparo et al., 1992). Such natural terrain has many mechanical properties that can influence running biomechanics. For example, humans and animals need to constantly adjust for changes in surface damping, compliance and smoothness during locomotion in the real world. To identify the energetic and biomechanical changes during running caused by increased surface height variability, we studied human running on an uneven surface designed to mimic natural terrain.

Step parameter adjustments are one potential factor that could contribute to increased energy expenditure during running on uneven terrain. In particular, humans adjust step width for maintaining lateral balance during walking (Hak et al., 2012; McAndrew et al., 2010) and could utilize the same strategy to improve running stability as well. A recent study showed that assisting with lateral balance during running resulted in reduced step width variability and energy expenditure in humans (Arellano and Kram, 2012). In contrast, if uneven terrain leads to increased step width variability, it may contribute to increased energetic costs to maintain balance.

Changes in surface height variability are likely to alter muscle activation patterns and mechanical work during running. Running on sand, for example, results in greater muscle activity, greater hip and knee motion, and greater positive mechanical work compared to running on a smooth flat surface (Lejeune et al., 1998; Pinnington et al., 2005). These changes are likely contributors to the increased energy expenditure for running on sand compared to a smooth, hard surface (Pinnington et al., 2005). In addition, we have previously found that human subjects showed greater hip and knee joint flexion motions during swing when walking on uneven terrain compared to even terrain (Voloshina et al., 2013). It is reasonable to expect similar modifications in swing leg dynamics for running on a similar uneven surface. In addition to increased muscle activity, running on the uneven surface may also disrupt patterns of muscle recruitment. Effective energy storage and return during locomotion requires muscle activation to produce a concerted contraction (Hof et al., 1983), or a contraction that minimizes the change in length of the muscle fiber and maximizes tendon and aponeurosis stretch and recoil. Because work produced from elastic energy storage and return contributes to about half of the total mechanical work performed during running (Cavagna et al., 1964), a reduction in elastic work would require increased muscle work and would be more energetically costly. As a result, these factors have the potential

to contribute to running energetic costs related to surface smoothness.

Leg stiffness is also likely to change with increased surface height variability. During human reaching in the presence of expected mechanical perturbations (Burdet et al., 2001; Franklin et al., 2007), arm stiffness tends to increase compared to reaching without perturbations. The nervous system may respond to expected lower limb perturbations similarly. In addition, Grimmer et al. have shown that human runners increase leg stiffness in anticipation of a single step-up when running on an uneven track (Grimmer et al., 2008). However, runners then decrease their leg stiffness for the actual step-up, possibly to smoothen out the perturbation to the center of mass trajectory. It is likely that runners would also adjust leg stiffness in response to running on uneven terrain.

In this study, we examined the energetic and biomechanical changes during running on uneven terrain when compared to running on smooth terrain. We used an uneven terrain surface that was attached to a standard exercise treadmill (Figure 4.1) to collect continuous energetic and kinematic data of human runners. We hypothesized that, on uneven terrain, subjects would show greater energy expenditure and step parameter variability. Based on previous research indicating increased limb stiffness under conditions of anticipated mechanical perturbations, we also expected runners to increase leg stiffness on uneven terrain compared to smooth terrain. Our overall objective was to provide insight into how the biomechanical adjustments lead to greater energy expenditure during running on uneven surfaces.

4.2   Methods

We modified a regular exercise treadmill by attaching an additional belt with wooden blocks of varying heights to the original treadmill surface. The blocks simulated an uneven surface on which subjects could run continuously while we collected biomechanical and metabolic data. Subjects also ran on a separate, smooth treadmill surface, resulting in two testing conditions termed 'uneven' and 'even.' For both surfaces the running speed was maintained at $2.3\,\text{m/s}$, while we collected kinematic, kinetic, metabolic and electromyographic data.

4.2.1   Subjects

Twelve young, healthy subjects participated in the study (7 male, 5 female; mean $\pm$ s.d.: age 24.3 ± 4.0 years, mass $68.6 \pm 7.1\,\text{kg}$ and height $175.5 \pm 7.1\,\text{cm}$). Subjects ran on the even and uneven surfaces during the same data collection. For running on both surfaces, we collected oxygen consumption ($N = 11$), step parameter data ($N = 12$), electromyographic
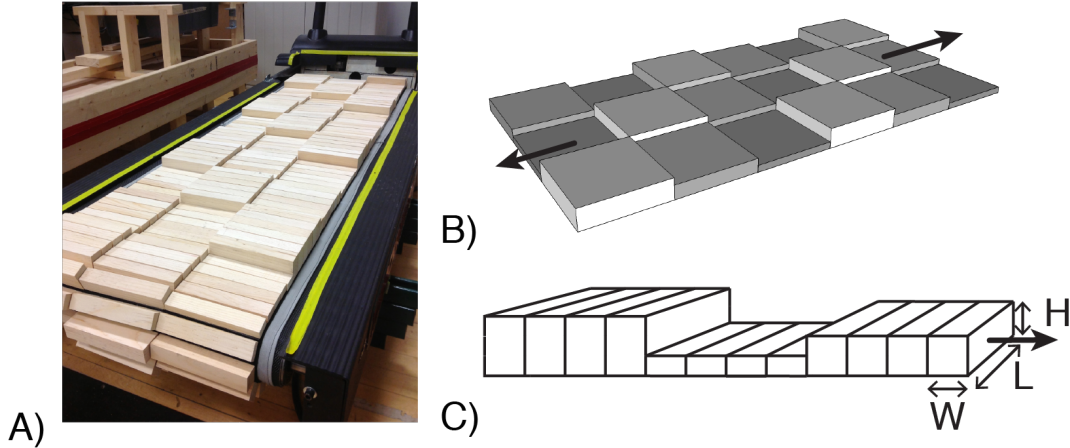
Figure 4.1: Uneven terrain treadmill for running. A) Uneven terrain treadmill used for the running studies. B) Schematic of the uneven surface, with stepping areas of three different heights (arrows indicate the treadmill's long axis). C) Close-up of the blocks comprising the stepping areas. Dimensions: H, 1.27 cm; L, 15.2 cm; W, 2.54 cm

data ($N = 10$) and joint kinematics and kinetics data ($N = 11$). Due to technical issues, some data were not collected for particular subjects, resulting in a value of N less than 12 in some data subsets.

Prior to the experiment, all subjects provided written informed consent. Experimental procedures were approved by the University of Michigan Health Sciences Institutional Review Board.

4.2.2 Running Surfaces and Trial Procedures

We created an uneven surface treadmill belt (Figure 4.1) that we attached to the regular treadmill belt of a modified exercise treadmill (JAS Fitness Systems, Trackmaster TMX22, Dallas, TX). To create the uneven surface belt, we sewed one side of the hook-and-loop fabric onto thick, non-stretch fabric. The other side of the hook-and-loop fabric was glued onto wooden blocks with a width of 2.55 cm, a length of 15.2 cm and of three varying heights (1.27, 2.54 and 3.81 cm). Then, we attached the blocks to the belt, oriented lengthwise across the belt. As a result, the blocks could curve around the treadmill rollers, due to their relatively short width. The blocks comprised 15.2 x 15.2 cm stepping areas (after Voloshina et al. (2013)), in a pattern that was difficult for subjects to adopt. We then placed the uneven surface belt on top of the regular treadmill belt and connected the ends of the second belt using zip-ties to form one continuous surface. Subjects also ran on a separate, custom-built in-ground instrumented treadmill (Collins et al., 2009). The even surface served as the control condition and allowed us to determine the biomechanical effects of the uneven

surface on gait biomechanics and energetics.

For both surfaces, subjects ran at a speed of 2.3 m/s and with the trial order randomized for every participant. Subjects participated in just one trial for each condition, with each trial lasting 10 min and with a minimum of 5 min rest allowed between trials. On both surfaces, subjects were instructed to run normally and not look down at their feet unless they felt it was necessary. Generally, subjects chose not to look at their feet during running. After the running trials were completed, subjects walked at 1.0 m/s for an additional 10 min on each surface, while we collected metabolic data to use as a comparison to our previous study on walking on uneven terrain (Voloshina et al., 2013). Subjects wore running shoes of their choice for the experiments.

4.2.3 Metabolic Rate

We measured the rate of oxygen consumption ($\dot{V}_{O2}$) for all running trials using an open-circuit respirometry system (CareFusion Oxycon Mobile, Hoechberg, Germany). We recorded respirometry data for all 10 min of the running and walking trials and also for 7 min during quiet standing prior to each data collection. We allowed subjects the first 7.5 min of the trial to reach steady-state energy expenditure and only used the last 2.5 min of data to calculate the metabolic energy expenditure rate of each subject. To find the metabolic rate, $\dot{E}_{met}$), we used standard empirical equations as described by (Brockway, 1987; Weir, 1949). The net metabolic rate was found by subtracting the standing metabolic power from the metabolic power of all running conditions. All net metabolic power was normalized by subject body mass (kg).

4.2.4 Kinetics and Kinematics

For both even and uneven conditions, we recorded the positions of 31 reflective markers using a 10-camera motion capture system (frame rate: 100 Hz; Vicon, Oxford, UK). We placed markers on the pelvis and lower limbs as described by (Voloshina et al., 2013) and taped them onto the skin or spandex shorts worn by the subjects. Although trials lasted for 10 minutes, the first 7.5 min allowed subjects to reach steady-state dynamics and we only used the last 2.5 minutes of data to calculate step parameters such as step width, length and height. For each subject and trial, the 2.5 minutes of data analyzed consisted of a minimum of 250 steps and up to 400 steps. To reduce motion artifact, we low-pass filtered all marker data at 6 Hz (fourth-order Butterworth filter, zero-lag). We defined step width, length and height as the distance between the lateral, fore-aft and vertical distances between the calcaneous markers on the two feet at their respective heel-strike instances. Step height

measurements were used only to determine changes in step height variability caused by the uneven surface. We calculated the effective leg angle as the angle relative to horizontal made by the straight-line distance from the greater trochanter marker to the calcaneous marker of the stance foot. The effective leg angle and the position of the calcaneous markers acted as a means to determine the time of heel-strike. This method of determining heel contact agreed well with the onset of the vertical ground reaction force. In addition, we normalized all measurements to subject leg length measured prior to each data collection and defined as the mean distance between the greater trochanter and calcaneous markers of both legs.

We recorded ground reaction forces using a custom-built in-ground instrumented treadmill (Collins et al., 2009) for the even condition and two in-ground force platforms for the uneven condition. For the uneven condition, we placed the treadmill on top of two supports, each of which rested solely on an in-ground force platform (sample rate: 1000 Hz; AMTI, Watertown, MA, USA). To obtain total ground reaction forces, we added the recorded forces from each of the force plates. For the even condition, subjects ran on one belt of the split-belt instrumented treadmill and we recorded only one set of forces (sample rate: 1000 Hz). Force platforms were re-zeroed prior to each trial. Force data used to determine the time of heel contact and to calculate the average vertical ground reaction forces for each subject, were low-pass filtered at 25 Hz (fourth-order Butterworth filter, zero lag). However, forces synced to kinematic data and used for inverse dynamics analysis were low-pass filtered at 6 Hz (fourth-order Butterworth filter, zero lag) due to the high noise sensitivity of the inverse dynamics calculations. We used Visual-3D (C-Motion, Germantown, MD, USA) to conduct inverse dynamics analysis and to determine joint angles, moments and powers in the sagittal plane for the stance limb. For both running conditions, we determined any position offset of the force vector relative to the running surface and corrected for its location in Visual-3D. For the even condition, this correction was minimal. However, for the uneven condition, the ground reaction force was measured across two force plates located substantially below the surface of the treadmill. To compensate for this, we transformed the measured forces and torques at the force platforms into a common reference frame with an origin at the height of the treadmill surface, and added them together. This introduced a small error into the inverse dynamics calculations, as the actual ground reaction force was applied on the terrain, which was up to 2.54 cm higher than the surface of the treadmill. We estimate the center of pressure error introduced by this simplification to be less than 1.5 cm based on projecting a force from the highest point on the terrain to the surface of the treadmill. Mean subject forces were normalized to subject weight and then averaged over subjects.

4.2.5 Electromyography

For all trials, we recorded and processed electromyography (EMG) signals as previously described by Voloshina et al. (2013). Bipolar surface electrodes (sample rate: 1000 Hz; Biometrics, Ladysmith, VA, USA) were placed over the belly of four lower leg and four thigh muscles. In particular, we recorded EMG data from the tibialis anterior (TA), soleus (SO), medial gastrocnemius (MG), lateral gastrocnemius (LG), rectus femoris (RF), vastus medialis (VM), vastus lateralis (VL) and the semitendinosus of the medial hamstring (MH) muscles of the right leg only. The surface electrodes had a diameter of 1.0 cm, an inter-electrode distance of 2.0 cm, and an EMG amplifier bandwidth of 20 Hz - 460 Hz. Only the last 2.5 min of data were used for analysis. EMG data were first high-pass filtered at 20 Hz (fourth-order Butterworth filter, zero lag) and then full-wave rectified. For each subject, we then averaged the data over steps to create EMG means for each muscle and normalized these means to the maximum mean value for the two running conditions to minimize inter-subject variability (Yang and Winter, 1984). These signals were then averaged over subjects to create representative EMG profiles. We also found the standard deviation of the EMG signal at each time point, for each subject. These standard deviations were also averaged over subjects, to create mean standard deviation envelopes for each running condition. Although variability in muscle activity cannot directly be related to changes in energy expenditure, it can demonstrate the amount of perturbation experienced due to uneven terrain. In addition, we quantified changes in muscle activation by averaging, over the stride time, the normalized subject EMG profiles for each subject and condition. These subject average values were then averaged over subjects to produce one mean value, for each muscle and condition, indicative of muscle activity. We also used the mean subject EMG profiles to calculate muscle mutual contraction (MC), or 'wasted' contraction as defined by (Thoroughman and Shadmehr, 1999), for three pairs of antagonistic muscles (SO/TA, MH/VM, and MH/VL):

$$\text{MC} = \int \min(f_1, f_2)\mathrm{d}t$$

such that f_1 and f_2 are the mean EMG profiles of the two antagonistic muscles and $\min(f_1, f_2)$ is the minimum of the two profiles at each time point (Voloshina et al., 2013). In other words, when mean EMG profiles from two muscles do not overlap, we can expect zero mutual contraction, whereas any overlap would produce a non-zero, shared activity level. We computed the integrals over the entire stride and in 1% increments, to determine where in the stride cycle mutual contraction occurred. The purpose of calculating mutual contraction was not to determine the amount of co-activation relative to what each muscle pair could have done during running, but to test for differences in co-activation strategies between the

two surfaces.

4.2.6 Leg Stiffness

In order to compare the sensitivity of our results, we calculated leg stiffness values using two methods. First, we reduced subject dynamics to that of a spring-mass model (McMahon and Cheng, 1990) and defined leg stiffness to be the ratio between the vertical ground reaction force and the change in effective leg length:

$$k_{max} = \frac{F_{max}}{\Delta L_{max}}$$

where the effective leg length was the straight-line distance from the greater trochanter marker to the fifth metatarsal marker of the stance foot, normalized to subject leg length. We defined ΔL as the difference in leg length at heel-strike and any other point during stance, such that maximum leg length deflection, ΔL_{max}, occurred near mid-stance when leg length was shortest. In addition, we defined, F_{max} as the maximum vertical ground reaction force after the impact force. We then calculated leg stiffness, k_{max}, for each stride as the ratio between the peak vertical ground reaction force and the maximum leg length deflection (Günther and Blickhan, 2002).

We used an alternate method for calculating leg stiffness as a means to ensure that methodology did not alter the conclusions of the study. We computed the second leg stiffness, k_{fit}, by finding a linear fit to the curve produced by plotting effective leg length against the vertical ground reaction force over a stride. The slope of this linear fit defined the approximate leg stiffness (Günther and Blickhan, 2002). For both calculations, we found leg stiffness at each step for every subject and then averaged the strides to find subject means for both running conditions. The mean inter-subject leg stiffness for each running surface was the average leg stiffness across subjects.

4.2.7 Data and Statistical Analyses

We defined variability for step parameters, joint parameters (consisting of joint angles, torques and powers) and EMG data as the average standard deviation of each parameter across subjects, per running trial. For example, for step parameter data, variability was calculated by averaging the standard deviation of consecutive step distances or periods over time for each subject, across subjects. Similarly, joint parameter and EMG variability were found by averaging the standard deviation of the parameter at each time point, per condition, across subjects. We then reported the mean variability (and the standard deviation of the variability over subjects) for each condition. We used repeated-measures ANOVAs to assess
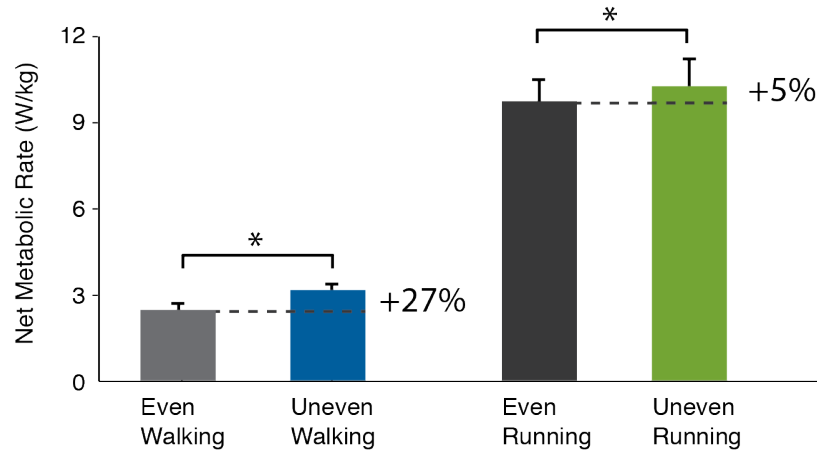
Figure 4.2: Net metabolic rate for running on even and uneven terrains. All net metabolic rates are normalized to subject mass and show the absolute changes in energetics when walking and running on uneven terrain compared to smooth terrain. Percentages indicate percent increases in energetic cost caused by uneven terrain when compared to even walking or running. Asterisks signify a statistically significant difference between the even and uneven walking and running conditions (*post hoc* pair-wise comparisons, $\alpha = 0.05$).

differences between conditions. The significance level, α, was set at 0.05, and *post hoc* Holm-Sidak multiple comparison tests were conducted where appropriate.

4.3   Results

Running on uneven terrain resulted in increased energy expenditure compared to running on smooth terrain. Several biomechanical adjustments contributed to this increase in energetic cost. Subjects did not exhibit changes in mean step parameters between the two conditions, but there were differences in step parameter variability. Joint angles, torques and powers were mostly unaffected by the terrain and only the ankle joint showed a significant decrease in joint power. In addition, we observed increased muscle activity in three proximal leg muscles (vastus medialis, rectus femoris, and medial hamstring), and increased muscle mutual contraction between the vastus medialis and medial hamstring muscles. Subjects also demonstrated higher leg stiffness when running on uneven terrain compared to smooth terrain.

4.3.1   Metabolic Energy Expenditure

Running and walking on the uneven terrain resulted in significant increases in energy expenditure when compared to running and walking on the even surface (Figure 4.2). During

	Even		Uneven		p − value	
	Mean(s.d)	Step.var.(s.d)	Mean(s.d)	Step.var.(s.d)	Mean	Step.var.
Width	0.055 (0.029)	0.022 (0.004)	0.059 (0.033)	0.028* (0.006)	0.353	<0.0001
Length	0.881 (0.051)	0.035 (0.009)	0.884 (0.044)	0.044* (0.011)	0.385	0.0002
Height	∼	0.004 (0.001)	∼	0.009* (0.002)	∼	<0.0001
Step period (s)	0.729 (0.041)	0.010 (0.003)	0.731(0.033)	0.013* (0.003)	0.427	0.0014

Table 4.1: Step parameters for running on even and uneven terrains. Parameters include step period and the mean step width, length, and height and their respective variabilities (all normalized to subject leg length, mean 0.944 m). Step variability is defined as the standard deviation of step distances over a trial, reported as a mean (±s.d.) across subjects. Asterisks signify a statistically significant difference between the even and uneven running conditions (*post hoc* pair-wise comparisons, $\alpha = 0.05$).

running, energetic cost increased from 9.72±0.65 W/kg to 10.2±0.94 W/kg ($p = 0.008$), or about 5% from even to uneven terrain. This percent increase in running energy expenditure was much lower than the percent increase found during walking on uneven terrain. In contrast to running, metabolic energy expenditure during walking on uneven terrain increased from 2.51±0.24 W/kg (mean±s.d.) to 3.19±0.14 W/kg ($p = 0.0004$), or by approximately 27%. This increase in metabolic cost was consistent with the 28% energy increase found in our previous study on walking on uneven terrain (Voloshina et al., 2013). This suggests that the biomechanical adaptations during walking in this study are likely the same as we have previously described, even though walking surfaces and subject footwear differed between the two studies. Although percent increases in energy expenditure were different between walking and running, the absolute increases in energetic cost were similar: 0.68 W/kg and 0.48 W/kg for walking and running, respectively. The mean standing metabolic rate was 1.46±0.17 W/kg.

4.3.2   Kinetics and Kinematics

We saw no changes in mean step parameters (width, length, height and period), although step variability increased for all parameters during running on uneven terrain compared to even terrain (Table 4.1). In particular, step width, length and height variability all increased significantly by approximately 27%, 26%, and 125% respectively ($p < 0.05$) on uneven terrain. In addition, step period variability on uneven terrain increased significantly by 30% ($p < 0.05$).

Subjects showed few changes in joint kinematics and kinetics during running on uneven terrain compared to even terrain, with most notable changes occurring at the ankle joint. During running on uneven terrain, joint angles in the sagittal plane showed slightly higher
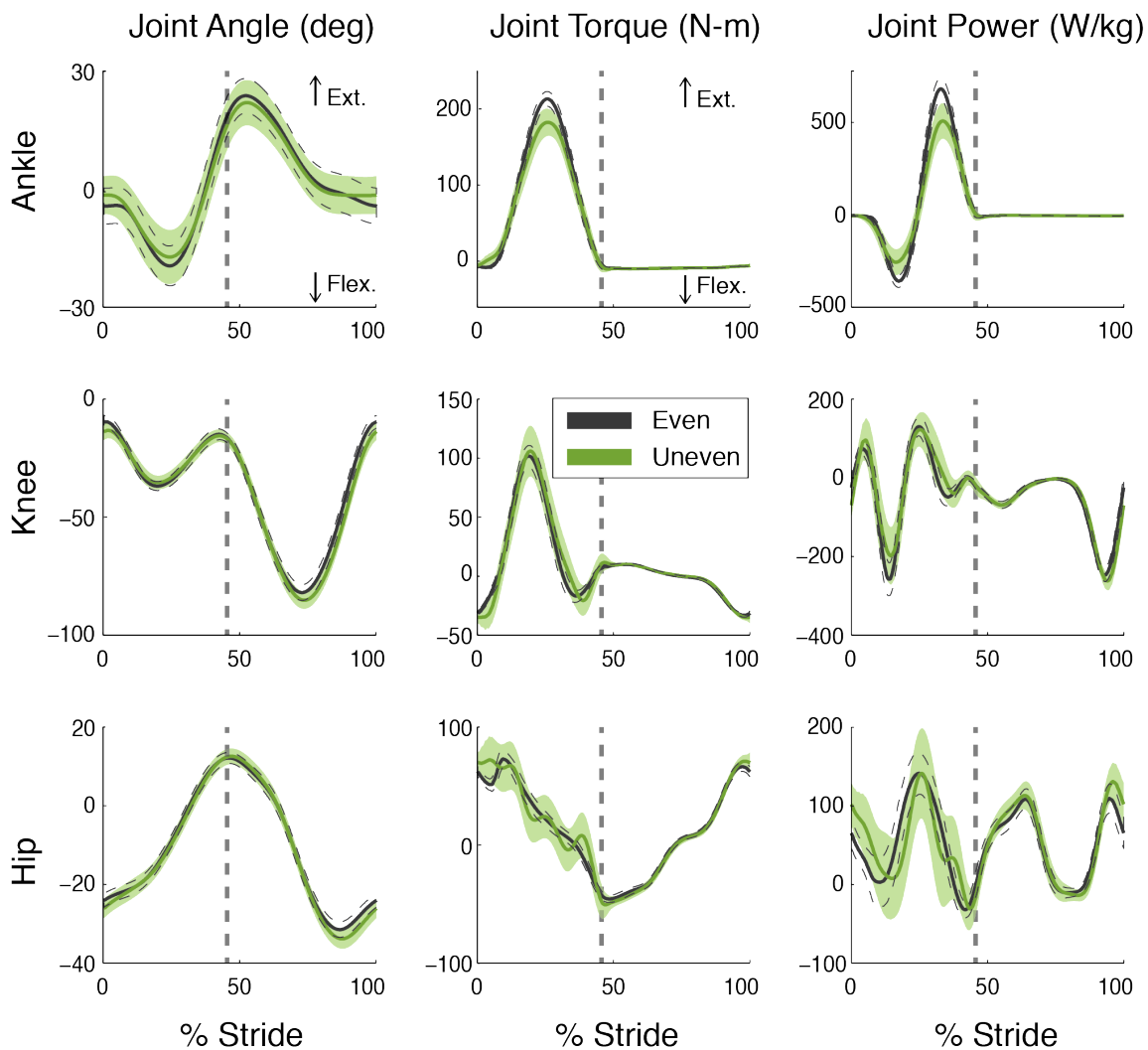
Figure 4.3: Joint angle, torque and power versus stride time for running on even and uneven terrains. Plotted in solid lines are the mean trajectories for the ankle, knee and hip against percent stride time for running during uneven and even terrain conditions. Shaded areas denote the mean standard deviation envelopes across subjects for the uneven condition; dashed lines for the even condition. Strides start and end at same-side heel-strike; dashed vertical gray line indicates toe-off.
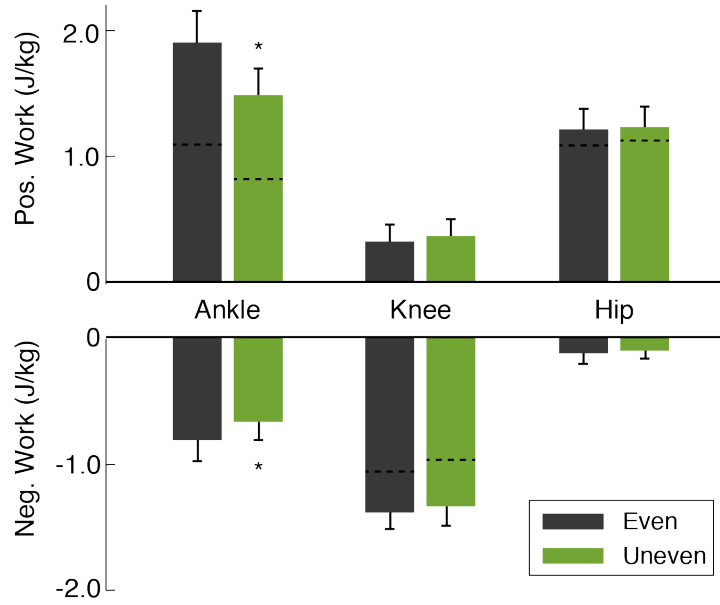
Figure 4.4: Joint work per stride for running on even and uneven terrains. Values are shown for positive and negative work for the three joints, with error bars denoting standard deviations. Dashed lines indicate net work for the specific joint and condition and asterisks signify a statistically significant difference between the even and uneven running conditions (post hoc pair-wise comparisons, $\alpha = 0.05$).

peak flexion angles in the knee and hip during mid-stance, possibly to allow for greater leg clearance (Figure 4.3). Qualitative examination of the ankle angle showed a slightly decreased range of motion on uneven terrain compared to even terrain, although subjects appeared to maintain a similar heel-strike footfall pattern on both surfaces. This reduced range of ankle motion suggests that subjects ran with slightly flatter feet when on uneven ground. The ankle joint also showed an approximately 14% decrease in peak joint moment, around mid-stance. In contrast, the knee and hip joints showed little change. Changes in joint power were only seen around the ankle and knee, with the two joints showing decreases in power around mid-stance (by 29 and 23%, respectively), when running on uneven terrain. Ankle power also decreased by 25% prior to push-off and at approximately 40% of stride time. The timing of toe-off with respect to stride timing did not differ between the two running conditions.

Joint motion variability was also greater on uneven terrain compared to even terrain (Figure 4.3). Surface unevenness increased ankle and knee angle variability by approximately 25%, and hip angle variability by 35% when compared to even terrain (all $p < 0.05$). Ankle moment variability also increased by about 60%, while knee and hip moment variability more than doubled on uneven terrain (all $p < 0.05$). Joint power variability increased by 50% for

the ankle and around 70% for the knee and hip (all $p < 0.05$).

Running on the uneven surface also affected amounts of positive and negative joint work done at the ankle (Figure 4.4). Positive ankle work decreased by 0.413 J/kg (22%) while negative ankle work decreased by 0.147 J/kg (18%; $p = 0.0001$ and $p = 0.0008$, respectively). Positive and negative joint work for the knee and hip were not statistically different between the two running conditions.

4.3.3 Muscle Activation

Subjects showed increases in muscle activity variability, mean muscle activity and muscle co-activation in the thigh muscles when running on uneven terrain compared to running on even ground (Figure 4.5). Significant increases in mean muscle activity were only noted in three of the thigh muscles; vastus medialis (VM), rectus femoris (RF) and medial hamstring (MH) activity increased by 7, 20 and 19%, respectively ($p < 0.05$). However, all muscles in the lower leg and the vastus lateralis (VL) showed no significant differences in mean muscle activity between conditions.

All but three muscles showed significant increase in EMG variability when running on the uneven terrain (Figure 4.5). Only two muscles in the lower leg and three muscles in the thigh showed increases in variability (standard deviation of muscle activity), with the mean increase in variability being slightly higher in the thigh muscles (mean 14% and mean 25% increase in the lower leg and thigh muscles, respectively). In the lower leg, both the soleus (SO) and lateral gastrocnemius (LG) showed 14% increases in standard deviation ($p < 0.05$), while the tibialis anterior (TA) and medial gastrocnemius (MG) showed no significant changes. For the thigh muscles, VM, RF and MH showed 15%, 35% and 26% increases in muscle variability, respectively ($p < 0.05$).

	Even		*Uneven*		*p − value*
	Mean	*s.d.*	*Mean*	*s.d.*	
TA/SO	105.7	36.34	109.5	32.83	0.6527
MH/VM	106.4	28.05	134.7*	34.31	0.0168
MH/VL	123.3	66.60	125.5	28.02	0.9244

Table 4.2: Muscle mutual contraction over the entire stride for running on even and uneven terrains. Values signify the dimensionless area under the minimum of the normalized EMG curves for the two muscles of interest. Three muscle antagonist pairs are compared: tibialis anterior/soleus (TA/SO), medial hamstring/vastus medialis (MH/VM), medial hamstring/vastus lateralis (MH/VL). Standard deviations are calculated across subjects. Asterisks signify a statistically significant difference between the even and uneven running conditions (post hoc pair-wise comparisons, $\alpha = 0.05$).
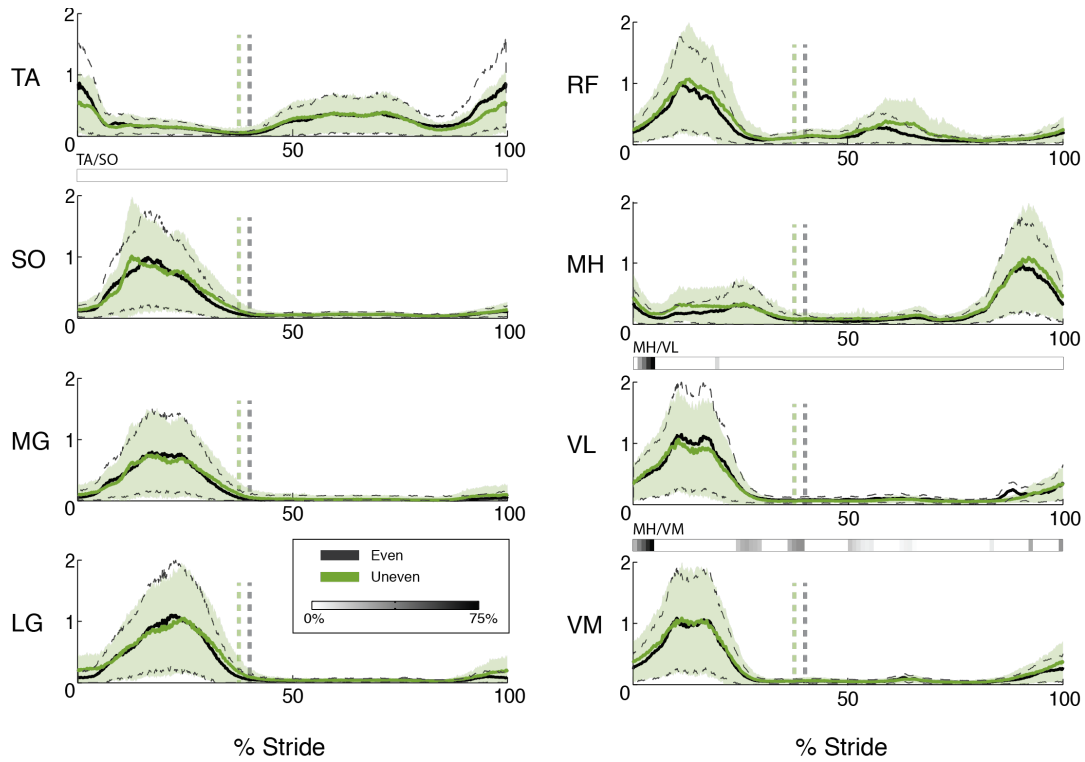
Figure 4.5: Averaged electromyographic (EMG) activity versus stride time for running on even and uneven terrains. All EMG profiles were normalized to the maximum mean muscle activity over the two running conditions, for each muscle and subject. Strides start and end at same-side heel-strikes. Dashed vertical gray line indicates toe-off. Shaded areas denote the mean standard deviation envelopes across subjects for the uneven condition; dashed lines for the even condition. Gray bars indicate statistically significant increases in mutual muscle contraction, with darker colors indicating larger percent increases from the even to the uneven running condition. TA, tibialis anterior; SO, soleus; MG, medial gastrocnemius; LG, lateral gastrocnemius; RF, rectus femoris; MH, medial hamstring; VL, vastus lateralis; VM, vastus medialis.
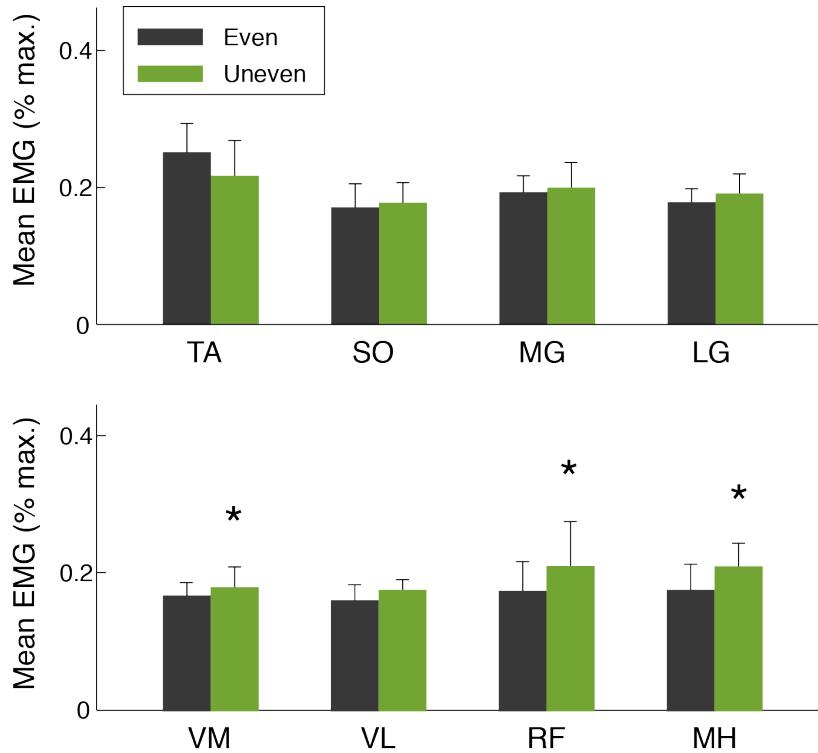
Figure 4.6: Mean rectified EMG activation values for running on even and uneven terrains. Mean subject EMG profiles were first normalized to maximum mean muscle activity over the two running conditions, for each muscle and subject, and then averaged over stride time to produce subject average EMG activity values. Subject average EMG activity was then averaged over subjects to produce mean EMG activity values. Bars indicate standard deviation across subjects. Asterisks signify a statistically significant difference between the even and uneven running conditions (post hoc pair-wise comparisons, $\alpha = 0.05$).

Out of the three pairs of antagonistic muscles, we observed increased muscle co-activation over the entire stride only in the MH/VM muscle pair (Table 4.2). However, when we broke down the stride into 1% increments, we noticed significant increases in muscle co-activation in the first 5% of the stride in the MH/VL muscle pair as well. Similarly, the MH/VM pair showed increased muscle co-activation during the first 5% of the stride but also slightly before and during toe-off. The muscle pair also demonstrated increased muscle co-activation during swing, although, due to minimal muscle activity of the two muscles during this time, these increases are likely inconsequential. The TA/SO muscle pair showed no significant increases in muscle co-activation at any point in the stride (Figure 4.5).
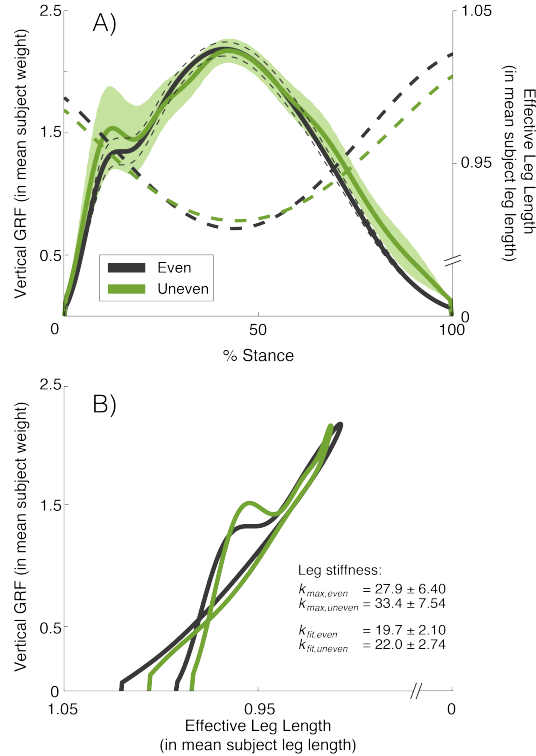
Figure 4.7: Vertical ground reaction forces, effective leg length and leg stiffness calculations for running on even and uneven terrains. A) Mean vertical ground reaction forces normalized to subject weight, in solid lines, and effective leg lengths normalized to mean subject leg length, in thick dashed lines, versus stance duration for running on even and uneven terrain. Shaded area denotes the mean standard deviation envelope across subjects for the vertical ground reaction force on the uneven condition; thin dashed lines indicate the envelope for the even condition. B) Normalized vertical ground reaction force plotted against the normalized effective leg length for the two running conditions. Mean leg stiffness values presented for two leg stiffness calculation methods: k_{max} equals the maximum force divided by the maximum leg length displacement and k_{fit} is the slope of the linear fit to the leg stiffness curve. Standard deviation values are across subjects.

4.3.4 Vertical Ground Reaction Forces and Leg Stiffness

Vertical ground reaction forces, normalized to subject weight, remained largely unchanged for running on uneven terrain compared to even terrain (Figure 4.7A). The maximum force, fmax, occurred around 40% of stance and had an average peak at 2.19±0.11 (mean±s.d.; dimensionless; $p = 0.753$). The peak maximum force was not statistically different for the two running conditions. However, the impact peak increased by approximately 17% (from 1.34±0.19 to 1.57±0.25; dimensionless) when running on uneven terrain compared to even terrain ($p = 0.0002$). In addition, vertical ground reaction force variability more than tripled when running on uneven terrain ($p < 0.05$).

Subjects ran in a slightly more crouched posture when on uneven terrain compared to

running on the even surface (Figure 4.7A). Subjects contacted the ground at heel-strike with a more bent leg, and hence a shorter leg length (0.992 ± 0.022 and 0.984 ± 0.022 for even and uneven terrains, respectively; dimensionless; $p = 0.0018$), defined as the straight-line distance from the greater trochanter marker to the fifth metatarsal marker of the stance foot and normalized to mean subject leg length. Similarly, leg length before toe-off decreased significantly from 1.02 ± 0.011 to 1.01 ± 0.015 (dimensionless; $p < 0.0001$). In addition, the minimum leg length during mid-stance was longer on uneven terrain (0.907 ± 0.014 and 0.912 ± 0.015 for even and uneven terrains, respectively; dimensionless; $p=0.0041$). This resulted in a 15% decrease in the maximum change in leg length, from 0.085 ± 0.023 on even ground to 0.072 ± 0.019 on uneven terrain (dimensionless; $p<0.0001$).

Primarily due to different leg length dynamics, subjects ran on stiffer legs when running on uneven terrain compared to running on even ground (Figure 4.7B). Using the more traditional leg stiffness calculation (defined as the ratio between the maximum vertical ground reaction force and the maximum leg length displacement), we found a 20% difference in leg stiffness between the two surfaces (from 27.9 ± 6.40 on even to 33.4 ± 7.54 on uneven terrain; dimensionless; $p < 0.0001$). Similarly, the second leg stiffness calculation (defined as the linear fit to the vertical ground reaction force versus leg displacement) showed a 10% increase in leg stiffness (from 19.7 ± 2.10 on even to 21.8 ± 2.74 on uneven terrain; dimensionless; $p < 0.0001$).

4.4   Discussion

In this study we quantified the changes in energetics and biomechanics between running on uneven terrain and on flat, smooth terrain. Our findings supported our hypotheses, primarily that running is more energetically costly on uneven terrain compared to even terrain. However, this increase was much smaller than the increase caused by the same surface during walking. More specifically, we found a 0.68 W/kg (27%) increase in metabolic cost during walking and a 0.48 W/kg (5%) increase during running. Although the percent changes were quite different between the two locomotion types, it is important to note that the absolute increases were very similar. These absolute energetic increases could be related to the total mechanical energy fluctuations caused by the uneven surface. For example, running uphill and downhill for an equal distance would result in greater energy expenditure than running on level ground for the same total distance (Margaria, 1968). If we equate the uneven surface to a series of steps up and down an incline, it would be reasonable to expect an increase in energy expenditure as well. If we consider the mean step length of our runners (0.884 m) and the maximum step height change of the uneven terrain (0.025 m), our

uneven terrain surface would be roughly equivalent to running up and down a 1.6% incline. In addition, we could expect this incline to result in an energy increase of approximately 0.35 W/kg (Margaria et al., 1963). However, the true energetic increase due to incline variations is likely much smaller. This suggests that other factors, other than changes in mechanical work, contribute to energy expenditure on uneven terrain during running.

As expected, we saw changes in step length and width variabilities across the two surfaces. Running on uneven terrain, runners showed 33% and 26% increases in step width and length variability, respectively ($p < 0.05$). This is consistent with past research, which has shown that challenges to locomotor stability tend to produce more step variability during walking (Thies et al., 2005; Voloshina et al., 2013). Greater step variability during walking also seems related to active stabilizing adjustments for maintaining lateral balance (Bauby and Kuo, 2000; Donelan et al., 2001). In contrast, during running humans tend to prefer narrow step widths close to the midline of the body (Cavanagh, 1987). This is because narrow step widths result in less lateral moments about the center of mass and tend to reduce energetic cost compared to larger step widths. Based on previous research (Arellano and Kram, 2011), reducing step width and step width variability during running led to a reduction in energy expenditure. However, our subjects only showed a 27% increase in step width variability and no change in the mean step width. These changes are relatively small and nowhere near the magnitude necessary to produce a 5% increases in energy expenditure (Arellano and Kram, 2011). This suggests that the energetic increase caused by changes in step parameters was negligible.

A significant finding of our study is that the absolute changes in energetic cost are independent of locomotor gait. Although percent increases in energetic cost were significantly different (27% and 5% for walking and running, respectively) the absolute changes were relatively close (0.68 W/kg and 0.48 W/kg for walking and running, respectively). The similar absolute changes for walking and running suggest that the dominant factor responsible for increases in metabolic cost during locomotion on uneven surfaces may be related to surface height variability and the corresponding vertical motion of the center of mass. It would be interesting to examine a range of surface height variabilities and their effects on walking and running energetics. This could provide insight into whether walking and running have similar biomechanical mechanisms responsible for energetic cost differences.

Another important finding of this is study is that the lower limb joints that compensate for locomotion on uneven terrain are very different between walking and running. During walking, ankle joint dynamics remain invariable while the knee and hip joints compensate with greater positive work production (Voloshina et al., 2013). In contrast, running on uneven terrain only significantly affects work done at the ankle joint. The most likely expla-

nation for this contrast in joint kinetic adaptations is the reliance on different biomechanical mechanisms for the two gaits. Running can be compared to a spring-mass system, with the lower limb functioning together as if it were a single compression spring (Farley and Ferris, 1998; McMahon and Cheng, 1990). In contrast, walking has inverted pendulum dynamics with differentiation by joint that is unlike running (Farley and Ferris, 1998; Alexander, 1992; Kuo, 2001; McGeer, 1990a). These differences in fundamental dynamics suggest that each gait has different benefits and drawbacks to joint specific adaptations on uneven terrain.

The decrease in ankle work seen during running on uneven terrain compared to even ground is likely due to the high load sensitivity of the ankle joint. Muscles at the distal joints rely on high-gain proprioceptive feedback and are often the first to encounter perturbations due to uneven terrain (Daley and Biewener, 2006). In contrast, the more proximal knee and hip joints are largely feed-forward controlled. This control strategy improves running stability by maintaining consistent limb cycling but has a more pronounced effect on the distal joints (Daley et al., 2007). In addition, we saw a small reduction in the ankle range of motion, which could have also led to a reduction in joint work. This reduction in ankle motion likely stabilized the joint in response to the unpredictable running surface. However, it could have also led to a reduction in energy storage and return in the Achilles tendon, leading to reduced work at the ankle joint. Recently, a number of research groups have demonstrated that ultrasound imaging can track both muscle fiber and tendon displacements during human running. Future experiments using ultrasound imagining could provide greater insight into the muscle-tendon mechanics on uneven terrain.

In conjunction with our hypotheses, subjects exhibited greater leg stiffness when running on uneven terrain compared to even terrain. There were changes in muscle co-activation but they were small in magnitude and were likely not the major drivers of leg stiffness adjustments across the surfaces. Vertical ground reaction force profiles were also largely unchanged, with only the impact peak magnitude increasing by 17%. This increase suggests that subjects landed with a higher contact force, likely due to flatter feet at ground contact. However, the main cause of increased leg stiffness is the change in lower limb posture. When running on uneven terrain, subjects contacted the ground at heel-strike with a shorter leg length, had a longer leg length during mid-stance, and a shorter leg length at toe-off. This change in posture, and in turn of leg stiffness, can be the result of several factors. Previous research on upper limb movements has shown that humans tend to stiffen their joints when presented with unfamiliar tasks, likely in anticipation of potential perturbations. Similarly, (Blum et al., 2007) have shown that a more crouched leg posture during avian running may be an adaptation mechanism, as it allows for lengthening and shortening of the limb. As a result, the more crouched running posture and overall larger leg stiffness on uneven terrain

is likely an adaptation response to an unfamiliar environment. In future studies, it may be interesting to look into the changes in leg stiffness throughout training periods, where subjects are allowed to become familiar with the surface over longer periods of time.

This study had several limitations related to kinetic measurements. The accuracy of the force measurements during uneven terrain running was one such limitation. As described previously, the uneven terrain treadmill was placed atop two supports, each of which was placed on top of a force platform. The forces recorded from each platform were then added together to obtain the total ground reaction forces. The treadmill was not rigidly attached to the supports and there was some slack in the belt to which the uneven surface was attached. As a result, the force data were noisier than data collected with our in-ground, instrumented treadmill. To account for the additional noise, we low-pass filtered the ground reaction force data using a cutoff frequency of 6 Hz, rather than a more traditional cutoff frequency of 25 Hz. We used the same filtering techniques for both surface conditions. To test the validity of comparing running on these different experimental setups, we compared a representative subject running on the in-ground instrumented treadmill to the same subject running on the regular treadmill on supports with a bare belt. Average peak vertical and anterior-posterior ground reaction forces, as well as average peak ankle moments, were within 4% of each other and highly correlated (i.e. R > 0.997). Mean center of pressure trajectories on the regular treadmill were also within 6% of mean center of pressure trajectories recorded on the instrumented treadmill. For the uneven surface, the terrain attached to the supported treadmill likely introduced additional variability to calculations of the center of pressure, because foot orientation during ground contact is highly variable on uneven terrain. However, this error would have been multidirectional and likely did not affect the mean results of the inverse dynamics calculations. Instead, the main effect on the inverse dynamics calculations would have been increased variability in parameters throughout the stance phase. Examination of standard deviations in the ankle profiles in (Figure 4.3) show slightly greater variability in the ankle moment calculations but increased variability is also present in the ankle angle data. The ankle angle data are independent of center of pressure calculations, so similar changes in variability seen in other parameters suggest that the effect of the center of pressure variability from the uneven terrain surface was not large.

Another limitation of the study was that subjects ran at only one prescribed speed. They could not negotiate the terrain by altering their speed as is possible when running on natural surfaces. We chose a slow running speed to maximize our subjects' comfort level and did not test a range of speeds. Running at faster speeds could have resulted in more pronounced biomechanical differences. We also tested only one pattern of stepping areas and one range of surface heights for the uneven terrain surface. However, since subjects did not appear to

get accustomed to the surface, we do not believe the inherent pattern of the uneven terrain affected gait dynamics. Larger surface height variability would have likely caused amplified biomechanical and energetic effects.

Additional limitations relate to subject training and the inherent difference between treadmill and overground running. For one, subjects were also not allowed multiple days to train and adjust to the terrain. It may be helpful in future studies to determine if there are long-term adaptation effects. In addition, subjects ran with a limited visibility of the terrain due to the length of the treadmill. All subjects were comfortable running on the treadmill and did not appear to be affected by limited visibility. However, it is possible that subjects may negotiate the terrain differently if more visibility were allowed. For overground locomotion, runners typically have extended visual feedback on the terrain and may choose different paths and foot placements in response to terrain properties.

In summary, we found that changes in mechanical work can explain approximately half of the energetic cost increase when running on uneven terrain surfaces compared to flat, smooth surfaces. The other half of the energetic cost increase may be related to less efficient energy storage and return in elastic tendons and ligaments. Future studies using ultrasound imaging could provide greater insight into muscle fiber and tendon dynamics on various terrains. We did find that human runners did not vary mechanical work done at their knee and hip joints when running on uneven terrain compared to smooth terrain. Instead, subjects reduced limb mechanical work done at the ankle joint when running on the uneven surface. Using a similar control approach for legged robots with biomimetic limb architectures might have benefits in increasing the relative stability of running as it alters the limb biomechanics closest to the foot-ground interface (Daley et al., 2007).

Acknowledgements

Funding

<div align="center">

CHAPTER V

The Cost of Walking on Uneven Terrain: a Model-based Analysis

</div>

Abstract

Human bipedal walking on uneven terrain is energetically expensive compared to walking on smooth terrain despite relatively minor changes in gait biomechanics between the different surfaces. We examined the mechanics of two simple models of walking (the rimless wheel and simplest walker) moving across uneven and smooth terrains to provide insight into the energetics of human locomotion. We performed analytical and numerical analyses of model biomechanical and energetic changes across up and down steps of equal magnitude. Our models demonstrated that the most energetically expensive gaits are those that maintain equal step durations for both up and down steps, regardless if powered by trailing limb push-off or leading limb hip work. We found that model predictions were within reason of biological data, and the results supported the conclusion that humans rely on energetically expensive hip work when walking on uneven terrain compared to smooth terrain. These findings provide insight into human gait in real world environments and could prove useful in the future design and control of bipedal robots.

5.1   Introduction

It is energetically more expensive for humans to walk on natural, complex terrain than on hard, flat surfaces typical of human-made environments. This greater energetic cost occurs during locomotion on uneven ground and on other unstructured surfaces, such as sand or snow (Davies and Mackinnon, 2006; Pandolf et al., 1976; Pinnington and Dawson, 2001; Soule and Goldman, 1972). Terrain unevenness, damping, stiffness, friction, and other

surface characteristics all affect gait biomechanics and can lead to increased metabolic costs. Surface unevenness, in particular, leads to increases in positive work at the hip and knee joints, which have been implicated as the main contributors to greater energy expenditure (Voloshina et al., 2013). Understanding the underlying mechanisms responsible for increased metabolic cost on unstructured terrain can potentially influence future designs of robotic exoskeletons, help with the development of various legged robots, and even influence clinical intervention during gait rehabilitation (Ferris et al., 2007; Gregorczyk et al., 2010).

A multitude of factors could contribute to the greater metabolic energy expenditure for walking on uneven terrain compared to on a smooth surface. Certain surface properties simply require more negative work to be performed against the ground or decrease the efficiency of the positive work produced. Walking on energy-dissipating surfaces, such as sand, requires more positive mechanical work than walking on hard surfaces (Lejeune et al., 1998). Locomotion on unstructured terrain also requires more effort for active gait stabilization. Empirical data and computational models have shown that, whereas fore-aft movements are stabilized passively, active stabilization is required in the lateral directions during human gait (Bauby and Kuo, 2000; Donelan et al., 2001). In addition, walking on uneven terrain results in more variable step widths and lengths compared to even terrain (Voloshina et al., 2013). Such gait adaptations have been shown to increase metabolic effort on smooth flat surfaces (O'Connor et al., 2012). Other adaptation examples may include increased ground clearance, changes in joint work distribution, or a more crouched posture. However, adaptations do not necessarily need to manifest themselves kinematically. Increased muscle co-activation, for example, could contribute to greater energy expenditure during walking on uneven terrain without changes in joint kinematic patterns. Less secure surfaces, such as a slippery walkway or railroad ballast, affect gait stability and lead to increased muscle co-activation about various joints (Cappellini et al., 2010; Wade et al., 2010). In our previous work, we have shown that walking on uneven terrain has resulted in slightly greater muscle co-activation between several pairs of antagonistic muscles in the leg, compared to walking on smooth terrain (Voloshina et al., 2013). Similar responses have also be noted when humans encounter unexpected drops in surface height (Nakazawa et al., 2004). It is possible that these changes occur to improve joint stability and that humans stiffen up joints preemptively to prepare for possible falls. Although it is difficult to quantify how changes in muscle co-activation relate to increased energy expenditure, it is reasonable to assume that additional muscle activity is a contributing factor. Because humans make multiple gait adaptations to terrain at the same time, it is very difficult to distinguish the specific effects of each adaptation on energetics in experimental studies.

One way of investigating the effect of terrain on gait energetics is through a model-based

analysis that focuses on one single gait characteristic. In this study, we aimed to isolate the effects of just one surface parameter (surface unevenness) on the mechanical and energetic aspects of gait. One possible reason for greater effort on uneven terrain is the need to perform additional work on the center of mass to move up and down an obstacle. Although net mechanical work will average to zero over multiple steps, displacing mass up and down requires positive and negative mechanical work, respectively. Both types of work require a net *positive* metabolic effort, so the amount of metabolic energy used for locomotion goes up. Margaria (1968) showed that when humans walk up and down inclines, they perform positive work with a 25% efficiency and negative work with a -120% efficiency. If we approximate uneven terrain walking to a series of up steps followed by an equal series of down steps, roughly equivalent to walking up and down inclines, then we can expect the energetic cost of walking on uneven terrain to increase linearly with drop height.

In a simple model analysis of moving the center of mass up and down obstacles, we assume no prior knowledge of the terrain and no ability to adapt to the encountered perturbations. It is possible that other mechanisms of mitigating fluctuations in potential energy might be used to compensate for uneven terrain. These mechanisms could include kinematic adaptations, increased energy loss at collision, and fluctuations in kinetic energy. However, an important issue in the gait dynamics is that the mechanical effects of active push-off by the trailing limb and collisions at heel-strike by the leading limb are highly sensitive to the relative timing of these events (Kuo, 2002). Unperceived terrain irregularities can disrupt this timing, which might increase energy consumption through the need for costly hip work (Kuo et al., 2005). The increase in energy expenditure during locomotion on uneven terrain is likely nonlinear, requiring a good understanding the dynamic processes that govern the energetics of walking.

To this end, we investigated two simple models of legged locomotion crossing uneven terrain. We used the rimless wheel (McGeer, 1990b) and the powered simplest walker (Alexander, 1995; Garcia et al., 1998; Kuo, 2001). We approximated uneven terrain by a surface that consisted of alternating up and down steps of equal height. Both models were driven by impulsive push-off and hip work. Although the surface used in this study was not as variable as natural terrain, using various combinations of push-off and hip work to power gait allowed us to mimic the unpredictability of natural surfaces. We analyzed analytically the effects of terrain irregularity on step timing and average forward velocity, and numerically simulated a range of compensatory strategies. We derived energetic predictions from these strategies and evaluated the strategies for both models. We then compared our results with empirical data from a previous study. Together, these analyses provide a clearer understanding of the bipedal adaptation methods on uneven terrain and their energetic consequences.

5.2   Model-based Predictions of Metabolic Effort

Moving up or down a step with height d changes the amount of potential energy stored in the center of mass (COM) of a legged system. If the overall motion is not adjusted to accommodate for the change in height, the COM will be displaced by a vertical distance d and the potential energy will change by $\Delta E = mgd$ (with m being the total system mass and g being gravitational acceleration). If we further assume that the velocity is not adjusted for each step, then the kinetic energy must remain the same and energetic fluctuations ΔE must be created by a mechanical work W performed over the course of the step:

$$W = mgd. \tag{5.1}$$

Humans perform positive and negative work with a 25% and -120% efficiency (Margaria, 1968). Approximating an uneven terrain by a series of alternating up and down steps (with height d), we can use this to compute an *average* amount of metabolic energy E_{met} used per step:

$$
\begin{aligned}
E_{met} &= \frac{1}{2} \left(\frac{mg\,(+d)}{0.25} + \frac{mg\,(-d)}{-1.2} \right) \\
&= 2.42 \cdot mgd.
\end{aligned}
\tag{5.2}
$$

In addition, if the average step length on even ground is given by x_e, we can directly compute the increase in the metabolic cost of transport (COT), ΔCOT_{met}, according to:

$$\Delta COT_{met} = \frac{E_{met}}{mgx_e} = 2.42 \frac{d}{x_e}. \tag{5.3}$$

However, the assumptions made above are not very reasonable. When humans move over a series of up and down steps, they adjust their motion to compensate for the unevenness of the terrain. This means that fluctuations in potential energy are accommodated in a different manner than through direct work. For example, one could slow down while stepping up and speed up when stepping down, thereby converting potential energy into kinetic energy. Similarly, one could take advantage of collisions to perform negative work passively rather than absorbing negative work through muscle effort. We examined these and other strategies using two simple models of locomotion.
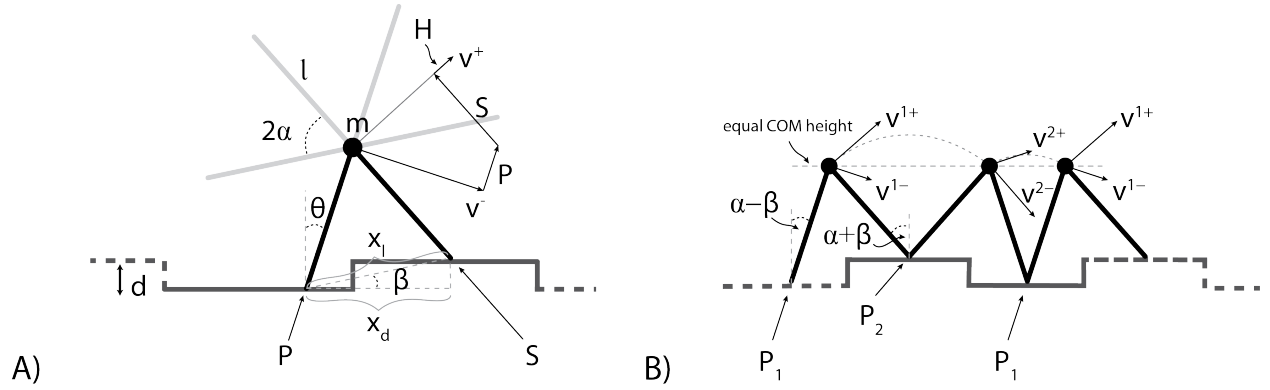
Figure 5.1: Schematic of the powered rimless wheel model. A) A mass, m, is located at the center of the wheel, with spokes of length l and 2α degrees apart. Angles θ and β are those of the stance leg relative to vertical and step height angle relative to horizontal, respectively. Push-off P is applied along the trailing leg redirecting the center of mass velocity. Upon heel-contact, a collision impulse S further redirects the center of mass velocity to be perpendicular to the new stance leg. Impulsive hip work H, directed along the motion of the center of mass after collision, brings the velocity after collision to the desired initial velocity of the step, v^+. Step length distances x_l and x_d are for level and uneven ground, respectively. B) Diagram of rimless wheel velocity indexing. Note that during all steps, the center of mass of the rimless wheel starts and ends at the same height, regardless of step height. Initial step angles are $\theta = \alpha + \beta$ and $\theta = \alpha - \beta$ for the up and down steps, respectively.

5.2.1   The Powered Rimless Wheel Model

We used a previously described model of the rimless wheel (McGeer, 1990b) to predict metabolic effort in response to surface height variability. The model consisted of a unit mass m at the center of the wheel and radially expanding spokes with length l at an inter-leg angle of 2α. As a spoke contacted the ground, a heel-strike impulse S redirected the center of mass velocity to be tangential to the new stance leg. The negative work done on the center of mass by the collision resulted in energy loss that needed to be replaced by the addition of positive work. In contrast to the model described by McGeer (1990b), this energy was not replaced by gravitational work (with the wheel moving down an incline). Instead, we used an impulsive push-off P, directed along the trailing leg, and impulsive hip work H, along the direction of motion of the COM after collision. Energy transfer is most energetically efficient if all positive work is done through a push-off immediately prior to collision of the following stance leg, with hip work equal to zero (Figure 5.1A) (Kuo, 2002). However, this is not always possible on uneven terrain since a preemptive push-off would require prior knowledge of the uneven surface in order to successfully regulate push-off timing and magnitude. We explored how push-off timing and surface unevenness affected the amount of work required for the rimless wheel to move at a constant speed.

5.2.1.1 Effects of Terrain on Step Timing and Average Velocity

The motion of the rimless wheel over a series of alternating up and down steps was analyzed as a series of steps k that we evaluated at contact events. At each contact, the magnitude of the center of mass velocity before heel-contact was given by v_k^- and after heel-contact by v_k^+. Because we were only interested in two-step periodic motion and the wheel was moving over terrain with regular up and down steps, we assumed that the velocities and wheel angles after each second contact were identical: $v_{k+2}^- = v_k^-$ and $\theta_{k+2} = \theta_k$. With this, we introduced the following naming convention:

- v^{1-} Velocity immediately before collision, following a down step

- v^{1+} Velocity immediately after collision, leading into an up step

- v^{2-} Velocity immediately before collision, following an up step

- v^{2+} Velocity immediately after collision, leading into a down step.

At every collision, one leg was on an up step and one leg on a down step, such that the COM height was equal at the start and end of each step, independent of whether the wheel was moving upwards or downwards (Figure 5.1B). Apart from the collisions, the rimless wheel was energetically conservative, the initial velocity of a step and its final velocity (measured before heel-contact of the following leg) were equal in magnitude. Assuming two-step periodic motion, this means that:

$$v^{2-} = v^{1+}$$
$$v^{1-} = v^{2+}. \tag{5.4}$$

Post impact velocities v^+ are a function of pre-impact velocities v^-, push-off P, and impulsive hip work H. Thus, the initial center of mass velocity of the following step (Figure 5.1A) can be computed as:

$$v^{1+} = v^{2+} \cos(2\alpha) + \sin(2\alpha)\frac{1}{m}P_1 + \frac{1}{m}H_1$$
$$v^{2+} = v^{1+} \cos(2\alpha) + \sin(2\alpha)\frac{1}{m}P_2 + \frac{1}{m}H_2 \tag{5.5}$$

where P_1 and P_2 are the respective push-off impulses for each step and H_1 and H_2 are step hip impulses. These equations are independent of step height d, which leads to two separate questions. First, how does step height influence initial step velocities, v^{1+} and v^{2+}, for the

up and down steps? Second, how do changes in push-off timing affect the amount of work done by push-off P and impulsive hip work H?

Both the initial step velocity, v^+, and the starting angle, θ_0, affect step duration t_e on even ground. Assuming a linearized pendulum motion about the stance foot and level ground, this time can be approximated by:

$$t_e = \sqrt{\frac{l}{g}} \ln \left(\frac{\dot{\theta}_0 \sqrt{l/g} - \theta_0}{\dot{\theta}_0 \sqrt{l/g} + \theta_0} \right), \tag{5.6}$$

where $\dot{\theta}_0 = v^+/l$ is the initial rotational velocity, and θ_0 the initial pendulum angle (McGeer, 1990b) (see Appendix A for details). On even ground, $\theta_0 = \alpha$ for all steps but, as d increases, this angle increases for up steps ($\theta_0 = \alpha + \beta$) and decreases for down steps ($\theta_0 = \alpha - \beta$) (Figure 5.1B). Step angle β was computed from the step height d according to $\beta = \arcsin \left(\frac{d}{x_l} \right)$. From this, we computed the average time for an up step and down step as:

$$t_d = \frac{1}{2} \sqrt{\frac{l}{g}} \left[\ln \left(\frac{v^{1+} \sqrt{l/g} - (\alpha + \beta) l}{v^{1+} \sqrt{l/g} + (\alpha + \beta) l} \right) + \ln \left(\frac{v^{2+} \sqrt{l/g} - (\alpha - \beta) l}{v^{2+} \sqrt{l/g} + (\alpha - \beta) l} \right) \right]. \tag{5.7}$$

Furthermore, distance covered over ground per step depended on step height d and was computed geometrically:

$$x_d = \sqrt{x_e^2 - d^2} = \sqrt{(2l \sin (\alpha))^2 - d^2}. \tag{5.8}$$

The average velocity $\bar{v}$ over two uneven steps can thus be written as:

$$\bar{v}_d = \frac{x_d}{t_d}. \tag{5.9}$$

As a result, changes in distance and time considerably decrease the average velocity $\bar{v}$. For example, for a gait with equal starting step velocities ($v^{1+} = v^{2+} = v^+$), Equation (5.7) simplifies to:

$$t_d = \frac{1}{2} \sqrt{\frac{l}{g}} \left[\ln \left(\left(\frac{v^+}{\sqrt{lg}} - \alpha \right)^2 - \beta^2 \right) - \ln \left(\left(\frac{v^+}{\sqrt{lg}} + \alpha \right)^2 - \beta^2 \right) \right]. \tag{5.10}$$

For $d = x_e \sin \left(\frac{v^+}{\sqrt{lg}} - \alpha \right)$, the step time becomes infinite. In other words, for a given initial velocity v^+ there is a limit to the step height d that the rimless wheel can traverse. If, on the other hand, we require a certain average forward velocity $\bar{v}$ as on level ground (as it is
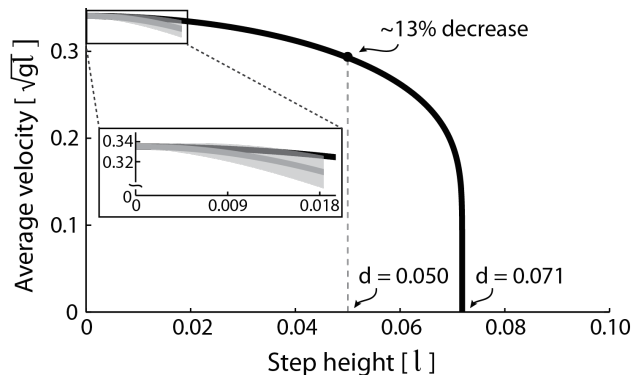
Figure 5.2: Rimless wheel average velocity with respect to changes in step height. Black line shows analytically calculated changes, grey line shows average simulated stochastic terrain results with one standard deviation shown in light grey envelope. Model parameters were based on a normalized initial velocity v^+ equivalent to walking at $1.0\,\mathrm{m/s}$ with a step length of $0.662\,\mathrm{m}$. For analytically calculated results, at a step height of 5% of leg length, average forward velocity decreases by approximately 13%. At approximately $d = 0.071$, the time required per step goes to infinity and the average forward velocity becomes zero. On stochastic terrain, the model could not complete trials after $d = 0.018$.

given, for example, in treadmill walking), the initial step velocity v^+ must be increased with higher steps d. This, in turn, requires a larger push-off impulse or more work done at the hip.

Given an initial velocity v^+ for level ground walking, we calculated the velocity limit for the rimless wheel when placed on uneven terrain. We based model parameters on human walking on level ground at a speed of $1.0\,\mathrm{m/s}$ and with a step length of $0.662\,\mathrm{m}$ (Voloshina et al., 2013). This was equivalent to a rimless wheel with a center of mass $m = 1$, leg length $l = 1$, an inter-leg angle of $\alpha = 0.390\,\mathrm{rad}$, a normalized average velocity of $\bar{v} = 0.342\sqrt{\lg}$ and normalized initial step velocities on level ground equivalent to $v^+ = 0.483\sqrt{\lg}$ and a push-off impulse of $P = 0.198$. Given these parameters, locomotion velocity decreases non-linearly with increased step height, such that at $d = 0.05l$, average velocity decreases by approximately $13\,\%$ (Figure 5.2). This decrease in velocity is primarily a result of a change in step duration, t_d (which increases by $15\,\%$). In contrast, step distance x_d only decreases slightly (by $0.2\,\%$). At a step height of approximately $d = 0.071l$ the velocity goes down to zero.

In addition, we simulated rimless wheel walking on stochastic terrain. The terrain consisted of steps of random heights, with maximum down and up steps being at $-2d$ and $+2d$, respectively. However, we dictated that each step alternate between an up and down step, making this surface only pseudo-random. Average change in step height was equal to d, which allowed us to compare stochastic terrain results to our analytical calculations. Each stochastic terrain trial started with level ground walking initial conditions and push-off mag-

59

nitudes. The rimless wheel then traversed the terrain for up to 100 steps. If the wheel could not complete all 100 steps, the trial was "incomplete" and was not used to calculate forward velocity averages. The rimless wheel completed 1000 trials for each height d, and no less than 600 successful trials were use to calculate velocity averages. Given this representation of stochastic terrain, the rimless wheel could not successfully complete enough trials after approximately $d = 0.018$ (Figure 5.2). This is likely because, with increased terrain variability, rimless wheel walking was more likely to degenerate as it encountered high enough steps it could not traverse given a fixed push-off magnitude. It is clear, however, even from a limited height range, that the average velocity of the rimless wheel on stochastic terrain decreased similarly (although faster) to the patterned terrain analyzed analytically. Gaits on stochastic terrain are also much more unpredictable and make it more difficult to draw any conclusions about gait biomechanics. In contrast, gait on the patterned terrain is more reliable but is still representative of walking on uneven terrain. As a result, we opted to conduct all further gait and energetic analyses using only the patterned terrain.

5.2.1.2   Effects of Push-off Timing on the Cost of Transport

Both the rimless wheel and the simplest walking model (discussed in more detail in the following section) can be powered by an impulsive push-off P of the trailing limb prior to collision and by impulsive hip work H of the leading limb immediately after collision. Between these two events, a collision impulse S redirects the motion of the COM. Push-off timing directly affects how the production of positive work is distributed between the foot and hip and, as a result, considerably affects model predicted power consumption (Kuo, 2002).

The work done by an impulse $\vec{J}$, on a particle with mass m and moving at an initial velocity $\vec{v}_{t_0}$, can be written as $W = \vec{v}_{t_0}\vec{J} + \frac{1}{2m}|\vec{J}|^2$. If we assume that hip work is instantaneous after collision, that the push-off impulse is always perpendicular and the hip impulse is always along the center of mass direction of motion, then:

$$W_P = \frac{1}{2m}P^2 \tag{5.11}$$

$$W_H = v^+H - \frac{1}{2m}H^2 \tag{5.12}$$

where v^+ is the post-impact velocity, and W_P and W_H are the work done by the push-off and hip impulses, respectively (see Appendix B for details). As shown in Equation (5.5), the post impact velocity, or the starting velocity of a step, is dependent on both the push-off and hip impulses, such that $v^+ = v^- \cos(2\alpha) + \sin(2\alpha)\frac{1}{m}P + \frac{1}{m}H$. The energetically

60

optimal strategy is to fully replace all collision losses through a preemptive push-off P (Kuo, 2002). Assuming no hip impulses, push-off magnitudes P_1 and P_2 for the up and down steps, respectively, can be calculated according to:

$$P_1 = m\frac{v^{1+} - v^{2+}\cos\left(2\alpha\right)}{\sin\left(2\alpha\right)}$$

$$P_2 = m\frac{v^{2+} - v^{1+}\cos\left(2\alpha\right)}{\sin\left(2\alpha\right)}. \tag{5.13}$$

Work performed by an impulsive push-off is strictly positive. Taking into account the 25 % efficiency at which humans perform positive work (Margaria, 1968), the metabolic cost of transport over two steps is computed as:

$$COT_{met,P} = \frac{1}{0.25}\frac{W_{P_1} + W_{P_2}}{2mgx_d} = \frac{P_1^2 + P_2^2}{m^2 gx_d}. \tag{5.14}$$

However, performing all work with a preemptive push-off P requires knowledge of the time of collision, which is not always possible on an uneven surface. This means that if push-off is missed, all energy lost during collision must be performed through hip work H. If $P_1 = P_2 = 0$, impulses H_1 and H_2 for the up and down steps must be equal to:

$$H_1 = m\left(v^{1+} - v^{2+}\cos(2\alpha)\right)$$

$$H_2 = m\left(v^{2+} - v^{1+}\cos(2\alpha)\right). \tag{5.15}$$

Unlike push-off work, hip work can be positive or negative. We defined W_H^+ and W_H^- as the positive and negative hip work, respectively. With the 25 % and -120 % efficiency for positive and negative work, the metabolic cost of transport over two steps evaluates to:

$$COT_{met,H} = \frac{1}{0.25}\frac{W_{H_1}^+ + W_{H_2}^+}{2mgx_d} + \frac{1}{-1.2}\frac{W_{H_1}^- + W_{H_2}^-}{2mgx_d}. \tag{5.16}$$

In addition to the cases stated in Equations (5.13) and (5.15), additional strategies exist that use a mix of both, push-off and hip work.

5.2.1.3 Numerical Analysis

To better understand the increase in work required to locomote on uneven terrain, we numerically simulated the dynamics of the rimless wheel model (McGeer, 1990b). We performed the simulation over two steps, consisting of one up and one down step of equal height d. Numerical integration began immediately after heel-strike and ended immediately after
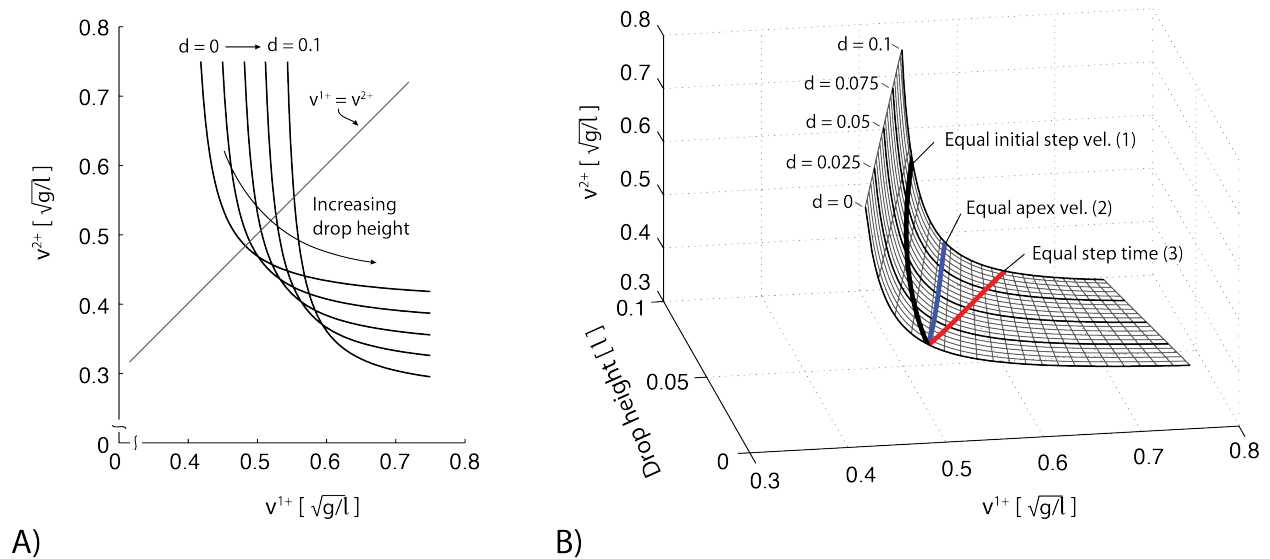
Figure 5.3: A selected range of initial step velocities, v^{1+} and v^{2+}, for the rimless wheel with respect to changes in drop height, d. All combinations of v^{1+} and v^{2+} result in the same average velocity $\bar{v}$, such that a larger v^{1+} leads to a smaller v^{2+} and the other way around. A) Relationship between v^{1+} and v^{2+} with changes in height, starting from $d = 0$ to $d = 0.1$. B) The initial step velocity plotted with respect to drop height d, with the think black lines corresponding to the lines plotted in A.

heel-strike following the second step. As previously mentioned, we selected model parameters analogous to human walking on level ground at a speed of $1.0\,\mathrm{m/s}$ and with a step length of $0.662\,\mathrm{m}$ (Voloshina et al., 2013). By enforcing a desired average velocity $\bar{v}$ over the two steps and by affixing the magnitude of v^{1+}, we could uniquely determine the necessary second initial step velocity v^{2+}. Over a range of heights, we identified the necessary initial velocities for the up and down steps, v^{1+} and v^{2+}, that would maintain the chosen average forward velocity (Figure 5.3). We were interested in three different *gait strategies*, that led to an exact v^{1+} and v^{2+} relationship:

1. Initial velocities, v^{1+} and v^{2+}, are equal for each given step height. This strategy assumes no prior knowledge of the terrain.

2. Initial velocities, v^{1+} and v^{2+}, are chosen to result in equal apex velocity for both the up and down step. When the center of mass velocity at apex is equal for both steps, the change in velocity during each step must equal the change in potential energy $W = mgd$, similarly to the increase in cost discussed in Equation (5.3).

3. Initial velocities, v^{1+} and v^{2+}, are chosen such that the durations of the up and down steps are equal and feet strike the ground in an evenly timed sequence. This results

in a much larger initial velocity for the up step, v^{2+} compared to the down step initial velocity, v^{1+}.

The energetic cost of each gait strategy does, however, depend on both the drop height and the method with which energy is input into the system. Recall that the initial step velocities can be obtained through various combinations of push-off and hip work, and that the chosen combination of energy input strategy directly affects the cost of transport (Equations 5.14 and 5.16). This leads to a number of cost of transport surfaces, given a choice of v^{1+} (and a corresponding v^{2+}) (Figure 5.4). In particular, we examined the following three *energy input strategies*:

1. The first energy input strategy (S1) used push-off work where possible with additional hip work only when necessary. For optimal performance, this method required a complete knowledge of the terrain surface and a continuous adaptation of push-off magnitudes. To compute the COT, we first obtained the push-off values P that produce the required v^{1+} and v^{2+} for $H = 0$. Without further constraints, it is mathematically possible for some values of P to be negative or to be large enough to cause negative values for the collision impulses S. Both cases are not reasonable in practice. For this reason, we constrained all push-off impulses to be $0 < P < \tan(2\alpha)v^{+}$, and computed H as required. These bounds ensured that push-off and collision impulses were always positive. As a result, there was only a small region in which gaits could be obtained strictly through positive push-off (Figure 5.4A, light grey shaded surfaces). Most of the solutions were powered by positive work done by push-off during one step and by negative work done by the hip during the other step. There was only a small region (dark grey shaded in Figure 5.4) where push-off values had to be constrained as they would have led to negative collision impulses.

2. The second energy input strategy (S2) produced all work through hip impulses H (Figure 5.4B). Because hip work can be positive and negative and since it happens post collision, there is no need to bound the values of H. Using only the hip to power the gait was clearly a suboptimal strategy, but it is the only option when it is not possible to produce push-off work at the necessary time in the stride cycle.

3. The third energy input strategy (S3) assumed that no adaptation of push-off magnitude occurred when walking over uneven terrain, although push-off was timed correctly. For all drop heights and velocity combinations, we set the push-off impulse to $P = 0.2$, which was the push-off magnitude used during symmetric, level ground walking (Figure 5.4C). The hip impulse then supplied any additional work, as it was required to match the required v^{1+} and v^{2+}.
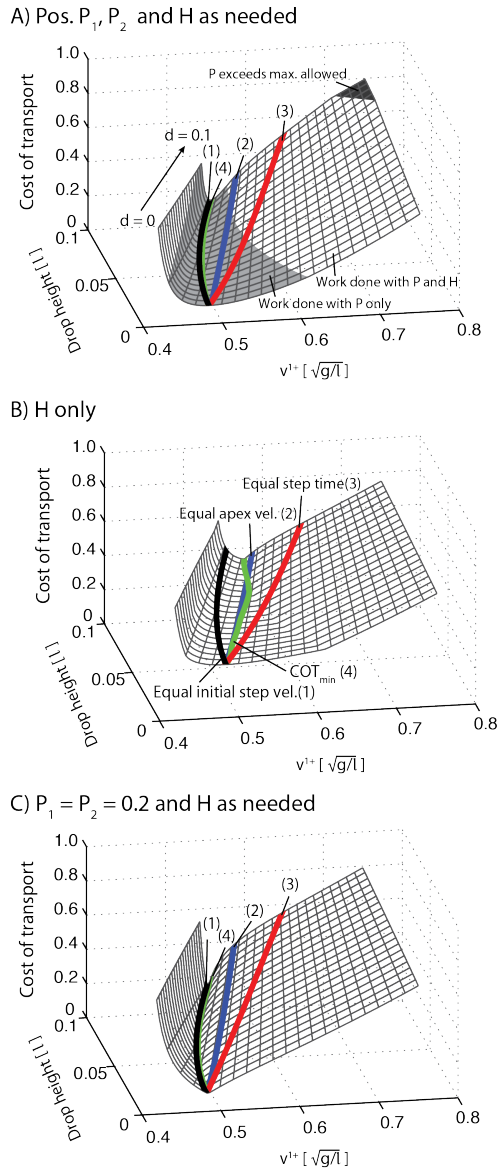
Figure 5.4: Effects of step height on the energetic cost of transport of the rimless wheel model. Given a selected range of initial step velocities, three energy input strategies are used: A) All positive push-off values P, with hip impulse H providing additional work when necessary. Shaded areas indicate work done through only P, a combination of P and H, and where at least one P exceeded the maximum value allowed. B) Only the hip impulse was used to produce positive work, C) Push-off impulses $P_1 = P_2 = 0.2$. Hip impulses provided the remaining positive work necessary to maintain a given forward average velocity.
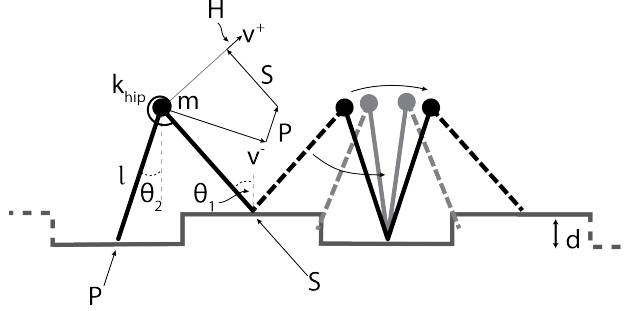
Figure 5.5: Schematic of the powered simplest walking model. The walker has legs of length l, a torsional hip spring k_{hip}, and a point mass m located at the hip. Each step is powered by a push-off impulse P, hip impulse H or both. Prior to heel-contact the center of mass is moving with a velocity of v^-. Upon heel-contact, a collision impulse S redirects the center of mass velocity to the initial velocity of the following step, v^+. The up and down steps are of height d. Angles θ_1 and θ_2 denote the angles between the stance leg and vertical and the swing leg and vertical, respectively.

For each of the three energy input strategies, an optimal choice of v^{1+} (and consequently v^{2+}) can be identified that minimizes the cost of transport at each drop height. This optimal choice of v^{1+} is shown for each of the cases in Figure 5.4. For the first and third energy input strategies, that allow for an active push-off P, the optimal choice was very close to the case where $v^{1+} = v^{2+}$. For the second strategy that relies only on hip work, the optimal choice was closer to solutions that generate equal apex velocities.

5.2.2 The Powered Simplest Walking Model

To investigate the effects of leg swing, we extended our study to a second model, the powered simplest walker (Garcia et al., 1998; Kuo, 2001). The model consists of two legs of leg length l, a unit mass m at the hip, mass-less legs, and feet with mass m_f. A torsional hip spring, with a spring constant k_{hip}, applies a torque between the stance and swing legs (Figure 5.5). Angles of the stance and swing leg with respect to vertical are θ_1 and θ_2, respectively. Assuming that $m_f \ll m$ (Garcia et al., 1998), we approximated the equations of motion for this system as:

$$\ddot{\theta}_1 = \frac{g}{l} \sin(\theta_1) \tag{5.17}$$

$$\ddot{\theta}_2 = \frac{k_{hip}}{m_f l^2} (\theta_1 - \theta_2) + \frac{g}{l} (\sin(\theta_1 - \theta_2) \cos(\theta_1)) - \dot{\theta}_1^2 \sin(\theta_1 - \theta_2).$$

Because the legs and feet were of negligible mass, the swing leg had no effect on the stance leg dynamics in this approximation.

Identical to the rimless wheel, the simplest walking model underwent an inelastic collision
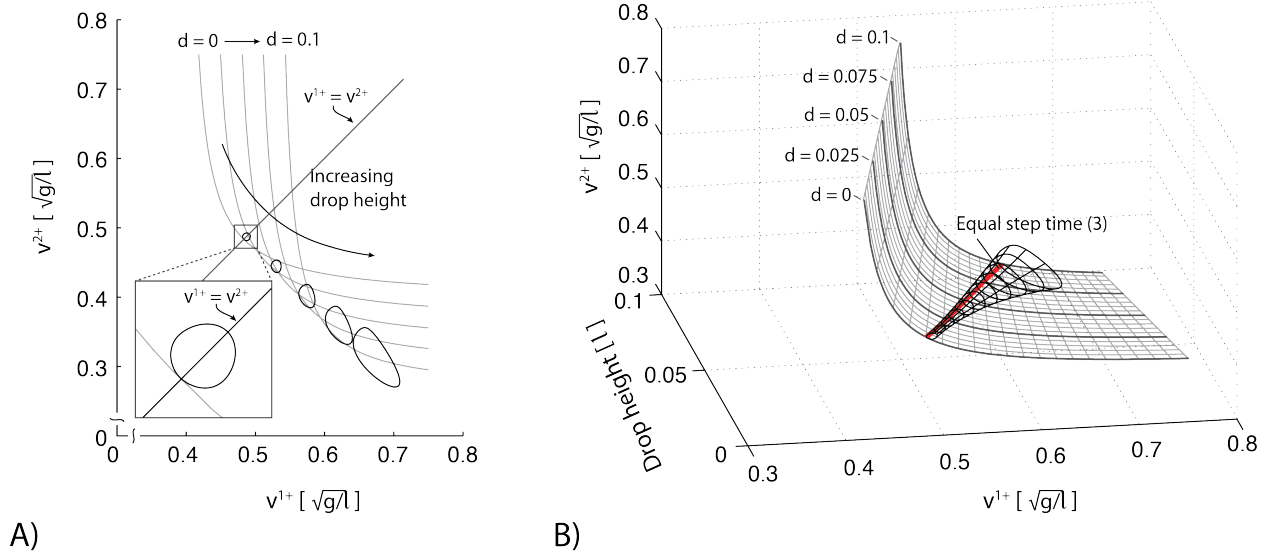
Figure 5.6: A selected range of initial step velocities, v^{1+} and v^{2+}, for the rimless wheel with respect to changes in drop height, d. A) Relationship between v^{1+} and v^{2+} with changes in height, starting from $d = 0$ to $d = 0.1$, plotted for the simplest walker (black lines) with the rimless wheel relationship for reference (grey lines). Inset shows close-up of the simplest walker and rimless wheel solutions for $d = 0$. Note, there are two solutions for the simplest walker where $v^{1+} = v^{2+}$, with one solution tangent to the rimless wheel surface. B) Initial step velocity plotted with respect to drop height d (black tube) with the rimless wheel surface for reference (grey surface). One side of the tube is collocated to the line indicating rimless wheel solutions with equal step durations.

S at every heel-strike. Energy lost during this collision was replaced through an instantaneous push-off impulse P applied immediately prior to heel-strike and through an impulse H at the hip applied after the collision. Unlike the rimless wheel, however, locomotion of the simplest walking model had variable step lengths, dependent on leg angles θ_1 and θ_2. As a consequence, the COM height varied from step to step, and Equation (5.4) of the rimless wheel no longer held true. Without any simplifications, the step-to-step transitions must be stated as:

$$v^{1+} = v^{1-} \cos\left(\theta_1^{1-} - \theta_2^{1-}\right) + \sin\left(\theta_1^{1-} - \theta_2^{1-}\right) \frac{1}{m} P_1 + \frac{1}{m} H_1 \tag{5.18}$$

$$v^{2+} = v^{2-} \cos\left(\theta_1^{2-} - \theta_2^{2-}\right) + \sin\left(\theta_1^{2-} - \theta_2^{2-}\right) \frac{1}{m} P_2 + \frac{1}{m} H_2.$$

5.2.2.1 Numerical Analysis

Because v^+, v^-, θ_1, and θ_2 were coupled through the complex dynamics of Equation (5.17), we identified periodic gaits numerically. We searched for these gaits over one up and one down step of height d. Stride integration began immediately after heel-strike of the first

66

step and ended after heel-strike of the second step. Continuous integration was interrupted after heel-strike, and a new initial stance leg velocity v^+ was set. The post-impact swing leg velocity was computed according to:

$$\dot{\theta}_2^+ = \dot{\theta}_1^- \cos\left(\theta_1^- - \theta_2^-\right)^2 \tag{5.19}$$

where, upon collision, the angle and velocity magnitudes previously associated with the stance leg were now associated with the swing leg. Similar to the rimless wheel, we specified one of the post-impact stance leg velocities v^{1+}, and computed v^{2+} to ensure a predefined average locomotion velocity. This velocity was consistent with normalized human walking data at $1.0\,\mathrm{m/s}$ (Voloshina et al., 2013) and set to $\bar{v} = 0.342\,\sqrt{\lg}$. Further model parameters were the hip mass $m = 1$, the leg length $l = 1$, and a the ratio of hip spring and foot mass $\frac{k_{hip}}{m_f} = 1.0482$. We selected hip spring stiffness such that the solution for the simplest walker with $v^{1+} = v^{2+}$ and at drop height $d = 0$ produced a gait equivalent to the rimless wheel solution at the same point (Figure 5.6A, inset). That is, the swing leg dynamics were tuned so that $\theta_1^{1+} = \theta_2^{1+} = \theta_1^{2+} = \theta_2^{2+} = \alpha$. Over a range of heights, we identified initial step velocities for the up and down steps, v^{1+} and v^{2+}, that resulted in a two-step periodic gait with the desired average forward velocity.

In contrast to the rimless wheel, solutions for the simplest walker were severely limited with respect to possible initial step velocities v^{1+} and v^{2+}. In fact, the space of possible solutions was tubular (Figure 5.6A). Starting from the simplest walker solution where $v^{1+} = v^{2+}$ and at $d = 0$, an increase in v^{1+} first led to a small decrease of v^{2+}. However, as v^{1+} increased, v^{2+} began to increase as well. This is in stark contrast to the rimless wheel, in which v^{2+} decreased monotonically. At a certain point, the rate of increase of v^{2+} becomes infinite, v^{1+} can no longer increase beyond this limit and larger values of v^{2+} can only be accommodated by reducing v^{1+} again. The solutions begin to wrap around and there is a second periodic solution where $v^{1+} = v^{2+}$. However, this solution had higher initial step velocities (yet with the same average walking speed). As a result, solutions on level ground were symmetric with respect to the $v^{1+} = v^{2+}$ line, and a closed band was formed. A similar shape could be found for all drop heights d, leading to a tube that widens as drop height increases (Figure 5.6B). One side of the tube was collocated to the line indicating rimless wheel solutions with equal step durations. For the walker, attainable step times were determined by the duration of the passive leg swing, which was roughly equal for the up and down steps.

Similar to the rimless wheel, we examined the cost of transport given three energy input strategies: positive work done by push-off P with additional hip work as needed (S1),

A) Pos. P_1, P_2 and H as needed

B) H only

C) $P_1 = P_2 = 0.2$ and H as needed
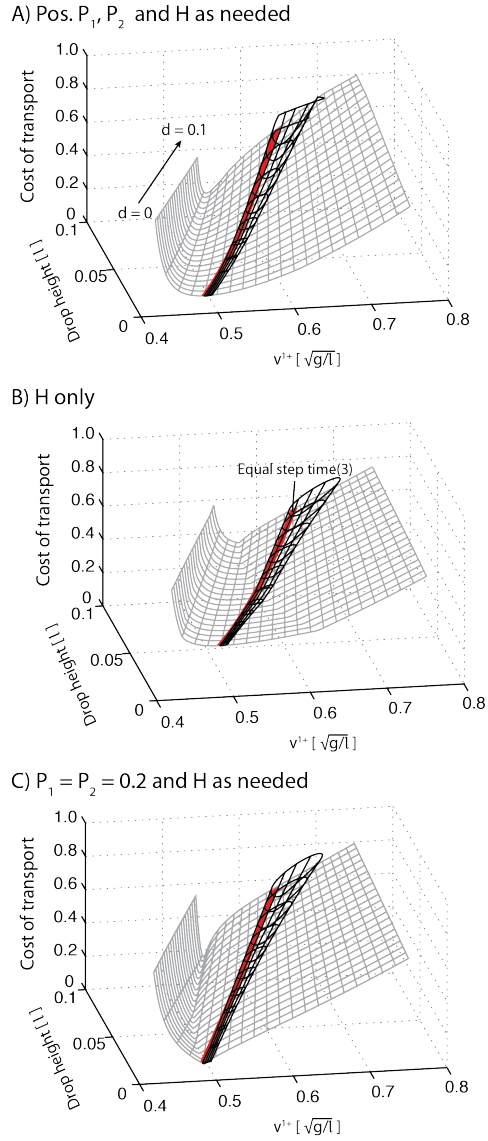
Figure 5.7: Effects of step height on the energetic cost of transport of the simplest walking model. Given a selected range of initial step velocities, three energy input strategies are used: A) All positive push-off values P, with hip impulse H providing additional work when necessary, B) Only the hip impulse was used to produce positive work, C) Push-off impulses $P_1 = P_2 = 0.2$. Hip impulses provided the remaining positive work necessary to maintain a given forward average velocity. Rimless wheel cost of transport surfaces shown in light grey for comparison.
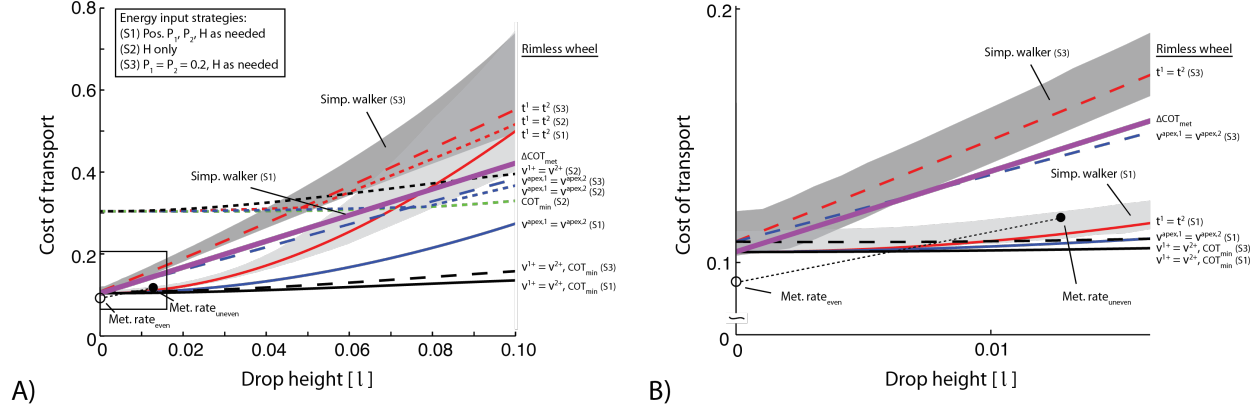
Figure 5.8: Model predicted increases in cost of transport with changes in drop height. A) Three energy input strategies are presented: 1) All positive push-off values P, with hip impulse as needed, 2) Hip impulse only and 3) Push-off impulses $P_1 = P_2 = 0.2$ with hip impulse as need. Lines depict specific solutions for the rimless wheel, and shaded areas depict solutions for the simplest walker. Energy input strategy 2 for the simplest walker not shown. The solid thick lines shows the change in cost of transport if we assume that energy increases on uneven terrain are strictly due to energy fluctuations and the positive work associated with them, as described by Equation 5.3. Note its proximity to the equal apex velocity line for S3. normalized human metabolic rate on even ground shown with hollow dot and for uneven terrain with black dot. B) Close up of square shown in part A.

positive work done by the hip impulse only (S2), and all push-off values set to a constant magnitude ($P = 0.2$) with additional hip work as needed (S3). Due to the tubular shape of the velocity solutions, the simplest walker cost of transport spaces were also tubular (Figure 5.7). Regardless of energy input strategy, all surfaces lay adjacent to the rimless wheel solutions that depict equal step durations. This resulted in all simplest walker solutions being significantly more energetically costly than the most energy efficient rimless wheel gaits. However, as with the rimless wheel, the first energy input strategy was also the most energetically efficient for the simplest walker.

5.3   Comparison of Results

For the rimless wheel model, we observed the lowest cost of transport for all drop height conditions during gaits powered by positive push-off impulses (light grey shaded surface, Figure 5.4A). In particular, solutions where the two initial velocities are equal to each other were the least energetically expensive (Figure 5.4A,C). As initial step velocities tend away from energetically optimal, one of the push-off impulses becomes zero, as the other impulse grows large enough to provide sufficient energy for both steps. However, this strategy required negative hip work during one of the steps, and additional energy to power gait. Eventually, the

69

increase in energetic cost as a result of doing hip work and the imbalance between push-off magnitudes outweighed the benefits of having a preemptive push-off. This strategy became more energetically expensive than powering gait through hip work alone. At this point, a constant push-off magnitude used on level ground with supplemental hip work was the most energetically efficient solution (Figure 5.4C).

The three energy input strategies had a similar effect on the simplest walker cost of transport. Although the simplest walker was more inefficient overall, the most energetically optimal strategy at smaller drop heights d was to use positive push-off and compensate with hip work as required (Figure 5.7A). Similar to the rimless wheel, at higher drop heights there exist simplest walker solutions that use a constant push-off and are less energetically expensive (Figure 5.8). The overall energetic efficiency of the simplest walker is highly dependent on the fact that solutions for this model tend to be collocated to rimless wheel solutions with equal step durations. Regardless of the energy input strategy, gaits with equal step times tend to be more energetically expensive, especially at higher drop heights (Figure 5.8). Leg swing happens passively in the simplest walking model, and step duration is largely determined by the time it takes the swing leg to complete a full pendulum motion. This time is influenced only marginally by the motion of the stance leg and thus roughly equal for the up- and down steps.

On level ground, both models predicted the energetic cost of human walking fairly accurately. When human subjects walked on an even surface with a net metabolic rate of $2.65\,\mathrm{W/kg}$ (Voloshina et al., 2013), it resulted in a cost of transport of 0.093. This was roughly equivalent to the lowest cost of transport for both simple models of 0.104. In the experimental study, human subjects also walked on an uneven surface with a 2.50cm maximum drop height. Once surface variability was normalized to leg length and averaged over all possible step heights, the mean step height was approximately equal to $d = 0.0128$. On such a surface, metabolic energy expenditure went up to $3.38\,\mathrm{W/kg}$ or a cost of transport of 0.118, approximately a 28% increase (Figure 5.8). As a result, the human cost of transport on uneven terrain lies approximately between rimless wheel solutions with equal time durations that use positive push-offs (S1) and solutions with equal apex velocities that use a fixed push-off (S3). It also clearly lies above the most energetically optimal energy input and gait strategies (where $v^{1+} = v^{2+}$ for S1 and S3). In contrast, the increase in the cost of transport as estimated by Equation (5.3) was much higher than the biological data. As previously mentioned, this is likely because such a strategy assumes no knowledge of or adaptation to the terrain and severely overestimates the energy increase associated with walking on uneven ground.

5.4 Discussion

In this study, we explored the particular effects of terrain unevenness on the cost of transport of the rimless wheel and the simplest walker models (McGeer, 1990b; Alexander, 1995; Garcia et al., 1998; Kuo, 2001). We simulated an uneven surface that consisted of equal up and down steps, and found periodic gaits for both models over a range of drop heights. Such a regularly patterned surface is clearly different from natural, more stochastic terrain. However, it captures the most important aspects of terrain variability, particularly with respect to the mechanical dynamics of walking.

We found that the observed increase in metabolic effort can be attributed to two effects. The first effect is purely mechanical: locomotion over uneven terrain leads to an increase in step duration, as described by Equation (5.10). This must be balanced by larger initial step velocities and results in higher collision losses that must be replaced by larger push-off or hip impulses (Equations (5.13) and (5.15)). The effect increases non-linearly with step heights and higher steps tend to cost disproportionately more than shorter steps. This allows for a number of *gait strategies*, essentially balancing velocities between up and down steps to produce certain gait characteristics. The second effect is related to event timing. Locomotion over uneven terrain makes it more difficult to predict events such as toe-off or heel-strike. This knowledge is key in energy optimal locomotion in which most work is performed through push-off, which must be timed immediately before heel-strike. Otherwise, additional energy-expensive hip work is necessary to maintain a constant forward velocity (Kuo, 2002; Kuo et al., 2005). Gaits that rely on only push-off impulses are comparable to walking with a complete knowledge of the terrain. In contrast, when all work is done through the hip, this is similar to locomotion while blindfolded, unaware of the characteristics of the following step. We mimicked the effects of natural terrain on gait timing by examining several *energy input strategies*. The strategies ranged from all work done through push-off impulses to all work done by the hip.

Depending on the gait and energy input strategies, model predicted increases in the cost of transport caused by uneven terrain were highly variable. Optimal strategies require work to be done only through push-off and with nearly identical initial step velocities, while the most expensive strategies involve large amounts of hip work and equal step duration gait patterns. For some gait types, the choice of gait and energy input strategy is merely a function of terrain knowledge. The more that is known about upcoming terrain, the better the push-off timing and magnitude can be adjusted towards optimal strategies. Other gait types exhibit a clear trade-off between gait and energy input strategies. The rimless wheel model, for example shows that unequal step durations (with equal initial step velocities) are

preferable to equal step durations (which require a much higher initial velocity for the up step). In the passive walking model, solutions are limited to gaits with equal step durations. To reduce energetic cost, unequal step durations can only be created by actively slowing down or speeding up the motion of the swing leg. However, this would require additional hip work and would in turn increase energy consumption, demonstrating a clear trade-off.

When we compare our results to data reported for humans walking on an uneven surface with a 2.5 cm variability (Voloshina et al., 2013), it is clear that humans always at least partially rely on push-off work. A push-off missed entirely would require all work to be done through the hip, leading to energetic increases much higher than those observed experimentally. At the same time, the increase in energy consumption is higher than an optimal strategy (equal initial velocities, all work done through push-off) would predict (Figure 5.8). It is our assumption, that humans vary push-off magnitude only partly, and rely mostly on additional hip work to compensate for terrain unevenness (most similar to energy input strategy S3). In addition to energetic predictions, this assumption is also consistent with changes in joint work that have been shown in human subjects walking on uneven terrain. Compared to walking on level ground, humans walking on uneven terrain tend to mainly increase positive work done at the hip. Positive knee work also slightly increases, while work done at the ankle does not change from the even to uneven surface. Producing work at the hip has previously been shown to be energetically more expensive, since the hip does not rely on passive energy storage and return from tendons (Sawicki et al., 2009). As a result, this change in joint work is primarily responsible for the 28 % increase in energetic cost, with changes in step width, length and their variabilities also potentially having minor contributions. These empirical conclusions, with most change seen at the hip joint, suggest that humans rely strictly on additional hip work when navigating uneven terrain. Although distinct changes in ankle work were not observed in human walking in response to uneven terrain, the changes in knee work and increased variability throughout gait imply that the strategy relying on increased push-off magnitudes is still plausible. In addition, the increase in metabolic cost seen on humans was substantially lower than the increase predicted by considering energy fluctuations due to up and down steps alone (Equation (5.3), Figure 5.8, ΔCOT_{met} line). Together, these results imply that humans are not optimal during locomotion on uneven terrain and still rely on energetically expensive hip work. However, humans are also not completely inefficient and still manage to show substantial adaptation to the walking surface.

The aforementioned trade-off between energetic optimality and a passive leg swing can also be observed experimentally. For locomotion on uneven terrain with a 2.5 cm variability, step duration is more variable, yet not as variable as predicted by a passive model. That is,

humans actively control swing time and step durations in order to allow for more energetically efficient gait strategies (see Appendix C for estimates of the increase in energy expenditure due to changes in swing time). In particular, human step period shortened by 3.7% when walking on uneven terrain compared to level ground (Voloshina et al., 2013). In contrast, for an analogous step height and using the most energetically efficient gait and energy input strategies, the model predicted decrease in step period was close to 8%. However, human step period variability, defined as a standard deviation of average step duration, also increased significantly by 26.7% (Voloshina et al., 2013). If this increase in step period variability is controlled, then it is fair to expect more positive work done at the hip. Step variability also likely leads to increased variability in push-off timing relative to heel-strike of the following leg, affecting the efficiency of energy transfer from step to step.

While our predictions roughly match the experimental data, the simplicity of the used models and the simplified uneven terrain clearly limit our model-based approach. As a result, gait variability was also strongly limited. However, terrain structure (stochastic vs. patterned) would not have altered the effects of various energy input strategies, since these strategies assumed either full or zero knowledge of the terrain. For gait timing, however, the non-linear effect of varying step heights has to be taken into account. As previously mentioned, higher steps are disproportionally more costly than shorter steps and this effect would alter the results on truly stochastic terrain. This is because, if step sizes are distributed uniformly, higher steps will have a larger impact on the average cost of transport. In the extreme case, a single very high step can bring the walking model to a complete halt, rendering overall locomotion velocity zero. For reasonable terrain variability, however, we found that our results scaled similarly to stochastic terrain and that our deterministic pattern served as a good proxy for uneven terrain.

Control of locomotion is an important part of gait that we did not discuss in this study. Instead, our models relied on simple impulse control, which allowed us to isolate how uneven terrain affected model energetics. However, in addition to changes in energetics, simple model analysis shows an increased risk of falling on stochastic terrain (Su and Dingwell, 2007). In particular, a simple passive walker model exhibited similar changes in gait variability as has been previously observed in humans, potentially predicting fall risk. Control optimization methods for walking models have also been proposed to improve gait stability on uneven terrain (Byl and Tedrake, 2008, 2009), although these methods have not considered energetics. Additional research would be necessary to determine how more sophisticated control methods could affect the energetic efficiency of continuous perturbation rejection. This could be especially useful for more complex models, such as those that include knee joints and potentially an upper body. A torso, for example, has been shown to be useful in stabilizing

walking in response to smaller perturbations (Maus et al., 2010). It is possible that performing an energetic analysis proposed in this paper, in addition to gait stability analysis and control, would allow more insight into how humans balance the trade-off between stability and energetic cost.

In this study, we characterized various model gait adaptations on uneven terrain for the rimless wheel and simplest walker models. We particularly focused on the effects of various gait and energy input strategies on model cost of transport and compared model outcomes to human empirical results. However, the patterned nature of our uneven surface limited the effects of gait timing on the energetic cost of transport. Future studies could focus on evaluating the effects of terrain variability on the biomechanics and energetics of gait. In addition, our models relied on simple impulse control and did not take gait stability into consideration. It may be useful to evaluate the trade-off between stability and gait energetics in the future, to allow more insight into gait adaptations on uneven terrain. However, the models presented in this study are reasonable estimates of how lower limb dynamics affect overall energetic cost. As a result, these findings could potentially prove useful in the design and control of biped robots, exoskeletons and any robotic assistive devices.

Acknowledgements

Funding

CHAPTER VI

Concluding Remarks

In this work, I explored the relationship between changes in energy expenditure and biomechanics during human locomotion on uneven terrain, compared to smooth level ground. I have used both empirical and model-based approaches, in order to gain more insight into the factors affecting energetic cost. In particular, I designed a novel treadmill modification method that allows for continuous human locomotion on an uneven surface (Chapter 2). I then used this treadmill to quantify the energetic and biomechanical changes caused by uneven terrain during human walking and running (Chapters 3 and 4). The results from these studies indicated that the increase in energy expenditure was likely largely caused by mechanical factors. As a result, my final study analyzed the effects of continuous up and down perturbations and various energy input methods on the cost of transport of the rimless wheel and simplest walker models (Chapter 5). In this final chapter, I discuss how my results contribute to the understanding of human locomotion on uneven terrain and their potential implications for the clinical and robotic fields.

6.1 Implications for clinical environments

Physical therapy to aid neurological recovery, such as after stroke, incomplete spinal cord injuries, or other gait disorders, is crucial in restoring patient mobility. Stroke, alone, affects nearly 900,000 new patients in the United States each year (Go et al., 2013), severely limiting gait and other activities of daily living. Rehabilitation is often driven by verbal cues and manual assistance from the therapist, robotic assistance, and body weight support training (Belda-Lois et al., 2011; Jaffe et al., 2004). Most exercises are task-specific and target only those motions that are deemed necessary for every day activity (Belda-Lois et al., 2011). In addition, overground walking is mainly trained on smooth, flat ground. As a result, even after rehabilitative therapy, many stroke survivors still struggle with impaired balance, motor weakness and decreased walking speed. This often leads to difficulty with navigating terrain, stepping over obstacles, decreased endurance and higher fall risks (Jaffe et al., 2004; Said et al., 1999; Winter et al., 1990). Therefore, supplementing rehabilitation exercises with

additional training on uneven surfaces will likely improve patient mobility and reduce fall risk.

Several studies focusing on gait rehabilitation post stroke have suggested using obstacle avoidance as an additional metric to evaluate gait and as a potential exercise to improve mobility (Jaffe et al., 2004; Said et al., 1999). In particular, (Jaffe et al., 2004) have evaluated the effects of obstacle avoidance training on gait parameters for both real and virtual obstacles. Over six sessions, both types of training resulted in increased self-selected walking velocity, increased ability to clear obstacles and overall endurance. In addition, improved gait parameters were retained even after 2 weeks, with some parameters even showing continued improvement. It is reasonable to expect that training on uneven surfaces would improve performance similarly. For example, patients could practice walking on an uneven terrain treadmill (described in Chapter 2) with a body-weight support system that would allow them to try new gait strategies in a safe environment and with therapist assistance. Interchangeable surfaces of varying surface height variability could be used with patients with varying levels of impairment. As patients continue with physical therapy, they can train on surfaces of increased difficulty, in order to encourage further improvement. It is important to note that a significant limiting factor in gait training after neurological injury is patient rate of fatigue. Healthy subjects walking on an uneven surface with a 2.5 cm height variability exhibited a 28% increase in energy expenditure, compared to walking on smooth terrain (Chapter 3). It is likely that patients undergoing rehabilitation therapy will fatigue faster with uneven terrain training. As a result, it would be crucial to supplement uneven terrain training with additional exercises that focus on adaptations necessary during walking on uneven terrain (such as producing more positive work at the knee and hip). Together with traditional therapy, training on uneven terrain could significantly improve the rate and magnitude of recovery for patients after neurological injuries.

6.2   Implications for robotic control

Hardware designs for biped robots have greatly advanced in recent years, but developing controllers for stable walking or running on uneven terrain still poses a challenge. Past research has mostly focused on ways to stabilize robotic gait after discrete disturbances rather than on adapting to continuously changing terrain. These stabilization methods usually drive the robot back to steady-state gait, or locomotion that is invariable from step to step. Since such a gait cannot be defined for uneven surfaces, robotic controllers used for walking in unfamiliar environments tend to evaluate gait on a step-by-step basis. Although this improves the robustness of the robot, it limits its natural dynamics, response speed

and greatly increases the energetic cost for generating locomotion. In contrast, humans can safely navigate and adapt to a variety of complex surfaces. These adaptations are naturally more energetically expensive, but they assist with maintaining stability during continuous surface height perturbations. Since human locomotion research has often served as biological inspiration for robotic designs, an understanding of human responses to uneven surfaces could provide suggestions for robotic design and control aimed at improving gait robustness and efficiency.

Locomotion of legged robots is commonly controlled by algorithms that rely on extensive knowledge of robot and environment mechanics. Models of the robot and the environment can be represented with detailed analytical equations that allow for joint trajectories and foot placement locations to be calculated on a step- by-step basis to ensure stability. One of the most commonly used methods to evaluate robot stability during gait is the Zero-Moment Point approach. This method relies on finding a point on the ground where the sum of all forces and torques on the robot will be equal to zero, thus ensuring static equilibrium (Vukobratovic and Stepanenko, 1972). Often, Zero-Moment Points are planned preemptively, with a full knowledge of the environment and the walking trajectory. However, they can also be estimated in real-time using various sensors on the robot that can characterize the movement of the robot and detect external forces. The robot can then generate forces, governed by additional control algorithms, which would counter any destabilizing effects. Many variations of these additional control algorithms exist to improve robotic gait but controllers that rely on the Zero- Moment Point concept are computationally intensive, slow, and produce unnatural movements. In addition, such control is generally robust to only very small perturbations and is energetically expensive, as every joint must be precisely driven at every moment.

Recently, research has also focused on using controllers that incorporate the natural dynamics of the robot. Animals often rely on the elastic properties of their muscles and tendons in order to store and return energy at specific times during the step cycle (Alexander and Bennet-Clark, 1977). The Achilles tendon during walking, for example, begins to stretch soon after the foot contacts the ground and then recoils to provide energy during push-off. This mechanism is completely passive and does not require active control, analogous to a spring. Similarly, the swinging motion of the leg during locomotion can be described by pendular equations of motion, completely ignoring the contributions of muscles (Mochon and McMahon, 1980). As a result, such passive dynamics have been integrated into legged models and even simple bipedal robots, which can walk and run completely passively down a slope, with gravity acting as the only input of energy (McGeer, 1990a,b). Passive-dynamic machines have since been extended to level ground walking, with simple on-off hip actuation

providing the necessary energy for locomotion (Collins et al., 2005). When scaled, such passive dynamic walkers are energetically comparable to humans, whereas robots relying on continual control use up to ten times the energy to traverse the same distance. In addition to energetic efficiency, incorporating passive dynamics into robotic control also improves robustness to perturbations (Collins et al., 2005). More complex robotic designs that incorporate passive elements, such as springs, have also been developed. With more sophisticated controllers, these robots can demonstrate a variety of gaits that are stable, energetically efficient, and still incorporate the natural dynamics of the system (Sreenath et al., 2011). However, adaptation to uneven surfaces during locomotion cannot fully rely on passive dynamics. Walking on uneven terrain would require modifications to the control algorithms regulating gait but how these modification should be applied has so far been unclear.

This thesis has several implications for robotic design and control. Humans adapt to uneven terrain during walking mainly by adjusting positive work production at the knee and hip (described in Chapter 3). In particular, changes in joint moments and power occur primarily at toe-off and shortly after heel-strike (Figure 2.2). Implementing similar changes in joint moment and work production at the same time in the stride may also improve the response of robotic systems to continuously changing terrain. Of course, fully relying on work done through push-off would be the most energetically efficient strategy (Kuo, 2002; Kuo et al., 2005). However, this would require complete knowledge of the terrain and is impractical for independent, biped robots. In contrast, producing work only at the hip is the most energetically expensive gait powering option, as shown by simulated walking models (Chapter 5). So, to alleviate the energetic increase associated with walking on uneven terrain, it may be beneficial for robots to still rely on passive elements and energy input at the ankle or knee joints, even when walking on uneven surfaces. For example, robot controllers could rely on sensors to determine where in the stride cycle heel-contact occurs. Based on this metric, torque at the ankle and hip would be adjusted accordingly. Or, once on an uneven surface, the robot could maintain a constant amount of work produced at the ankle and then compensate at the hip to maintain a certain forward velocity. Assuming passive elements in the robot, such strategies could significantly improve gait robustness and efficiency. For running robots, gait adaptation strategies described in Chapter 4 would be implemented instead. As uneven terrain seems to only affect ankle moments during human running (Figure 3.3), positive work produced in a robotic ankle would need to be reduced. In addition, humans exhibited slight increases in leg stiffness and changes in leg posture when running on uneven terrain. These are possibly adaptations for improved stability on an unfamiliar surface, which could also improve robotic gait. In addition, similar control schemes could also be implemented

on exoskeletons aimed at improving performance or multi-joint prosthetic devices.

6.3 Future directions and conclusions

This thesis has focused on quantifying the relationship between the biomechanical and energetic changes caused by uneven terrain during human walking and running. I have designed and constructed a novel uneven terrain treadmill and presented both empirical and model-based analyses of human locomotion on uneven ground. I used only one uneven surface for the empirical studies, with a given height variability and a particular pattern. Although subjects did not show any adaptations to the terrain pattern, it may be useful for future studies to focus on how changes in terrain variability affect energy expenditure. In addition, changes in walking speed and time given to adapt to the terrain may also affect gait biomechanics. It is also important to note that the models presented in this work, the rimless wheel and simplest walker, are very simplified representations of human gait. Although they have provided much insight into the causes of energetic increase during walking on uneven terrain, more sophisticated models are needed for a more detailed understanding of walking over uneven terrain. Future studies may want to focus on multi-jointed models and more sophisticated control of the moments produced at each joint. This would undoubtedly further the design of robotic devices and their control algorithms. The work presented in this thesis serves as a significant basis for future studies and will hopefully contribute to the development of more effective clinical interventions during gait rehabilitation, as well to the design and control of bipedal robots, exoskeletons and prostheses.

APPENDIX A

Effects of up and down steps on average forward velocity

There is a direct relationship between the average linear velocity and the initial leg contact angle and angular velocity. To find this relationship let us first consider that average velocity must be equal to:

$$\bar{v} = \frac{\Delta x}{\Delta t} \tag{A.1}$$

where Δx and Δt are the linear distance travelled and the time it takes to travel this distance, respectively. In our case, we are considering locomotion on uneven terrain involving two asymmetric steps (on up- and one down- step). As a result, the total distance travelled over two steps can be expressed as:

$$\Delta x = x_d = 2\sqrt{x_e^2 - d^2}$$
$$= 2\sqrt{\left(2l \sin\left(\alpha\right)\right)^2 - d^2} \tag{A.2}$$

where d is the step height, x_e is the step length on even ground and α is half the angle between the legs of the rimless wheel. If we consider θ the angle of the stance leg relative to vertical, then we can find the time needed to take a step on level ground, t_l, by solving the equations of motion of the simple inverted pendulum:

$$\ddot{\theta} = \frac{g}{l} \sin\left(\theta\right). \tag{A.3}$$

Assuming small angle θ, the relationship becomes:

$$\ddot{\theta} = \frac{g}{l}\theta \tag{A.4}$$

and solving the differential equation results in:

$$\theta(t) = C_1 e^{t\sqrt{g/l}} + C_2 e^{-t\sqrt{g/l}} \tag{A.5}$$

$$\dot{\theta}(t) = \sqrt{\frac{g}{l}} \left(C_1 e^{t\sqrt{g/l}} - C_2 e^{-t\sqrt{g/l}} \right) \tag{A.6}$$

Solving for C_1 and C_2 at time $t_0 = 0$:

$$\theta_0 = C_1 + C_2$$

$$\dot{\theta}_0 = \sqrt{\frac{g}{l}} \left(C_1 - C_2 \right).$$

Therefore:

$$C_1 = \frac{\theta_0 + \dot{\theta}_0 \sqrt{\frac{l}{g}}}{2} \tag{A.7}$$

$$C_2 = \frac{\theta_0 - \dot{\theta}_0 \sqrt{\frac{l}{g}}}{2} \tag{A.8}$$

At apex, θ is equal to zero and Equation (A.5) becomes:

$$C_1 e^{t\sqrt{g/l}} = -C_2 e^{-t\sqrt{g/l}}.$$

Solving for t, we get that the time to reach apex is equal to:

$$t_l = \frac{1}{2} \sqrt{\frac{l}{g}} \ln \left(-\frac{C_1}{C_2} \right).$$

Substituting Equations (A.7) and (A.8) and multiplying by two gives us the time needed for one full step:

$$
\begin{aligned}
t_l &= \sqrt{\frac{l}{g}} \ln \left(-\frac{\theta_0 - \dot{\theta}_0 \sqrt{l/g}}{\theta_0 + \dot{\theta}_0 \sqrt{l/g}} \right) \\
&= \sqrt{\frac{l}{g}} \ln \left(\frac{\dot{\theta}_0 \sqrt{l/g} - \theta_0}{\dot{\theta}_0 \sqrt{l/g} + \theta_0} \right)
\end{aligned} \tag{A.9}
$$

where θ_0 is the initial angle of the stance leg relative to vertical and $\dot{\theta}_0 = \dfrac{v^+}{l}$ is the initial rotational velocity.

If we consider that the two step motion is periodic and assume that the push-off impuls

P is equal for each step, then the relationship between initial and final velocities for the two steps can be written as:

$$v^{1-} = v^{1+} = v^{2-} = v^{2+} \qquad \text{(A.10)}$$

where the negative and positive superscripts indicate initial and final velocities, and the 1 and 2 superscripts indicate velocities for the up- and down- steps, respectively. Because the initial velocities are the same regardless of step height changes, only the initial angle θ_0 changes for the two steps. If β is the angle the step length forms with the horizontal due to changes in surface height, then θ_0 is equal to $(\alpha + \beta)$ and $(\alpha - \beta)$ for the up and down steps, respectively. From here, we can use Equation (A.9) to find the time needed to complete both steps:

$$t_d = \sqrt{\frac{l}{g}} \left[\ln \left(\frac{v^{1+}\sqrt{l/g} - (\alpha + \beta)\, l}{v^{1+}\sqrt{l/g} + (\alpha + \beta)\, l} \right) + \ln \left(\frac{v^{2+}\sqrt{l/g} - (\alpha - \beta)\, l}{v^{2+}\sqrt{l/g} + (\alpha - \beta)\, l} \right) \right] \qquad \text{(A.11)}$$

From this we get that the average velocity on the uneven surface is:

$$\bar{v}_d = \frac{2\sqrt{(2l\sin(\alpha))^2 - d^2}}{\sqrt{\dfrac{l}{g}} \left[\ln \left(\dfrac{v^{1+}\sqrt{l/g} - (\alpha + \beta)\, l}{v^{1+}\sqrt{l/g} + (\alpha + \beta)\, l} \right) + \ln \left(\dfrac{v^{2+}\sqrt{l/g} - (\alpha - \beta)\, l}{v^{2+}\sqrt{l/g} + (\alpha - \beta)\, l} \right) \right]} \qquad \text{(A.12)}$$

For the case of level ground walking, where $d = 0$, $\beta = 0$, and $v^{1+} = v^{2+} = v^+$ the equation for the average velocity $\bar{v}$ reduces to:

$$\bar{v}_l = \frac{2\sin\alpha}{\sqrt{\dfrac{l}{g}} \ln \left(-\dfrac{\alpha l + v^+\sqrt{l/g}}{\alpha l - v^+\sqrt{l/g}} \right)}. \qquad \text{(A.13)}$$

APPENDIX B

Work done by push-off and hip impulses

Let us define our arbitrary impulse vector, $\vec{J}$, as:

$$\vec{J} = \int\limits_{t_0}^{t_f} \vec{F} \, dt \tag{B.1}$$

where $\vec{F}$ is a force applied during the time interval between t_0 and t_f. From this, work done by the impulse on a mass m can be calculated as:

$$W = \int\limits_{t_0}^{t_f} \vec{F} \vec{v} \, dt \tag{B.2}$$

where $\vec{v}$ is the sum of the velocity at the time of the impulse (v_{t_0}) and the additional velocity increase due to the force, such that $\vec{v} = \vec{v}_{t_0} + \dfrac{\vec{F}t}{m}$. As a result, work done by the impulse can be re-written such that:

$$
\begin{aligned}
W &= \int\limits_{t_0}^{t_f} \vec{F}(\vec{v}_{t_0} + \frac{\vec{F}t}{m}) \, dt \\
&= \int\limits_{t_0}^{t_f} \vec{F}\vec{v}_{t_0} \, dt + \int\limits_{t_0}^{t_f} \frac{\vec{F}^2 t}{m} \, dt \\
&= \vec{v}_{t_0}\vec{F}t \Big|_{t_0}^{t_f} + \frac{1}{2m}\vec{F}^2 t^2 \Big|_{t_0}^{t_f} \\
&= \vec{v}_{t_0}\vec{J} + \frac{1}{2m}|\vec{J}|^2.
\end{aligned}
\tag{B.3}
$$

The above equation describes work done by an arbitrary impulse acting on the center of mass. To determine work done specifically by a push-off impulse, it is important to note

83

that the push-off P is always perpendicular to the center of mass direction of motion. As a result, work done by the push-off simplifies to:

$$\begin{aligned} W_P &= \frac{1}{2m}|\vec{P}|^2 \\ &= \frac{1}{2m}P^2. \end{aligned} \tag{B.4}$$

In contrast, impulsive hip work H always acts along the center of mass direction of motion. If we assume that hip work is done instantaneously after collision (rather than distributed over the entire stance phase) then:

$$\begin{aligned} W_H &= \vec{v}_{t_0}\vec{H} + \frac{1}{2m}|\vec{H}|^2 \\ &= v_{t_0}H + \frac{1}{2m}H^2. \end{aligned} \tag{B.5}$$

If we define the final velocity after the hip impulse to be v^+, it will be equal to $v^+ = v_{t0} + \dfrac{H}{m}$. In turn, hip work can be re-written as:

$$W_H = v^+H - \frac{1}{2m}H^2 \tag{B.6}$$

APPENDIX C

Effects of swing period on energy expenditure

For small angles, θ, the natural period T_0 of a simple pendulum can be written as:

$$T_0 = 2\pi\sqrt{\frac{l}{g}} \tag{C.1}$$

where l is the length of the pendulum and g is gravitational acceleration. Adding a torque at the base of the pendulum to increase or decrease the natural period of the pendulum can be equated to a change in gravitational acceleration, such that:

$$\bar{g} = \frac{l}{(T/2\pi)^2} \tag{C.2}$$

where $\bar{g}$ is the modified gravitational acceleration dependent on the desired pendulum period T. In addition, the change in energy from the starting position of swing to mid-swing (when the pendulum is vertical) can be calculated as:

$$\Delta E = mgl\left(1 - cos\left(\theta\right)\right). \tag{C.3}$$

As a result, additional energy E_{add} required to modify the duration of swing with respect to
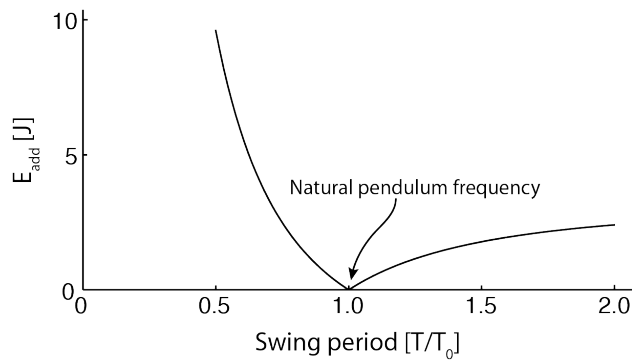

Figure C.1: Additional energy required to modify the swing period of a representative lower limb.

the natural energy of the system is found using:

$$E_{add} = ml\left(\bar{g} - g\right)\left(1 - cos\left(\theta\right)\right). \tag{C.4}$$

If we consider a representative subject from (Voloshina et al., 2013) with mass 66.1 kg and height 1.73 m, we can estimate the center of mass of the lower limb to be approximately 11.3 kg and located 0.415 m away from the greater trochanter (Winter, 2009). Given such parameters, a completely passive limb swinging from a starting angle of $\alpha = 0.390$ (roughly equivalent to a step length of 0.662 m) will have a $\Delta E = 3.22$ J and a natural frequency of 1.28 Hz. Almost three times the natural energy will be required to double the swinging period of the leg (Fig. C.1).

BIBLIOGRAPHY

Alexander, R. M. (1992). A model of bipedal locomotion on compliant legs. *Philos. Trans. R. Soc. Lond. B. Biol. Sci.* **338**, 189–98.

Alexander, R. M. (1995). Simple models of human movement. *Applied Mechanics Reviews* **48**, 461–470.

Alexander, R. M. and Bennet-Clark, H. C. (1977). Storage of elastic strain energy in muscle and other tissues. *Nature* **265**, 114–117.

Andres, R. O., Holt, K. G. and Kubo, M. (2005). Impact of railroad ballast type on frontal plane ankle kinematics during walking. *Appl. Ergon.* **36**, 529–534.

Arellano, C. J. and Kram, R. (2011). The effects of step width and arm swing on energetic cost and lateral balance during running. *J. Biomech.* **44**, 1291–1295.

Arellano, C. J. and Kram, R. (2012). The energetic cost of maintaining lateral balance during human running. *J. Appl. Physiol.* **112**, 427–434.

Bauby, C. E. and Kuo, A. D. (2000). Active control of lateral balance in human walking. *J. Biomech.* **33**, 1433–40.

Belda-Lois, J.-M., Mena-del Horno, S., Bermejo-Bosch, I., Moreno, J. C., Pons, J. L., Farina, D., Iosa, M., Molinari, M., Tamburella, F. and Ramos, A. (2011). Rehabilitation of gait after stroke: a review towards a top-down approach. *J. Neuroeng. Rehabil.* **8**, 66.

Bertram, J., D'antonio, P., Pardo, J. and Lee, D. (2002). Pace length effects in human walking:"Groucho" gaits revisited. *J. Mot. Behav.* **34**, 309–318.

Blickhan, R. (1989). The spring-mass model for running and hopping. *J. Biomech.* **22**, 1217–1227.

Blum, Y., Rummel, J. and Seyfarth, A. (2007). Advanced swing leg control for stable locomotion. *Autonome Mobile Systeme 2007* pp. 301–307.

Brockway, J. M. (1987). Derivation of formulae used to calculate energy expenditure in man. *Hum. Nutr. Clin. Nutr.* **41**, 463–71.

Burdet, E., Osu, R., Franklin, D. W., Milner, T. E. and Kawato, M. (2001). The central nervous system stabilizes unstable dynamics by learning optimal impedance. *Nature* **414**, 446–449.

Byl, K. and Tedrake, R. (2008). Metastable walking on stochastically rough terrain. *Proc. of Robotics: Science and Systems* pp. 6490–6495.

Byl, K. and Tedrake, R. (2009). Metastable walking machines. *Int. J. Robot. Res.* **28**, 1040–1064.

Cappellini, G., Ivanenko, Y., Dominici, N., Poppele, R. and Lacquaniti, F. (2010). Motor patterns during walking on a slippery walkway. *J. Neurophysiol.* **103**, 746–760.

Cavagna, G. A., Saibene, F. P. and Margaria, R. (1964). Mechanical work in running. *J. Appl. Physiol.* **19**, 249–256.

Cavanagh, P. R. (1987). The biomechanics of lower extremity action in distance running. *Foot Ankle* **7**, 197–217.

Cavanagh, P. R. and Kram, R. (1985). Mechanical and muscular factors affecting the efficiency of human movement. *Med. Sci. Sports Exerc.* **17**, 326.

Collins, S., Ruina, A., Tedrake, R. and Wisse, M. (2005). Efficient bipedal robots based on passive-dynamic walkers. *Science* **307**, 1082.

Collins, S. H., Adamczyk, P. G., Ferris, D. P. and Kuo, A. D. (2009). A simple method for calibrating force plates and force treadmills using an instrumented pole. *Gait Posture* **29**, 59–64.

Daley, M. A. and Biewener, A. A. (2006). Running over rough terrain reveals limb control for intrinsic stability. *Proc. Natl. Acad. Sci. USA* **103**, 15681–15686.

Daley, M. A. and Biewener, A. A. (2011). Leg muscles that mediate stability: mechanics and control of two distal extensor muscles during obstacle negotiation in the guinea fowl. *Philos. T. Roy. Soc. B* **366**, 1580–1591.

Daley, M. A., Felix, G. and Biewener, A. A. (2007). Running stability is enhanced by a proximo-distal gradient in joint neuromechanical control. *J. Exp. Biol.* **210**, 383–394.

Davies, S. and Mackinnon, S. (2006). The energetics of walking on sand and grass at various speeds. *Ergonomics* **49**, 651–660.

Dean, J. C. and Kuo, A. D. (2009). Elastic coupling of limb joints enables faster bipedal walking. *J. R. Soc. Interface* **6**, 561.

Doke, J. and Kuo, A. D. (2007). Energetic cost of producing cyclic muscle force, rather than work, to swing the human leg. *J. Exp. Biol.* **210**, 2390–2398.

Domingo, A. and Ferris, D. P. (2009). Effects of physical guidance on short-term learning of walking on a narrow beam. *Gait Posture* **30**, 464–468.

Donelan, J. M., Kram, R. and Kuo, A. D. (2001). Mechanical and metabolic determinants of the preferred step width in human walking. *Proc. Roy. Soc. B* **268**, 1985.

Donelan, J. M., Shipman, D. W., Kram, R. and Kuo, A. D. (2004). Mechanical and metabolic requirements for active lateral stabilization in human walking. *J. Biomech.* **37**, 827–835.

Farley, C. T. and Ferris, D. P. (1998). Biomechanics of walking and running: center of mass movements to muscle action. *Exercise Sport. Sci. R.* **26**, 253–286.

Ferris, D. P., Liang, K. and Farley, C. T. (1999). Runners adjust leg stiffness for their first step on a new running surface. *J. Biomech.* **32**, 787–94.

Ferris, D. P., Louie, M. and Farley, C. T. (1998). Running in the real world: adjusting leg stiffness for different surfaces. *Proc. Biol. Sci.* **265**, 989–94.

Ferris, D. P., Sawicki, G. S. and Daley, M. A. (2007). A physiologist's perspective on robotic exoskeletons for human locomotion. *Int. J. Hum. Robot.* **4**, 507–528.

Franklin, D. W., Liaw, G., Milner, T. E., Osu, R., Burdet, E. and Kawato, M. (2007). Endpoint stiffness of the arm is directionally tuned to instability in the environment. *J. Neurosci.* **27**, 7705–7716.

Garcia, M., Chatterjee, A., Ruina, A. and Coleman, M. (1998). The simplest walking model: stability, complexity, and scaling. *J. Biomech. Eng.* **120**, 281–288.

Geyer, H., Seyfarth, A. and Blickhan, R. (2006). Compliant leg behaviour explains basic dynamics of walking and running. *Proc. Biol. Sci.* **273**, 2861–7.

Go, A. S., Mozaffarian, D., Roger, V. L., Benjamin, E. J., Berry, J. D., Borden, W. B., Bravata, D. M., Dai, S., Ford, E. S. and Fox, C. S. (2013). Heart disease and stroke statistics–2013 update: a report from the american heart association. *Circulation* **127**, e6.

Gordon, K. E., Ferris, D. P. and Kuo, A. D. (2009). Metabolic and mechanical energy costs of reducing vertical center of mass movement during gait. *Arch. Phys. Med. Rehabil.* **90**, 136–144.

Gregorczyk, K. N., Hasselquist, L., Schiffman, J. M., Bensel, C. K., Obusek, J. P. and Gutekunst, D. J. (2010). Effects of a lower-body exoskeleton device on metabolic cost and gait biomechanics during load carriage. *Ergonomics* **53**, 1263–1275.

Grimmer, S., Ernst, M., Günther, M. and Blickhan, R. (2008). Running on uneven ground: leg adjustment to vertical steps and self-stability. *J. Exp. Biol.* **211**, 2989–3000.

Günther, M. and Blickhan, R. (2002). Joint stiffness of the ankle and the knee in running. *J. Biomech.* **35**, 1459–1474.

Hak, L., Houdijk, H., Steenbrink, F., Mert, A., van der Wurff, P., Beek, P. J. and van Dieën, J. H. (2012). Speeding up or slowing down?: Gait adaptations to preserve gait stability in response to balance perturbations. *Gait Posture* **36**, 260–264.

Hof, A. L., Geelen, B. A. and Van den Berg, J. W. (1983). Calf muscle moment, work and efficiency in level walking; role of series elasticity. *J. Biomech.* **16**, 523–537.

Jaffe, D. L., Brown, D. A., Pierson-Carey, C. D., Buckley, E. L. and Lew, H. L. (2004). Stepping over obstacles to improve walking in individuals with poststroke hemiplegia. *J. Rehabil. Res. Dev.* **41**, 283–292.

Jensen, K., Johansen, L. and Karkkainen, O.-P. (1999). Economy in track runners and orienteers during path and terrain running. *J. Sport Sci.* **17**, 945–950.

Kerdok, A. E., Biewener, A. A., McMahon, T. A., Weyand, P. G. and Herr, H. M. (2002). Energetics and mechanics of human running on surfaces of different stiffnesses. *J. Appl. Physiol.* **92**, 469–478.

Kuo, A. D. (2001). A simple model of bipedal walking predicts the preferred speed-step length relationship. *J. Biomech. Eng.* **123**, 264–269.

Kuo, A. D. (2002). Energetics of actively powered locomotion using the simplest walking model. *J. Biomech. Eng.* **124**, 113.

Kuo, A. D., Donelan, J. M. and Ruina, A. (2005). Energetic consequences of walking like an inverted pendulum: step-to-step transitions. *Exercise Sport. Sci. R.* **33**, 88–97.

Lejeune, T. M., Willems, P. A. and Heglund, N. C. (1998). Mechanics and energetics of human locomotion on sand. *J. Exp. Biol.* **201**, 2071.

Margaria, R. (1968). Positive and negative work performances and their efficiencies in human locomotion. *Int. Z. Angew. Physiol.* **25**, 339–351.

Margaria, R. (1976). *Biomechanics and energetics of muscular exercise.* Clarendon Press Oxford.

Margaria, R., Cerretelli, P., Aghemo, P. and Sassi, G. (1963). Energy cost of running. *J. Appl. Physiol.* **18**, 367–370.

Marigold, D. S. and Patla, A. E. (2002). Strategies for dynamic stability during locomotion on a slippery surface: effects of prior experience and knowledge. *J. Neurophysiol.* **88**, 339–353.

Marigold, D. S. and Patla, A. E. (2007). Gaze fixation patterns for negotiating complex ground terrain. *Neuroscience* **144**, 302–313.

Maus, H.-M., Lipfert, S. W., Gross, M., Rummel, J. and Seyfarth, A. (2010). Upright human gait did not provide a major mechanical challenge for our ancestors. *Nature Comm.* **1**, 70.

McAndrew, P. M., Dingwell, J. B. and Wilken, J. M. (2010). Walking variability during continuous pseudo-random oscillations of the support surface and visual field. *J. Biomech.* **43**, 1470–1475.

McGeer, T. (1990a). Passive bipedal running. *Proc. Roy. Soc. B* **240**, 107–134.

McGeer, T. (1990b). Passive dynamic walking. *Int. J. Robot. Res.* **9**, 62–82.

McMahon, T. A. and Cheng, G. C. (1990). The mechanics of running: how does stiffness couple with speed? *J. Biomech.* **23**, 65–78.

McMahon, T. A., Valiant, G. and Frederick, E. C. (1987). Groucho running. *J. Appl. Physiol.* **62**, 2326–2337.

Minetti, A. E., Ardigo, L. P. and Saibene, F. (1993). Mechanical determinants of gradient walking energetics in man. *J. Physiol.* **472**, 725–735.

Mochon, S. and McMahon, T. A. (1980). Ballistic walking. *J. Biomech.* **13**, 49–57.

Murray, M. P., Kory, R. C. and Clarkson, B. H. (1969). Walking patterns in healthy old men. *J. Gerontol.* **24**, 169–178.

Nakazawa, K., Kawashima, N., Akai, M. and Yano, H. (2004). On the reflex coactivation of ankle flexor and extensor muscles induced by a sudden drop of support surface during walking in humans. *J. Appl. Physiol.* **96**, 604–611.

O'Connor, S. M. and Kuo, A. D. (2009). Direction-dependent control of balance during walking and standing. *J. Neurophysiol.* **102**, 1411–1419.

O'Connor, S. M., Xu, H. Z. and Kuo, A. D. (2012). Energetic cost of walking with increased step variability. *Gait Posture* **36**, 102–107.

Pandolf, K. B., Haisman, M. F. and Goldman, R. F. (1976). Metabolic energy expenditure and terrain coefficients for walking on snow. *Ergonomics* **19**, 683–690.

Patla, A. E. (1997). Understanding the roles of vision in the control of human locomotion. *Gait Posture* **5**, 54–69.

Pinnington, H. C. and Dawson, B. (2001). The energy cost of running on grass compared to soft dry beach sand. *J. Sci. Med. Sport* **4**, 416–430.

Pinnington, H. C., Lloyd, D. G., Besier, T. F. and Dawson, B. (2005). Kinematic and electromyography analysis of submaximal differences running on a firm surface compared with soft, dry sand. *Eur. J. Appl. Physiol.* **94**, 242–253.

Pontzer, H., Raichlen, D. and Sockol, M. (2009). The metabolic cost of walking in humans, chimpanzees, and early hominins. *J. Hum. Evol.* **56**, 43–54.

Poole, D. C. and Richardson, R. S. (1997). Determinants of oxygen uptake. *Sports Med.* **24**, 308–320.

Said, C. M., Goldie, P. A., Patla, A. E., Sparrow, W. A. and Martin, K. E. (1999). Obstacle crossing in subjects with stroke. *Arch. Phys. Med. Rehabil.* **80**, 1054–1059.

Sawicki, G. S., Lewis, C. L. and Ferris, D. P. (2009). It pays to have a spring in your step. *Exerc. Sport. Sci. R.* **37**, 130.

Sockol, M. D., Raichlen, D. A. and Pontzer, H. (2007). Chimpanzee locomotor energetics and the origin of human bipedalism. *Proc. Natl. Acad. Sci. USA* **104**, 12265–12269.

Soule, R. G. and Goldman, R. F. (1972). Terrain coefficients for energy cost prediction. *J. Appl. Physiol.* **32**, 706–708.

Sponberg, S. and Full, R. J. (2008). Neuromechanical response of musculo-skeletal structures in cockroaches during rapid running on rough terrain. *J. Exp. Biol.* **211**, 433–446.

Sreenath, K., Park, H.-W., Poulakakis, I. and Grizzle, J. W. (2011). A compliant hybrid zero dynamics controller for stable, efficient and fast bipedal walking on MABEL. *Int. J. Robot. Res.* **30**, 1170–1193.

Su, J. L.-S. and Dingwell, J. B. (2007). Dynamic stability of passive dynamic walking on an irregular surface. *J. Biomech. Eng.* **129**, 802–810.

Thies, S. B., Richardson, J. K. and Ashton-Miller, J. A. (2005). Effects of surface irregularity and lighting on step variability during gait:: A study in healthy young and older women. *Gait Posture* **22**, 26–31.

Thoroughman, K. A. and Shadmehr, R. (1999). Electromyographic correlates of learning an internal model of reaching movements. *J. Neurosci.* **19**, 8573–8588.

Voloshina, A. S., Kuo, A. D., Daley, M. A. and Ferris, D. P. (2013). Biomechanics and energetics of walking on uneven terrain. *J. Exp. Biol.* **216**, 3963–3970.

Vukobratovic, M. and Stepanenko, J. (1972). On the stability of anthropomorphic systems. *Math. Biosci.* **15**, 1–37.

Wade, C., Redfern, M. S., Andres, R. O. and Breloff, S. P. (2010). Joint kinetics and muscle activity while walking on ballast. *Hum. Factors* **52**, 560–573.

Weir, J. (1949). New methods for calculating metabolic rate with special reference to protein metabolism. *J. Physiol.* **109**, 1–9.

Winter, D. A. (2009). *Biomechanics and motor control of human movement.* John Wiley & Sons.

Winter, D. A., Patla, A. E., Frank, J. S. and Walt, S. E. (1990). Biomechanical walking pattern changes in the fit and healthy elderly. *Phys. Ther.* **70**, 340–347.

Winter, D. A. and Yack, H. J. (1987). EMG profiles during normal human walking: stride-to-stride and inter-subject variability. *Electroencephalogr. Clin. Neurophysiol.* **67**, 402–411.

Yang, J. and Winter, D. (1984). Electromyographic amplitude normalization methods: improving their sensitivity as diagnostic tools in gait analysis. *Arch. Phys. Med. Rehabil.* **65**, 517.

Zamparo, P., Perini, R., Orizio, C., Sacher, M. and Ferretti, G. (1992). The energy cost of walking or running on sand. *Eur. J. Appl. Physiol.* **65**, 183–187.